Diss. ETH No. 18618

A novel biofuel cell harvesting electrical energy from activated human macrophages

A dissertation submitted to the

SWISS FEDERAL INSTITUTE OF TECHNOLOGY

ETH ZURICH

for the degree of

Doctor of Sciences

presented by

MIHO SAKAI STALDER

Dipl. Ing. Mechanical Engineering, ETH Zurich

born December 25, 1969

citizen of Japan

accepted on the recommendation of:

Prof. Andreas Stemmer, examiner

Prof. Viola Vogel, co-examiner

Dr. Andreas Vonderheit, co-examiner

2009

Acknowledgments

I would like to thank Professor Andreas Stemmer, head of the Nanotechnology Group at ETH Zurich, for giving me the greatest opportunity to conduct my PhD work, with which I could fulfill my two major interests "something small and something biological". His encouragement and enormous support were invaluable during my PhD in the Nanotechnology Group. The unforgettable experiences in Woods Hole in the first period of my thesis (both day and night) became the nuts and bolts of my bio-lab life.

I would also like to thank Professor Viola Vogel, head of the Laboratory for Biologically Oriented Materials at the ETH Zürich, and Dr. Andreas Vonderheit for being co-referees of my thesis and for their insightful comments.

My appreciation also goes to the group members of the Institute of Biochemistry and Dr. Axel Niemann, the Institute of Cell Biology, at ETH Zurich for their generous support.

Moreover, I would like to thank Professor Ulrike Ehlert, head of the Department of Clinical Psychology and Psychotherapy at University Zurich, for giving me the opportunity to work on the fascinating collaboration, and also Sussane Huber and Ulrike Kübler for their cooperation in macrophage-tests.

I would also like to thank following people: Orane Guillaume-Gentil, the Laboratory of Biosensors and Bioelectronics at ETH Zurich, for nice discussion and providing me her PEG-g-PLL solution for the test; Dr. Grace Li, the Laboratory for Biologically Oriented Materials at ETH Zurich, for insightful discussion; Verena Lütschg, the Institute of Zoology at University Zurich, for encouraging discussion; Dr. Edith Schneider Gasser for her tuition of patch clamp, Anna Evans, the Nonmetallic Inorganic Materials Group at ETH Zurich, for useful comments; Dr. Robert Stark, the NanoBioMat Group at Ludwig-Maximilians-Universität München for his tips; Mr. Oettinger, the Graphitfolien-Papst and Vice President of Technology&Innovation in SGL Carbon (Germany), for happily providing nice graphite samples.

A special thanks goes to Dr. Laurence Vindevogel for her support and my

tutoring in cell culturing and bio-thinking, and Dr. Xun Wei for her tuition in electrochemistry. Working with them was also fun.

I am too grateful for words to Dr. Andreas Vonderheit for his countless support. During his time in the Nanotechnology Group and even after his duty, his reliable guide and support was very precious.

A lots of thanks go to the members of the Nanotechnology Group for their supports, friendly discussions and many other funny things during my PhD time: Antje Rey, Dr. Brian Cahill, Dr. Dominik Ziegler, Dr. Georg Schitter, Guy Birrer, Dr. Javad Farahani, Dr. Laurence Vindevogel, Livia Seeman, Dr. Manuel Aschwanden, Dr. Markus Beck, Dr. Nicola Naujoks, Ralph Friedlos, Raoul Enning, Reto Fioka, Dr. Roman Fedosseev, Dr. Roxana Stoenescu, Siegfried Graf, Dr. Stefan Lengweiler, Dr. Xun Wei, Dr. Yury Belyaev. I really appreciated the atmosphere in the office owing to Altan Gürsel, Dr. Andreas Vonderheit, Claudia Küttel. I thank them for academic and non-academic discussions enlarging my mind.

Finally, I would like to thank my friends and family in Japan and in Switzerland, and also in the rest of the world for their supports and encouragements.

Abstract

In small medical devices, a battery occupies the major portion of the device in terms of weight and volume. Attempt to replace the conventional battery with a biofuel cell employing enzymes, extracted from organisms, have been undertaken in last few decades. By modifying the electron transfer from the reaction site to the electrode, miniaturization of the device and enhancement of overall performance have been demonstrated. When implanted, however, the operational period is limited due to host defense reactions from the human body.

During the inflammatory response, macrophages are recruited to sites of pathogens and activated to synthesize radicals, primarily superoxide anion through nicotinamide adenine dinucleotide phosphate oxidase (NADPH oxidase). NADPH oxidase is a transmembrane protein transporting electrons across the plasma membrane. To capture electrons for power generation, we focused on this electron transfer through the plasma membrane and examined its utility for running a biofuel cell.

THP-1 human monocytic cells were chemically stimulated to differentiate into macrophages. Further they were activated to induce a phagocytic response. Western blot analysis confirmed the presence of NADPH oxidase complex proteins in activated macrophages, and the activity of NADPH oxidase was validated by measuring the superoxide anion production using a colorimetric method. During differentiation, cells became adherent to a plain gold electrode which served as the anode in a two-compartment fuel cell system. The fuel cell produced a current of 1.5-2 μA per 10^6 cells seeded. The current production in the fuel cell always corresponded to the NADPH oxidase activity. Moreover, our results of different inhibitory tests and the estimate of the amount of superoxide anion production during the current generation let us conclude that (i) the current observed in the fuel cell originates from NADPH oxidase in activated macrophages and (ii) there are more than one electron transport pathways from the cells to the electrode. One pathway involves superoxide anions produced upon stimulation, additional not yet identified electron transport

occurs independently of superoxide anions.

Kurzfassung

In medizinischen Kleinstgeräten nimmt die Batterie in der Regel den meisten Platz ein und beeinflusst das Gerät auch hinsichtlich des Gewichts massgeblich. In den vergangenen Jahren gab es Versuche, die herkömmlichen Batterien durch biologische Brennstoffzellen zu ersetzen, welche aus Organismen gewonnene Enzyme zur Energiegewinnung nutzen. Durch die Verbesserung der Elektronen-Übertragung zwischen der Reaktionsstelle und der Elektrode konnten diese Brennstoffzellen verkleinert und die Gesamtleistung der Geräte verbessert werden. Bei implantierten Geräten bleibt die Lebensdauer jedoch wegen der Abwehrreaktion des Körpers beschränkt.

Doch könnte gerade die Abwehrreaktion des Körpers eine wichtige Quelle für die Energiegewinnung sein. Während der Entzündungsreaktion werden Makrophagen rekrutiert und aktiviert, um Radikale – zuerst Superoxidanionen – durch Nicotinsäureamid-Adenin-Dinukleotid-Phosphat Oxidase (NADPH Oxidase) zu synthetisieren. NADPH Oxidasen sind Transmembran-Proteine, welche Elektronen durch die Plasmamembran transportieren. Die vorliegende Arbeit befasst sich mit diesem Elektronentransfer durch die Plasmamembran, da dieser für den Betrieb von Brennstoffzellen genutzt werden kann.

Konkret wurden menschliche monozytären THP-1 Zellen chemisch stimuliert, um sie zu Makrophagen zu differenzieren. Weiter wurden die Zellen aktiviert, um phagozytäre Reaktionen zu induzieren. Mit der Western Blot Analyse wurden NADPH Oxidase-Proteine des Multi-Protein-Komplexes in aktivierten Makrophagen nachgewiesen und die Aktivität der NADPH Oxidase wurde durch die Messung der Superoxidanion-Produktion mittels einer kolorimetrischen Methode bestätigt. Während der Differenzierung hafteten die untersuchten Zellen auf einer unbehandelten Gold-Elektrode, welche als Anode in einem Zweikammer-Brennstoffzellen-System diente. Diese Brennstoffzelle erzeugte Strom von 1.5-2 μA pro 10^6 gesäten Zellen. Die Stromproduktion der Brennstoffzelle entsprach immer der NADPH Oxidase-Aktivität. Zudem kann man aus den Ergebnissen der verschiedenen inhibitorischen Tests und der

geschätzten Menge der Superoxidanion-Produktion während der Stromproduktion folgern, dass (i) der gemessene Strom aus der NADPH Oxidase aktivierter Makrophagen stammt und (ii) dass es mehr als nur einen Transportweg für die Elektronen aus der Zelle zur Elektrode gibt. Zum Transport der Elektronen dienen einerseits die durch Stimulation der Zelle entstehenden Superoxidanionen und zum andern werden die Elektronen auf einem noch nicht identifizierten Weg unabhängig von Superoxidanionen transportiert.

Contents

This thesis includes material published in Biosensors and Bioelectronics, Volume 25, Issue 1, Pages 68-75.

Chapter 1

Introduction

After the development over the years, batteries nowadays have attained good size reduction and longevity. As power source for implantable medical devices, conventional batteries still form the biggest and heaviest part of the device, and require regular replacement, which entails surgical operation. Moreover, these batteries may contain toxic substances to acquire high performance.

Due to the constant increase of the energy demand and the consequential environmental problems, the exploration of clean, sustainable energy sources have been receiving considerable attention. One of the promising fields for substitutional energy is fuel cells.

Conventional fuel cells work by catalysis. For instance, in a proton exchange fuel cell, hydrogen molecules are oxidized on the anode catalyst and dissociate into proton and electron, and on the cathode-catalyst oxygen molecules are reduced to water reacting with the electrons. These catalysts are often expensive materials such as platinum.

In living nature, microorganisms catalyze the oxidation of substrates using enzymes. Since microorganisms produce these enzymes and replace them continuously as a part of their metabolism, utilizing microorganisms in fuel cells may allow a substitutional energy source for a battery which is less expensive and does not require to be recharged or replaced. This is realized in microbial fuel cells.

1.1 Microbial fuel cells

In a microbial fuel cell, inactive substrate is transformed via microbial catabolism into a form accessible for electrochemical oxidation [1], and so chemical energy contained in the substrate is converted to electrical energy.

Attempts in microbial fuel cell have already been reported since the beginning of the last century. In 1911 Potter demonstrated the time response of the potential difference between the electrodes, one of which was immersed in an E.coli culture, and proposed the adaptation of this technique to a galvanic cell [2]. 20 years later Cohen presented a bacterial half cell using diverse bacteria [3]. When conventional fuel cells started to be investigated for practical use in 1960s, first preliminary experiments of microbial fuel cell were undertaken employing glucose as a fuel source for bacterial metabolism [4, 5]. Though, most practical advances and developments have been accomplished after 1980 [6].

The anode compartment in a microbial fuel cell is typically anoxic, preventing that oxygen works as the electron acceptor and blocks the electron transfer to the anode. Therefore, microbes living in an anaerobic environment are preferably used, for instance, *Klebsiella pneumoniae* [7], *Escherichia coli* [8, 9], *Pseudomonas aeruginosa strain KRP1* [10], *Proteus vulgaris* [11–13] or *Actinobacillus succinogenes* [9]. The cathode is either suspended in aerobic solution or exposed to air, for the use of oxygen as an electron acceptor.

The product of microbial catabolism used as a fuel can be either in the intermediate state such as oxidized glucose, or the end product of the fermentation such as hydrogen (H_2). In the latter case H_2 is further applied as a fuel for conventional proton exchange fuel cell [14].

To improve the electrical yield of microbial fuel cells, bacteria have also been immobilized onto the anode. The immobilization of *Proteus vulgaris* resulted in faster and more efficient response to substrate addition [15]. A common method to gain higher yield of electron transfer is the addition of mediators. Mediators facilitate the electron transfer from the catalytic active site to outside of the biological cell. Mediators generate reduced products that are more electrochemically active than most fermentation products. The mediators can be applied as diffusive or as immobilized components. For electron shuttling through the plasma membrane, the mediators are often membrane-permeable substances with low molecular weight. Such redox-species have to be able to penetrate easily in the oxidized state and be chemically stable, and posses suitable redox potential. Furthermore the mediators should not interfere with other metabolic processes of the cells. Commonly used mediators for microbial fuel cells are methylene blue [4,16], thionine [9,16,17], 2-hydroxy-1,4-naphthoquinone [15, 18], or neutral red [19].

The immobilization of mediators allows the enhancement of electrical yield as well. Although stable binding of the mediator to the electrode surface is rather

difficult to achieve [20], 2,6-dimethyl-1,4-benzoquinone (DMBQ) [21], 2-hydroxy-1,4-naphthoquinone (HNQ) [22], or neutral red [9] have been successfully immobilized to facilitate electron transfer to the anode.

The drawback of utilizing a mediator is toxicity and sustainability of the system. Most mediators are not easily reoxidized in the anodic compartment. Therefore continuous replacement of mediators is required [23].

Some microorganisms have the ability to produce their own mediators to promote extracellular electron transfer. Iron (Fe(III)) reducing *Shewanella putrefaciens* [16], *Geobacter sulfurreducens* [24], or *Rhodoferax ferrireducens* [25] have been reported to have an electron transport chain in their outer membrane. Fe(III) is often an abundant electron acceptor for microbial respiration in subsurface environments and aquatic sediments [25]. The electrons transferred to extracellular space can be utilized to generate anodic current instead of reducing circumjacent Fe(III) [26].

Economic application of microbial fuel cells has been tested for practical use. Accomplishing waste water treatment, mixture of bacteria present in waste water are inoculated for the use in microbial fuel cells [27, 28]. Anaerobic sludge from a methanogenic reactor at a potato processing plant served as mixed culture of bacteria for microbial fuel cells [10]. The attempt to obtain electrical energy from marine sediment achieved a complete natural biofuel cell system, in which the sediment itself served as a natural proton permeable membrane and oxygen in seawater was reduced at the cathode [29].

Another complete biofuel cell system is realized in a photo-electrochemical biofuel cell. In the anodic compartment, the oxidation of water in the photosystem of cyanobacteria *Synechococcus* produces electrons that are transferred to the electrode, whereas in the cathodic compartment the water is produced through the reduction of oxygen [21].

In microbial fuel cells, mostly procaryotic cells are employed as catalysis organ due to the simplicity of biological structure. Procaryotic cells possess single or double layered lipid bilayer as outer membrane and lack a membrane-bound cell nucleus, or any other membrane-bound organelles, so that all biochemical processes are accessible through the outer membrane. Though eukaryotic cells also possess lipid bilayer as outer membrane, these cells contain organells organized into complex structures enclosed within membranes. Biochemical processes occur in many organelles in cytosol engulfed in another layer of membranes, therefore the energetic site is hardly accessible.

Nevertheless yeast *Saccharomyces cerevisae* has also been examined to run a biofuel cell similarly as a bacterial biofuel cell. Already Potter provided the proof of principle of the use of yeast for galvanic study [2], and then this idea was realized much later in biofuel cells utilizing methylene blue as mediator [30] or even without artificial mediators [31]. Yeast grow rapidly under both aerobic and anaerobic conditions and have simple nutritional requirements [30], therefore should be ideal biocatalyst for microbial fuel cells.

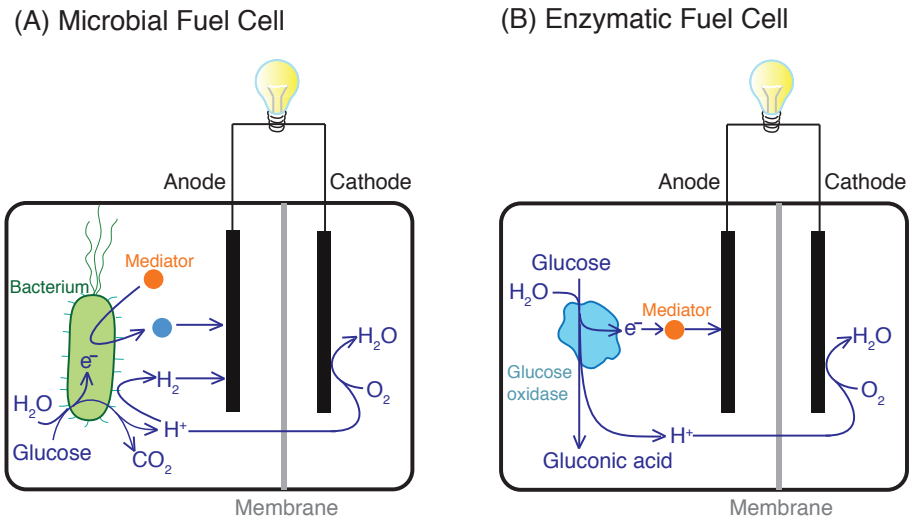

Figure 1.1: Schematic examples of biofuel cells. (A) A microbial fuel cell. Glucose is catabolized to CO_2 and proton by bacteria producing electrons. The electrons are either transferred to the anode via mediators, or utilized for fermentation to produce hydrogen used as a fuel. (B) An enzymatic fuel cell. Electrons released during the conversion of glucose to gluconic acid by glucose oxidase are transferred to the anode via mediators.

1.2 Enzymatic fuel cells

Past research of microbial fuel cells illustrates the difficulties and complexities of the electron transfer from the redox site to the electrode in the extracellular space. Additionally, such a biofuel cell cannot be applied as a power source for devices to be implanted, since microbes are often pathogenic. Therefore, catalytic sites (enzymes) have been extracted from bacteria and examined as biocatalyst for fuel cells [14, 32]. First enzymatic fuel cell with glucose as a fuel was demonstrated by Kimble et. al. in 1963 [33] in a two compartment fuel cell setup using glucose oxidase or D-amino acid oxidase for the glucose oxidation in the anode.

In contrast to microbes in microbial fuel cells that grow on the substrate, enzymes were not strongly adhered but rather suspended. To shorten the distance from catalytic active site to the electrode, it was reasonable that the tendency of research went towards immobilizing enzymes closer to the electrode. The immobilization of enzymes even provided a benefit for the lifetime of enzymes. Enzymes in solution are only stable for days, whereas immobilized enzymes can be stable for months [34].

To further increase of the power of enzymatic devices, as in microbial fuel cells, mediators are employed for shuttling electrons from catalytic site to the electrode. In 1980s Torstensson immobilized enzyme (D-glucose dehydrogenase) and mediator (meldola blue) onto carbon electrodes [35, 36]. The electron shuttling is most effective, if mediators are placed between enzymes and the electrode to form direct electron paths. Consequently enzymes and their cofactors or/and mediators have been "wired" on the electrode for electron-relay. Since carbon electrodes in the form of glassy carbon or carbon fibers can easily be modified chemically, various polymers are used to coat the carbon electrode enveloping anodic biocatalysts such as glucose oxidase or dehydrogenase and/or cofactor, e.g. NADP. Mediators have been also entrapped within the polymer at the anode [37, 38]. Instead of mediators, metal-polymer complex can be built to increase the conductivity. [32, 39] When redox polymer such as osmium-based redox polymer is used, it also serves as mediating system [40, 41]. Another approach for electrode modification employs covalent coupling of redox mediators to self-assembled monolayers on gold electrode surfaces. Pyrroloquinoline quinone (PQQ) is a redox coenzyme for enzymes such as glucose oxidase/dehydrogenase, diaphorase, or lactate dehydrogenase. Apo-glucose oxidase has been wired to PQQ-FAD (flavin adenine dinucleotide) monolayer on a gold electrode, resulting in enzyme-reconstitution by fitting FAD in apo-glucose oxidase and electron shuttling through PQQ-FAD to the electrode [14, 42].

Utilizing biological molecules in the cathodic compartment to catalyze the reduction of oxygen is an alternative to the classical use of platinum. The use of laccase in the cathodic suspension enabled oxygen reduction at a much lower overpotential than that required at a platinum electrode [43]. Laccase or bilirubin oxidase (BOD) have been immobilized to carbon electrode [37,38,44] by entrapping with redox polymer on carbon electrodes. In such cases, 2, 2'-azino-bis (3-ethylbenzo-) thiazoline-6- sulfonic acid) (ABTS) can be supplemented as a mediator [39, 43]. Gold electrodes have also been functionalized with microperoxidase via thiol monolayer [42, 45], or with cytochrome oxidase via

cytochrome c covalently bound to thiol monolayer [14, 46]. Some enzymes used for enzymatic fuel cells such as BOD have the maximum activity at lower pH. Running such a setup in phosphate buffer at physiological pH down-regulates the activity of enzymes and so the power of the fuel cells. Heller and colleagues encapsulate the redox center of these enzymes within redox polymers or hydrogels to raise the capability of oxygen reduction at the cathode [32, 44].

Giving selectivity to each electrode by wiring molecules allows one to omit the membrane in biofuel cells. By embedding BOD or laccase within osmium-based redox polymer [37, 38], non-compartmentalized complete biofuel cells have been realized promoting the miniaturization of the whole setup.

One of the most active areas in the research of enzymatic fuel cells is focused towards developing power sources for implantable devices within human body. Ideally one would use a biological metabolite fuel source such as glucose or lactate, available in physiological fluids [47]. Miniaturizing such a biofuel cell as a power source for drug delivery system has been proposed and is in development [37]. However, if implanted in human body, the fluctuation of anodic signal and the shortened lifetime of the device become serious problems. In case of glucose sensors, the sensitivity in vivo is only 50% of that in vitro [48].

For biosensors diverse reasons of such failure have been discussed [49] and these arguments can be extended to implanted enzymatic fuel cells as well. Main reasons for the sensitivity decrease in vivo include: (1) adsorption of proteins contained in the subcutaneous fluid; (2) the release of enzymes and radicals by macrophages and other cells involved in the foreign body response; (3) encapsulation of the sensor in a matrix of collagen laid down by fibroblasts; and (4) natural and phagocytotic degradation of enzymes or electrodes [48, 50] .

The acute inflammatory response starts immediately after the sensor is implanted. During the initial response, fluid carries plasma proteins and inflammatory cells migrate to the site of the foreign body such as biosensor [51]. Protein adsorption occurs within the first minutes of contact between the surface and the protein solution [52]. Adsorption of biomolecules smaller than 15kDa contribute to the greatest decrease in sensitivity for glucose sensors [53].

After the protein adsorption, phagocytic cells (neutrophils, monocytes, and macrophages) attempt to phagocytose the device and release enzymes and reactive oxygen species to destroy it. Due to the high amount of radicals released upon the foreign body response, depletion of oxygen in the tissue may occur and cause fluctuations in sensor response [48]. Since devices are relatively large, only "frustrated phagocytosis" occurs, seen as the release of reactive oxygen species

and enzymes degrading the device [51].

After a few days of the acute response, a chronic inflammatory response may set in or a modified version of the healing process begins which is the start of the fibrotic encapsulation process. To minimize these problems, different methods to prevent the adhesion of biomolecules have been attempted, e.g., flow system-based device architecture, biomimicry of surface by coating with humic acid, hyaluronic acid or phosphorylcholine, surface modification to form hydrogels. Moreover microdialysis was used as the sampling method, or radicals around the device were reduced by addition of superoxide dismutase (SOD) to promote the dismutation of superoxide to hydrogen peroxide [48]. Although natural degradation of enzymes causes the device failure as well, for most biosensor designs an excess of enzyme is used, therefore lost enzyme activity is very seldom a problem [54].

1.3 Long-term target of our project

For small portable medical devices, such as an glucose sensor, an apparatus is desired to be as small and light as possible. The usage of the conventional batteries in such has disadvantages in weights/ dimensions, requirement of the recharging and the replacement, and bio-incompatibility. Therefore this project has set the goal to develop a small energy source for a small medical device. Conventional fuel cells operated in ambient condition are still rare and require artificial supplement of substrates. Microbial fuel cells may reduce the frequency of the replacement, but suffer from bio-incompatibility. Enzymatic fuel cells, though pathogens are eliminated, suffer from limited lifetime. In most cases, implanted devices are exposed to the danger of being attacked by immune reaction of host body and losing their functionality rapidly.

To overcome the shortcomings of these energy sources, utilizing natural functions of human body as an energy source for a fuel cell would be an attractive option. Thus, this project addresses the feasibility of harvesting electrical energy using human living cells.

1.4 Transmembrane proteins

Human cells are encapsulated by the so-called plasma membrane separating the interior of the cell from the outside environment. Thinking about the biofuel cell operated by human cells, the electron transfer from the active reaction

site to extracellular space is an issue, as in microbial fuel cells. Employing permeable mediators may help, however, they are often toxic and may interfere with cellular functions. A transmembrane protein can play an important role since it is present at the interface between cytosol, where substantial cellular metabolisms happen, and the extracellular space, where the electrode is placed. The transmembrane protein is a protein embedded in the biological membrane and spans the entire membrane. As other membrane binding proteins, the function of transmembrane proteins is strongly connected to the regulation of various cellular vital functions. To maintain their cellular functions, electrical energy can be transferred over the plasma membrane using intra/extracellular reactions. For such a conversion between chemical energy and electrical energy, transmembrane proteins undertake an active or passive role. Deep investigation of the correlation between biological function and electrical energy has been started after the existence of a membrane potential in cells was ascertained in the middle of the last century [55, 56]. Mitchell then revealed the coupling between electron transport across membrane proteins and the production of biological energy [57]. This finding led to the discovery of different transmembrane electron transport mechanisms involving membrane proteins.

One of the major roles of transmembrane proteins is serving as a receptor for extracellular signaling molecules. When hormones, neurotransmitter, cytokines, or growth factors attach to the receptor, the cells become activated and generate a cascade of intracellular signals that alter the behavior of the cell [58].

Some transmembrane proteins are cell adhesion molecules. Cadherin, one such protein, maintains the cell-cell junction by connecting intracellular anchor proteins that bind to cytoskeleton and an extracellular matrix. Integrin is a famous cell adhesion molecule also responsible for signaling from extracellular matrix [59].

Another important function of transmembrane proteins is transport of molecules or ions. Since lipid bilayers are highly impermeable to most polar molecules or ions, transmembrane proteins undertake the transport of molecules or ions necessary for cell metabolism. Each of such transmembrane proteins are responsible for transferring a particular solute across the membranes [58]. Passive transport with a concentration gradient or electrochemical gradient occurs spontaneously, for example, through ion channels. The ion channels form aqueous pores across the lipid bilayer and allow inorganic ions of appropriate size and charge to cross the membrane along their electrochemical gradients. The channels are gated and usually open transiently in response to a specific

perturbation in the membrane, such as a change in membrane potential (voltage gated channels) or the binding of a chemical messenger as neurotransmitter (ligand-gated channels) [58]. An example of such a transport is seen in transmembrane ATPases. Mitchell has revealed the mechanism of transmembrane ATPase involved in transport of substances [57]. This synthase transforms upon transit of proton though membrane due to concentration gradient, creating ATP from ADP in the cytosolic side. By ATP hydrolysis, ATP synthase becomes an active transport system for pumping protons out across the membrane against the concentration gradient. Through this bilateral function, transmembrane ATPases import many of the metabolites necessary for cell metabolism and export toxins, waste, and solutes that can hinder cellular processes. Similar systems can been seen also for transport of ions (Na^+/K^+ATPase).

Transmembrane proteins that possess redox system can be utilized for electron transport through membrane. The electron transfer maintains the charge balance over membrane and is necessary for bioenergetics and redox homeostasis, proton extrusion and control of internal pH, and the generation of defensive reactive oxygen species by nicotinamide adenine dinucleotide/nicotinamide adenine dinucleotide phosphate (NADH/NADPH) oxidase [60]. NADPH oxidase is a transmembrane protein complex that transports electrons across biological membranes to reduce oxygen to superoxide and its function is activated during phagocytosis.

1.5 NADPH oxidase

Nicotinamide adenine dinucleotide phosphate-oxidase (NADPH oxidase) is a transmembrane enzyme that catalyzes the production of superoxide anion ($O_2^-\cdot$) from oxygen and NADPH with its electron transport mechanism. The overall reaction is:

$$NADPH + 2\,O_2 \longrightarrow NADP^+ + H^+ + 2\,O_2^-\cdot$$

Since the superoxide anion is a precursor of different reactive oxygen species used in the immune defense to degrade bacteria or invaders, NADPH oxidase plays a crucial role in host defense. Genetic defects in the NADPH oxidase cause several chronic granulomatous diseases (CGD). In these diseases, cells cannot produce enough reactive oxygen species and persistent bacterial infections occur [61, 62]. Inadequate superoxide anion production by NADPH oxidase is a major source of atherosclerosis, the thickening of artery walls due to the accumulation of cholesterol.

NADPH oxidase is a multicomponent enzyme complex containing six essential protein components, two membrane-bound elements and four cytosolic elements. These components are disassembled and dormant in resting cells, and upon activation, all components are assembled to become a functional NADPH oxidase.

1.5.1 Structure of NADPH oxidase

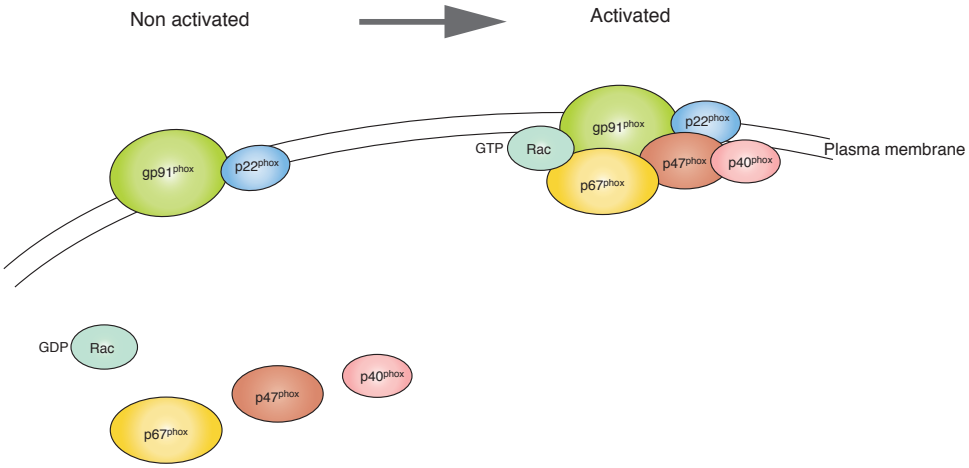

Figure 1.2: Schematic diagram of NADPH oxidase before and after activation. The cytosolic subunits p47phox, p67phox, p40phox, and RacGDP translocate to plasma membrane upon activation and form NADPH oxidase complex with the membrane bound subunits, gp91phox and p22phox.

1. Membrane-bound NADPH oxidase subunits

Two of the NADPH oxidase components are integral membrane proteins that attach to the biological membrane permanently. These components had been considered as one transmembrane component flavocytochrome b_{558}, until the technique of protein purification became well-developed. This flavocytochrome b_{558} was actually a heterodimer composed of one large and one small protein, namely gp91phox and p22phox [63].

gp91phox

gp91phox is the catalytic core of NADPH oxidase. This molecule contains all redox centers of NADPH oxidase, two molecules of haem and one molecule of flavin adenine dinucleotide (FAD). FAD has a NADPH- binding site, where the chain redox reaction of NADPH oxidase starts [64]. Therefore the redox reaction is selective for NADPH as a substrate [63]. gp91phox is dormant in resting cells and activated by the assembly of NADPH oxidase.

p22phox

p22phox is a membrane protein which closely associates with gp91phox in a 1:1 ratio forming the floavocytochrome b_{558}. The absence of p22phox in phagocytes from CGD patients results in no detectable level of gp91phox [63]. Therefore p22phox is thought to stabilize gp91phox by binding to it. p22phox is also known to provide high affinity binding sites for cytosolic NADPH oxidase subunits [64] promoting the stable interaction between p47phox, a cytosolic component, and gp91phox for NADPH oxidase activation.

2. Cytosolic NADPH oxidase subunits

p47phox

p47phox is the organizer of the NADPH oxidase assembly.

p47phox is phosphorylated on multiple sites through the action of several kinases, resulting in binding to p67phox (and possibly p40phox) through multiple binding sites, and then translocation of the subunits-complex to the membrane [65]. At the membrane, this protein interacts with p22phox through the SH3 domain which is first unmasked when phosphorylated, but also with cytoplasmic region of gp91phox stabilizing the attachment of p67phox to flavocytochrome b_{558} [64,66,67]. Loss of phosphates from p47phox attenuates the superoxide anion production [68].

p67phox

p67phox contains an activation domain essential for electron transfer through flavocytochrome b_{558} redox centers [69].

After binding with p47phox, this protein is translocated to the plasma membrane and attaches directly to membrane-bound component flavocytochrome b_{558} and then triggers the change in gp91phox in combination with RacGTP to

initiate oxidizing of NADPH and induce electron transport [64, 70]. Myeloid-related proteins in p67phox induce the switch between the partially and the fully "open" cytochrome b_{558} conformation [71].

p67phox is associated with the cytoskeleton and is involved in structural changes of the cells for movement and phagocytosis [66, 70].

The phosphorylation of p67phox is necessary for NADPH oxidase activity [63], however, the contribution of this phosphorylation event to the formation of activated NADPH oxidase is still not clear [72].

Furthermore, p67phox appears to be a bridging molecule that links p47phox and p40phox [65].

p40phox

p40phox is a component which may not be necessary for NADPH oxidase. Usually p40phox interacts with p47phox and p67phox with a 1:1:1 stoichiometry [63]. The interaction between p67phox-p40phox has a higher affinity than p47phox-p40phox interaction [73]. Since p40phox may be stable only when bound to p67phox [63], it may be constitutively associated to p67phox in both resting and activated cells [73].

Contradictory functions of p40phox have been discussed. On the one hand, the presence of p40phox may promote NADPH oxidase activity [74]. On the other hand, p40phox may induce down-regulation of NADPH oxidase activity because some domains of this protein compete against the interaction with other NADPH oxidase subunits [73] when not phosphorylated [75]. Even some reports have suggested that p40phox is separated from the active NADPH oxidase during activation [73].

Thus, p40phox is thought to be a modulatory unit of NADPH oxidase [63].

Rac-GDP/GTP

Rho-family small GTPase exists in two interconvertible forms: the GDP-bound inactive and GTP-bound active form. Rac is one of Rho-family small GTPase and its GTP-bound form is an essential element of the NADPH oxidase [76–78].

Rac in general exists in GDP-bound form in resting cells as cytosolic complexes with Rho GDP-dissociation inhibitor (RhoGDI) [79]. Upon cell stimulation, Rac becomes activated by exchanging GDP for GTP, dissociated from RhoGDI, and is subsequently recruited to the membrane. This translocation of Rac to the membrane occurs independent of the translocation of other cytosolic

subunits of NADPH oxidase [80, 81].

Diverse evidences showed that Rac-GTP may interact with p67phox [77, 81] and/or with gp91phox directly [79, 82], with or without binding to the phospholipid bilayer [82]. In any case, Rac stabilizes the NADPH oxidase complex in an active conformation [77].

Rac supports NADPH oxidase activity only in its GTP-bound active form [79] and hydrolysis of GTP bound to Rac, that occurs intrinsically and/or stimulated by GTPase activating protein (GAP), leads to disassembly and inactivation of the enzyme [75, 82].

Therefore Rac-GDP/GTP functions as molecular switch for turning on and off NADPH oxidase [75, 79].

1.5.2 Regulation of NADPH oxidase activity

Since generated reactive oxygen species via inflammatory systems may be injurious to adjacent cells, NADPH oxidase activity is regulated through various steps during its activation. Generally, NADPH oxidase activity in a cell may depend on a dynamic balance between the rate of assembly or activation and the rate of deactivation [75].

The activation of NADPH oxidase is commonly triggered by agonist binding to plasma membrane receptor. The expression of subunits of the enzyme complex is associated with the maturity of the cell and is regulated by intrinsic and/or extrinsic signaling molecules such as lipopolysaccharide, cytokines and growth factors. Upon such stimuli, protein kinases including PKCs are activated and phosphorylate NADPH oxidase subunits, and promote their translocation to the membrane via production of intracellular messenger molecules, such as phosphatidylinositol [66]. When phosphoinositide 3-kinases (PI3K) are activated by signaling from integrin or other receptors for hormones or growth factors in plasma membrane, lipids produced upon the activation of PI3K, such as phosphatidylinositol-3,4-bisphosphate (PI(3,4)P_2) or phosphatidylinositol-3-phosphate (PI(3)P), further activate protein kinases [83]. Activated protein kinase, for instance protein kinase C (PKC), phosphorylates p47phox and p67phox and the cytosolic subunit complex is built. The lipid products of PI3K may also interact with cytosolic subunits p47phox, p40phox, and also Rac-GTP to recruit them to the membrane [66, 68, 84]. Without phosphorylation, p47phox anti-inhibitory region is surface-exposed to prevent the interaction with other cytosolic subunits [63].

Upon stimulation the expression of membrane-bound subunits is induced

by the activation of transcription factors such as NFκB, and upon activation p22phox-gp91phox in intercellular storage sites translocate to the membrane.

The localization of *organizer* p47phox to the membrane brings the *activator* p67phox into contact with *redox core* gp91phox, and also brings the *modulator* p40phox to the complex. Finally, the *regulator* Rac-GTP interacts with gp91phox directly or indirectly and mediate to strengthen the interaction between p67phox and gp91phox, simultaneously *stabilizer* p22phox also strengthens the mutual interaction between subunits.

NADPH oxidase needs GTP-bound form of Rac (Rac-GTP) for its activity. When hydrolyzed by GTPase, which is activated by GTPase-activating protein (GAP) in membrane or cytosol, NADPH oxidase becomes down-regulated.

Various models have been discussed regarding the regulation NADPH oxidase by Rac-GTP. Rac-GTP may (i) anchor to the plasma membrane, and have no gp91phox-regulatory functions but promote the activation of gp91phox by p67phox, (ii) bind to gp91phox directly and attribute to its activation, or (iii) bind to gp91phox but only as a stabilizer of the complex [79].

1.5.3 Phagocytic and non-phagocytic NADPH oxidase

A phagocyte is a cell that ingests and destroys microorganisms or debris via a process known as phagocytosis. The phagocyte utilizes its NADPH oxidase to produce reactive oxygen species with the objective to kill such foreign matter. Reactive oxygen species are important components of cellular signaling, regulation of gene expression, and cell differentiation as well [63]. A cell which possesses NADPH oxidase to produce reactive oxygen species not primarily for phagocytic purpose is called a non-phagocytic cell.

The phagocytes are mainly leukocytes such as monocytes, macrophages, neutrophils, tissue dendritic cells and mast cells. Homologs of phagocytic NADPH oxidase are found in various cells such as fibroblasts, vascular smooth muscle cells, endothelial cells, renal mesangial cells, and tubular cells, and widespread through human body from inner ear, thyroid, colon, kidney blood vessels, lymphoid tissue, to testis [63, 85]. While the nonphagocyte NADPH oxidases are functionally distinct from the phagocyte NADPH oxidases, the structural features of many nonphagocyte oxidase proteins are similar to those of their phagocyte counterparts [86]. However, regulation of non-phagocytic NADPH oxidase doesn't follow the same paradigm established for the phagocytic NADPH oxidase [65], therefore activation mechanisms of non-phagocytic NADPH oxidase are markedly different from that of phagocytic NADPH oxidase

[63].

While phagocytic NADPH oxidase is activated upon stimulation, non-phagocytic NADPH oxidase is constitutively active, but also responds to hormones, growth factors, cytokines, and mechanical stress [85]. Although not involved in defense, non-phagocytic NADPH oxidase shares with phagocytic NADPH oxidase the capacity to transport electrons across the membrane, and produces low amount of superoxide anion under physiological conditions to regulate the cellular function by intracellular or intercellular signaling pathways [79, 85]. The inhibitory responses of non-phagocytic cells to stimuli may differ from that of phagocytic cells, and even enhance NADPH oxidase activity [87].

Abnormal acute and chronic upregulation of non-phagocytic NADPH oxidase results in pathogenesis of diverse diseases such as cancer, cardiovascular disease, atherosclerosis, diabetes, neurodegenerative diseases (Alzheimer's disease and Parkinson's disease), and aging [88].

1.6 "Professional" phagocytes

Leukocytes (white blood cells) play a major role in host defense against both infectious disease and foreign materials, producing high amounts of reactive oxygen species using electron transfer through phagocytic NADPH oxidases. These cells are categorized in three groups, granulocytes (neutrophils, basophils, eosinophils), lymphocytes (B cells, T cells, NK cells), and monocytes/monocyte-derived macrophages. Leukocytes are all produced and derived from a multipotent cell in the bone marrow known as a hematopoietic stem cell which can be diversely differentiated according to the necessity of body regulation. For example, some bacterial infections cause a selective increase in neutrophils, while infections with some protozoa and other parasites cause a selective increase in eosinophils [58].

Phagocytosis involves distinct steps including (i) attachment to receptors, (ii) engulfment with the formation of phagocytic vacuoles, (iii) encapsulation of foreign bodies, (iv) killing or degradation by reactive oxygen species. The main killing mechanism depends on the assembly and activation of NADPH oxidase to produce superoxide anion [89].

When pathogens invade the body, the regulatory cytokines are released by lymphocytes, which induce the recruitment and the activation of phagocytes. Phagocytes migrate into tissue and exhibit chemotaxis to the affected area. The phagocytes assemble NADPH oxidase complexes on the membrane that

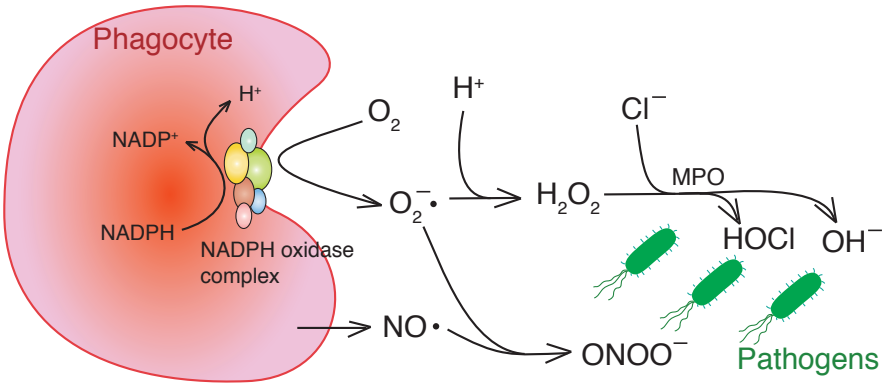

Figure 1.3: Production of reactive oxygen species by phagocytes. Upon activation, phagocytes release superoxide anion and nitric oxide and promote the formation of other radicals such as hydrogen peroxide, peroxynitrite, hypochlorous acid, and hydroxyl radical to kill or degrade pathogens.

catalyze the production of a series of highly toxic reactive oxygen species such as superoxide ($O_2^-\cdot$), hydrogen peroxide (H_2O_2), hypochlorous acid (HOCl), hydroxyl radical (OH^-), nitric oxide ($NO\cdot$), and peroxynitrite ($ONOO^-$) (Fig. 1.3). Once superoxide is produced, it will spontaneously or enzymatically dismute into hydrogen peroxide. Nitric oxide is formed as a product of the conversion of L-arginine to L-citrulline by the constitutive and inducible nitric oxide synthases (NOS) of phagocytes and reacts with superoxide anion to produce another radical $ONOO^-$ in a diffusion controlled reaction [58]. The production of these toxic compounds is accompanied by a transient increase in oxygen consumption by the cells, called respiratory burst. The release of these oxygen-derived radicals acidifies the phagosome, a vacuole formed by phagocytosis, to degrade bacterial cell walls and proteins. Not only superoxide anion, as stated in section 1.5.3, but also other radicals serve as mediators in several physiological responses including the release of proinflammatory cytokines. The secretion of phagocytes are versatile, including polypeptide hormones and enzymes to reactive oxygen species, ranging in molecular mass from 32 (superoxide anion) to 440,000 (fibronectin), showing biological activities ranging from induction of cell growth to provocation of cell death [90]. The release of such products during phagocytosis can lead to chronic inflammation [89].

During phagocytosis, cytosolic granules fuse with the invaginating plasma membrane around the engulfed microorganism to form a phagolysosome into

which they release radicals to create a highly toxic microenvironment. This degranulation normally prevents release of the toxic components into the extracellular environment. However, some targets may be too large to be fully phagocytosed or they avoid engulfment, resulting in frustrated phagocytosis. In this case cells release phagocytic radicals to the extracellular space instead of the intracellular cavity that engulfs the substances to be degraded [91].

Major "professional" phagocytes are neutrophils and macrophages . Their function and the structure of their NADPH oxidase are similar, nevertheless with slight distinctions.

Neutrophils are the most numerous of the leukocytes (ca. 60% of leukocytes) in the human body and provide the first line of defence to infection by ingesting their targets into an enclosed phagocytic vacuole [86, 92]. Though the accumulation of neutrophils and monocytes, the precursor of macrophages, is characteristic for the acute inflammation, the phagocytosis activity of neutrophil is dominant in early stages. Neutrophils exhibit more immediate radical production on stimulation (peaking within 10 minutes, depending on the stimulus), whereas monocyte-derived macrophages gradually increase production of superoxide anion with peak production at ≈ 1 hour that decays over time, but still detectable after several hours [93]. For chronic inflammation the presence of macrophages, monocytes, and lymphocytes is the characteristic feature [91].

Activation agents for neutrophil NADPH oxidase do not necessarily trigger the activation of monocytes/macrophages NADPH oxidase, indicating differential regulation likely through alternative signal transduction pathways. This fact is also reflected in the small difference of their NADPH oxidase structure. Instead of Rac1 in monocytes/macrophages NADPH oxidase, Rac2 is a component of the neutrophil NADPH oxidase [93].

Whereas macrophages will generally survive the severe conditions during killing operation and continue to patrol tissues for other pathogens, neutrophils usually die [58], even get digested by macrophages [94].

Macrophages are categorized in two classes depending on their arena, resident macrophages and inflammatory macrophages. The resident macrophages are constitutively present in tissues where microbial invasion or accumulation of dust is likely to occur, whereas the inflammatory macrophages are differentiated from monocytes circulating in blood, in response to activating stimuli.

Since Ebert and Florey first reported their observation of the monocyte migration from blood vessels into the tissue, developing into macrophages in 1939 [95], the mechanism of this monocyte differentiation into macrophages has

been widely investigated. The elucidation of this differentiation mechanism is a key to understand the mechanism of diseases like atherosclerosis. When monocytes differentiate into macrophages, they localize in the subendothelium and begin to accumulate lipid due to the change in lipid metabolism through cell-mediated oxidation of low-density lipoprotein (LDL) in macrophages [96]. This lipid grows gradually to atheromatous plaque [97].

Circulating monocytes can be differentiated either to macrophages or dendritic cells, depending on stimulation. Specific cytokines or growth factors alone or in different combination switch the differentiation of monocytes to macrophages or dendritic cells [98]. The macrophages and the dendritic cells are both antigen-presenting cells, that possess antigen material on their surface. The dendritic cells show much higher level antigen presentation and play an important role in mediating immune cell communication by direct contact of cell-surface proteins or secreting cytokines, the latter may recruit activated macrophages to allow phagocytosis. In contrast to macrophages, dendritic cells are able to induce primary immune responses from naive T cells to novel antigens in human [99].

Macrophages respond to both specific and nonspecific stimuli [89] and their activation passes two steps. In the first "primed" stage, which can be induced by interferons, interleukins, or growth factors, macrophages exhibit enhanced surface antigen presentation and oxygen consumption, but reduced proliferative capacity. In the second "activated" stage, which can be induced by LPS, bacteria, growth factors, or PMA, macrophages show inability to proliferate, high oxygen consumption through NADPH oxidase, killing facultative and intracellular parasites, tumor cell lysis, and maximal secretion of mediators of inflammation such as TNF-α, interleukins, and reactive oxygen species and nitric oxides [91].

1.7 Objective of this thesis

Our project aimed at an electrical energy source using living human cells. The transmembrane electron transfer to extracellular space is a preferable candidate to harvest electrons from living cells. One of the strongest electron transfers is seen during phagocytosis, where excessive oxygen uptake is observed to produce superoxide anion by single-electron reduction of oxygen. The production of electrons is catalyzed by NADPH oxidase, a transmembrane protein with

electron transport mechanism. When pathogens intrude into the human body, signal transduction is triggered via diverse intercellular/intracellular secretory substances, which activate NADPH oxidase in phagocytes.

This thesis embarked on examining the feasibility of a biofuel cell utilizing the electron transfer mechanism of NADPH oxidase in phagocytes. In host defense, monocyte-derived macrophages are one of the strongest phagocytes contributing to both acute and chronic inflammation and show prolonged activated state compared to other phagocytes. Therefore monocytes were employed for the operation of our biofuel cell in this thesis project. By using monocytes, the mimicry of the interaction of monocytes to the invaded site was also realized.

Human monocytic cells THP-1 were chemically stimulated to undergo differentiation into macrophages and then activate their NADPH oxidase. The cells seeded on a plain gold electrode generated current in a biofuel cell setup upon activation. Series of inhibitory tests proved the NADPH oxidase was a source of the current generation in the biofuel cell. The analysis of these tests showed the contribution of superoxide anion to the electron transfer between the cells and the electrode. This analysis also indicated the existence of another mediating factor of the electron transfer.

Chapter 2

Assay Development

2.1 Cells

NADPH oxidase is a transmembrane protein with electron transfer function and present in a variety of cells, whereas its strongest activity is seen in professional phagocytes. Since monocyte-derived macrophages are present in both acute and chronic inflammation and possess prolonged phagocytic activity, these cells are suitable candidates for our examination of the current generation by living human cells. Due to high variation in physiological activity of primary cells, testing with a cell-line cells is reasonable.

Throughout this thesis the human monocytic cell line THP-1 was used for experiments. THP-1 cells were derived from peripheral blood of a 1-year old boy with acute monocytic leukemia [100] and resemble the human monocytes with respect to numerous criteria such as morphology, secretory products, oncogene expression, expression of membrane antigens, and expression of genes involved in lipid metabolism [97]. THP-1 cells appear to be blocked at a relatively late stage of differentiation [100] but still exhibit metabolic and morphological similarities to human monocytes [101]. This cell line can be easily differentiated to macrophages by phorbol esters such as phorbol 12-myristate 13-acetate (PMA), active vitamin D compound, retionic acid, or cytokines (tumor necrosis factor-α (TNF-α), interferon-γ (IFN-γ)).

Although the states of differentiation of THP-1 induced by various agents may differ [101], differentiated THP-1 cells, in general, demonstrate the characteristics of mature macrophages like the expression of adhesion molecules, such as inter-cellular adhesion molecules (ICAM) and vascular cell adhesion molecules (VCAM), or phagocytic capacity. It is also reported that differentiated THP-1 cells behave more like native monocyte-derived macrophages compared to other

human myeloid cell lines, such as HL-60, U937, KG-1, or HEL cell lines [97].

Therefore, THP-1 cells represent a useful model for differentiation studies of human monocytes, and as an in vitro model of human macrophages in studies of macrophage involvement in inflammatory functions, including diseases such as atherosclerotic processes [101].

2.2 Cell stimulation

2.2.1 Chemicals

NADPH oxidase is known to be activated by receptor-mediated and receptor-independent protein kinase C stimuli, such as opsonized zymosan (OPZ), formyl-methionyl-leucyl-phenylalanine (fMLP), active vitamin D compound, or phorbol 12-myristate 13-acetate (PMA). Also various cytokines regulate the activity of NADPH oxidase. Lipopolysaccharide (LPS) is another commonly used stimulus which mimics the presence of bacteria or their fragments. Other extracellular signaling molecules which bind to receptors in the plasma membrane, such as C5a, C3b or iC3b, may trigger some part of the NADPH oxidase activation as well. [97, 102].

PMA is commonly used as an artificial stimulator to induce the NADPH oxidase activity in leukocytes. PMA activates protein kinase C (PKC) receptor-independently via phosphotidyl inositol-3 kinase (PI3K) signaling pathway [63, 66], which regulates transcription factors, cell proliferation, growth, differentiation, and apoptosis [89]. For phagocytosis, this signaling pathway is known to activate the production of reactive oxygen species through the potentiated expression of p40phox and p47phox [89]. Indeed, the up-regulation of the expression of p47phox by PMA stimulation has been reported together with the fact that this stimulus induces the phosphorylation of p22phox in monocytes [103]. PMA increases the expression of cytokines and monocyte differentiation antigens as well [101]. In the presence of PMA, THP-1 cells stop proliferation and demonstrate macrophage-like morphology, attaching and spreading on the substrate [101]. A respiratory burst could be induced in THP-1 cells with a direct protein kinase C activator such as PMA, but not with chemokines alone [104].

OPZ is a serum-coated yeast cell wall, a mimicry of a yeast pathogen, and activates calcium-dependent PKC and cytosolic phospholipase A2 (cPLA2) pathways [93, 105]. Like PMA, OPZ produces a strong, continuous NADPH oxidase activity, with a pronounced lag phase. The activity of NADPH oxidase

upon OPZ sitmulation, however, sustains shorter compared to PMA stimulation [106].

Another PKC activator is fMLP. fMLP is derived from bacterial protein degradation or from mitochondrial proteins upon tissue damage [107]. Stimulation of the fMLP receptor activates the PKC and induces calcium flux receptor [108]. fMLP is a strong chemoattractant and induces adherence of phagocytes as well [107]. Compared to the NADPH oxidase activity induced by PMA which is long-lasting and very intensive, fMLP induces milder NADPH oxidase activity [106].

Active vitamin D compound, 1,25-$(OH)_2D_3$, is known to promote the induction of monocytic differentiation to macrophages [109]. Using a signal transduction pathway completely different from PMA [97], active vitamin D compound increases the antigen-presenting activity of macrophages and the production of immunoregulatory molecules such as cytokines. Although active vitamin D compound enhances the production of PKCs and superoxide anion comparable to PMA [110], this was less effective on loss of proliferation and adhesion of the cells [111], since active vitamin D compound decreases the production of pro-inflammatory cytokines and promotes the production of anti-inflammatory cytokines [112].

LPS is a major component of the outer membrane of Gram-negative bacteria and so is a pathogen-associated immunostimulant. Binding to the receptor complex (TRL/CD14) of phagocytes, LPS activates NF-κB signaling pathway and promotes the secretion of pro-inflammatory cytokines, especially TNF-α, and growth factors [89, 113, 114] and primes phagocytes to produce radical oxygen species [115]. Stimulating phagocytes with LPS in combination with PMA intensifies the secretion of pro-inflammatroy cytokines drastically [116]. It is also reported that LPS, in combination with fMLP, enhances the expression of cytosolic NADPH oxidase subunits, p47phox, p67phox and Rac, however, simultaneously limits the phosphorylation of p47phox [115].

Cytokines are signaling molecules essential for cellular communication. For host defense cytokines are secreted by damaged or inflamed tissue and local endothelial cells, and are sources of chemoattractant causing phagocytes to become polarized and crawl toward the affected sites [58]. Cytokines are categorized into pro-inflammatory and anti-inflammatory cytokines. Both are necessary for the regulation of the immune function. Phagocytes themselves also secret cytokines as signaling in autocrine and paracrine network. It is reported that many cytokines alone do not induce differentiation of phagocytes, however, the combination of different cytokines may mimic the full spectrum of activity

induced by PMA [97].
Interleukins (IL) are a group of cytokines that are involved in defense mechanism. IL-1α and -β, pro-inflammatory cytokines produced by macrophages, monocytes and dendritic cells increase the expression of adhesion molecules to enable transmigration of leukocytes [117].
Macrophage colony-stimulating factor (M-CSF) is a cytokine produced by a variety of cells inducing lymphocytes, monocytes, fibroblasts, endothelial cells, myoblasts and osteoblasts. This cytokine regulates cellular proliferation, differentiation, and survival of blood monocytes, tissue macrophages, by inducing cytokine and protease secretion. In monocytes and macrophages M-CSF induces the synthesis of cytokines such as IL-1, granulocyte-colony stimulating factor (G-CSF), IFN, TNF and also oxidative metabolism [118]. Combinations of IFN-γ and M-CSF resulted in enhancement of the expression of pro-inflammatory cytokines such as IL-1β and TNF-α and of intercellular adhesion molecule-1 (ICAM) and vascular cell adhesion molecule-1 (VCAM) in THP-1 cells [117].
IFN-γ is produced predominantly by natural killer (NK) cells and T cells once antigen-specific immunity develops. The production of IFN-γ is controlled positively and negatively by cytokines secreted by antigen-presenting cells [119]. IFN-γ is known to promote the upregulation of cell adhesion molecules (ICAMs and VCAMS) via Janus kinase-signal transducers and activators of transcription (JAK-STAT) signaling pathway [58]. This stimulus also shows growth-inhibitory effect in phagocytes by activating STAT signaling pathway, whose contribution to the cell differentiation process is well known. Macrophages stimulated with IFN-γ upregulate receptors bind to extracellular pathogens [119]. The increase of the cytokine production was also observed if the IFN-γ was combined with TNF or IL-2 [117]. IFN-γ also enhances the expression of subunits of NADPH oxidase. The upregulation of gp91phox [119–121], p67phox expression [63, 119], and expression of p47phox [122] have been observed.
TNF-α is synthesized mainly by macrophages in response to an effective stimulus such as LPS or different cytokines including IFN-γ and interleukins [113]. TNF-α is one of the earliest major pro-inflammatory mediators [113, 123] and is involved in activation of NF-κB and MAPK pathways. Through the activation of these pathways TNF-α potentiates the mRNA expression of NADPH subunits (p47phox, p67phox, and gp91phox) [124]. Besides the regulation of immune function, this cytokine also induces apoptosis.
Another commonly used cytokine for cell activation is transforming growth factor β1 (TGF-β1). This stimulus inhibits proliferation and promotes differentiation

of THP-1 [125], though this protein is also known to inhibit the secretion and activity of many other cytokines and suppress inducible nitric oxide synthase (iNOS) with other immunosuppressive action in macrophage [126].

Based on the information above, the use of PMA, IFN-γ/TNF-α and LPS for the activation of THP-1 cells was examined.

Although PMA is an artificial stimulus, the activation level of NADPH oxidase is greater than other PKC activators. Synergistic effects of the combination of IFN-γ with TNF-α on upregulation of NADPH oxidase system in monocytes [120, 127] and on activation of NF-κB pathway in macrophages [123] have been reported. These are reflected by the enhancement of superoxide anion release from IFN-γ /TNF-α primed cells upon PMA stimulation [127].
Moreover, stimulating phagocytes with PMA and LPS enhances the secretion of IFN-γ/TNF-α profoundly [116].

2.2.2 Method of stimulation

For proving the principle of a biofuel cell system with human cells, high cell activity is desired to obtain high signal to noise ratio in the current measurement. Since a high level of superoxide anion production is a clear indication of phagocytic activity, an optimal cell stimulation protocol was searched, which allows cells to produce superoxide anion in high amount and for a prolonged period of time. The combination of stimuli, the order of stimulation, and the concentration of stimuli were examined.

First, THP-1 cells were treated with each stimulus and changes were visually observed under the light microscope (Fig.2.1). When cells were stimulated with PMA alone or combined with other stimuli, the morphological change of the cells such as elongation and spread, which are the typical feature of monocyte differentiation into macrophage, was seen. On the cytokine stimulation the cells exhibited cluster formation and slight adherence to culture wells. In both cases cell proliferation was suppressed, while PMA had a stronger effect. LPS stimulation did not cause any change in cell morphology and proliferation.

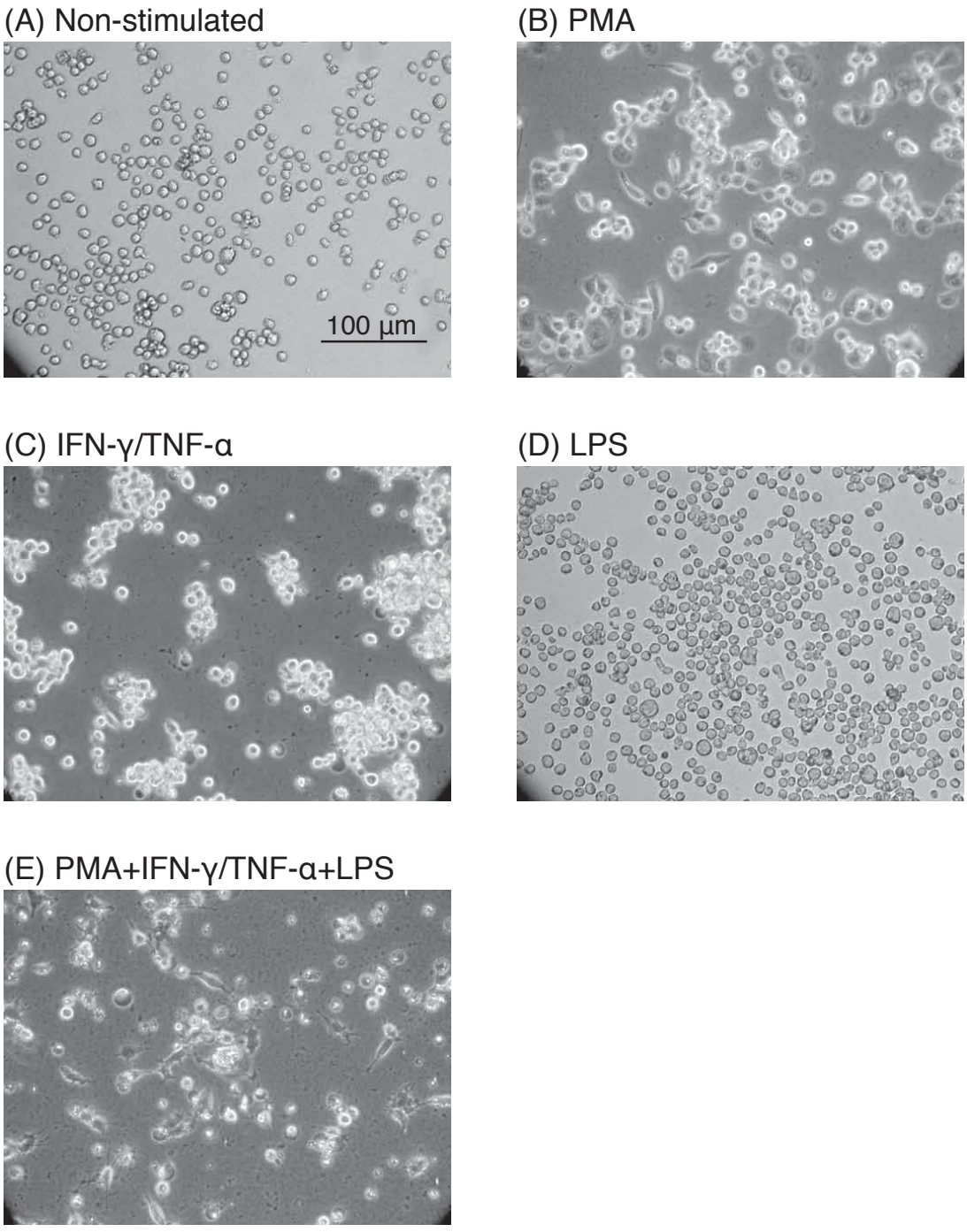

Figure 2.1: Morphological change of THP-1 cells on different stimuli after 1 day. (A) THP-1 cells before stimulation. The cells were incubated in culture media containing (B) 50 nM PMA, (C) 20 ng/ml IFN-γ and 20ng/ml TNF-α, (D) 300 ng/ml LPS, (E) all stimuli together. Images were acquired with Zeiss Axiovert 40CFL light microscope with 20$\times$ objective. (B,C,E) were obtained in phase contrast mode.

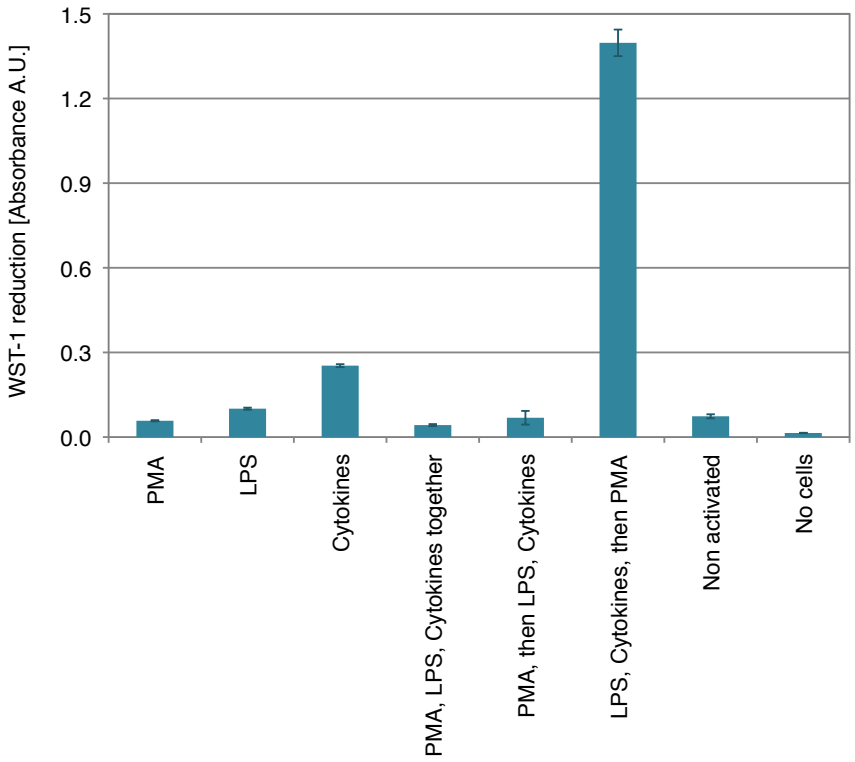

Figure 2.2: Superoxide anion production from THP-1 cells upon different stimulation methods. The standardized protocol is described in Section 2.5.3. Superoxide anion production was measured by the amount of reduced WST-1 using a spectrophotometer. The cells were incubated in culture media with stimulation of (from left to right) PMA; LPS; IFN-γ/TNF-α; PMA + LPS + IFN-γ/TNF-α all together; first PMA then LPS + IFN-γ/TNF-α were added before the measurement of superoxide anion; first LPS + IFN-γ/TNF-α then PMA was added before the measurement of superoxide anion; no stimuli; the most right sample did not contain cells but all stimuli. The concentration of each stimulus used was: PMA 50 nM, 20 ng/ml IFN-γ, 20ng/ml TNF-α, 300 ng/ml LPS. The experiment was performed once in duplicate.

Secondly, superoxide anion production from the cells after different stimulation was examined (Fig. 2.2). The single use of either PMA or LPS did not induce high superoxide anion production. Only the combination of cytokines, IFN-γ and TNF-α induced low amount of superoxide anion production. Strong enhancement in superoxide anion production was achieved when the cells were stimulated first with LPS, IFN-γ and TNF-α, thereafter with PMA. This result did not correspond to previously reported evidence reported that THP-1 cells were activated with PMA alone for superoxide anion release [111, 128, 129]. Even longer incubation with PMA did not induce significant superoxide anion release

from THP-1 cells in our experiments.

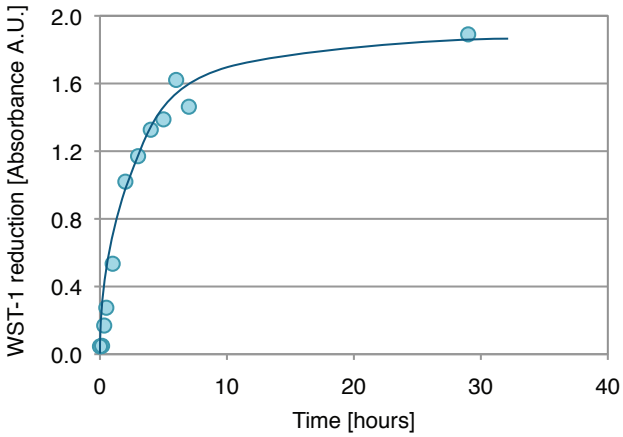

Figure 2.3: Time course study of superoxide anion production from activated THP-1 cells. After differentiation with 20 ng/ml IFN-γ, 20ng/ml TNF-α and 300 ng/ml LPS in the culture media, cells were incubated with 50 nM PMA in HBSS containing 100 μM WST-1 for different time periods and the supernatants were collected for the superoxide anion measurement.

Additionally the temporal pattern of the superoxide anion production from the cells was investigated by collecting samples at different time points during the activation. As shown in Fig. 2.3, when the cells were pre-incubated with LPS, IFN-γ and TNF-α, the superoxide anion production after adding PMA exhibited a rapid increment, suggesting that THP-1 cells were differentiated into macrophage-like cells on the stimulation with LPS, IFN-γ and TNF-α, and were further triggered to release superoxide anion only on PMA stimulation. Thus, throughout this thesis, THP-1 cells were stimulated by LPS together with IFN-γ and TNF-α for differentiation, and then by PMA for activation.

Next, the optimal concentrations of each stimulus for the activation of THP-1 cells were examined. Since an excess of stimulus could induce reverse effects, the minimum amount sufficient for full activation of the cells was adopted.

The concentration of LPS did not have strong a effect on the superoxide anion production from the cells (Fig. 2.4). However, the stimulation with higher concentration of LPS tended to induce more superoxide anion production from cells, and when the cells were stimulated without LPS, sometimes less morphological change in the cells was seen. In this thesis, 300 ng/ml of LPS was used for the cell stimulation.

The concentration of different cytokines also influenced the superoxide anion

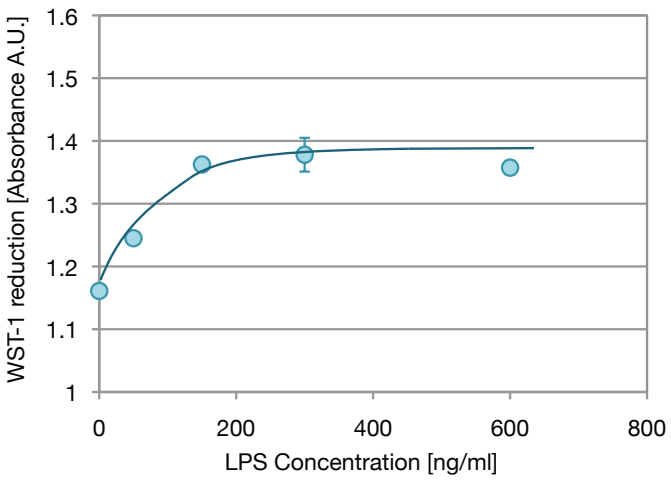

Figure 2.4: Effect of different LPS concentrations on THP-1 activation. The standardized procedure is described in Section 2.5.3. In brief, after cell stimulation with LPS, 20 ng/ml IFN-γ and 20 ng/mlTNF-α for 2 days, cells were incubated with 50 nM PMA in HBSS containing 100 μM WST-1 for 4 hours. The superoxide anion production was measured by the absorbance of the supernatant. The LPS concentrations examined were 0, 50, 150, 300, 600 ng/ml. The experiment was performed once in duplicate.

release from THP-1 cells (Fig. 2.5). At low concentration of IFN-γ, a change in the concentration of TNF-α caused no difference in superoxide anion production. When the concentration of IFN-γ was increased, higher concentration of TNF-α enhanced the cell activity. Thus, as a default, we used 20 ng/ml of both IFN-γ and TNF-α for our cell stimulation.

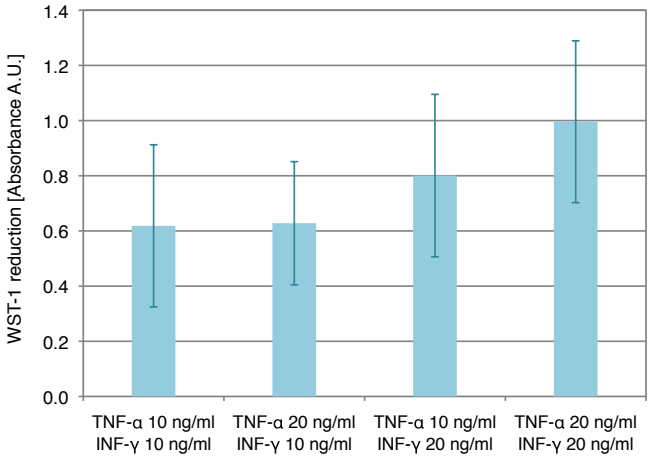

Figure 2.5: Effect of different concentrations of TNF-α and IFN-γ on THP-1 activation.The standardized procedure is described in Section 2.5.3. In brief, after cell stimulation with 300 ng/ml LPS, IFN-γ and TNF-α for 2 days, cells were incubated with 50 nM PMA in HBSS containing 100 μM WST-1 for 4 hours. The superoxide anion production was measured by the absorbance of the supernatant. Three independent experiments were conducted.

If PMA was used as the only stimulus for the activation of THP-1 cells, with the elevation of PMA concentrations, gradual increase of cell elongation or cell spreading was observed (Fig. 2.6), which are features of the differentiation of monocytes into macrophages. According to the level of the morphological change, we set the lowest concentration of PMA at 50 nM to examine the superoxide anion production from the cells.

Apparently the superoxide anion production was not influenced by the PMA concentration (Fig. 2.7). Thus, we concluded that 50 nM of PMA represents the level necessary for the maximum activation of the cells.

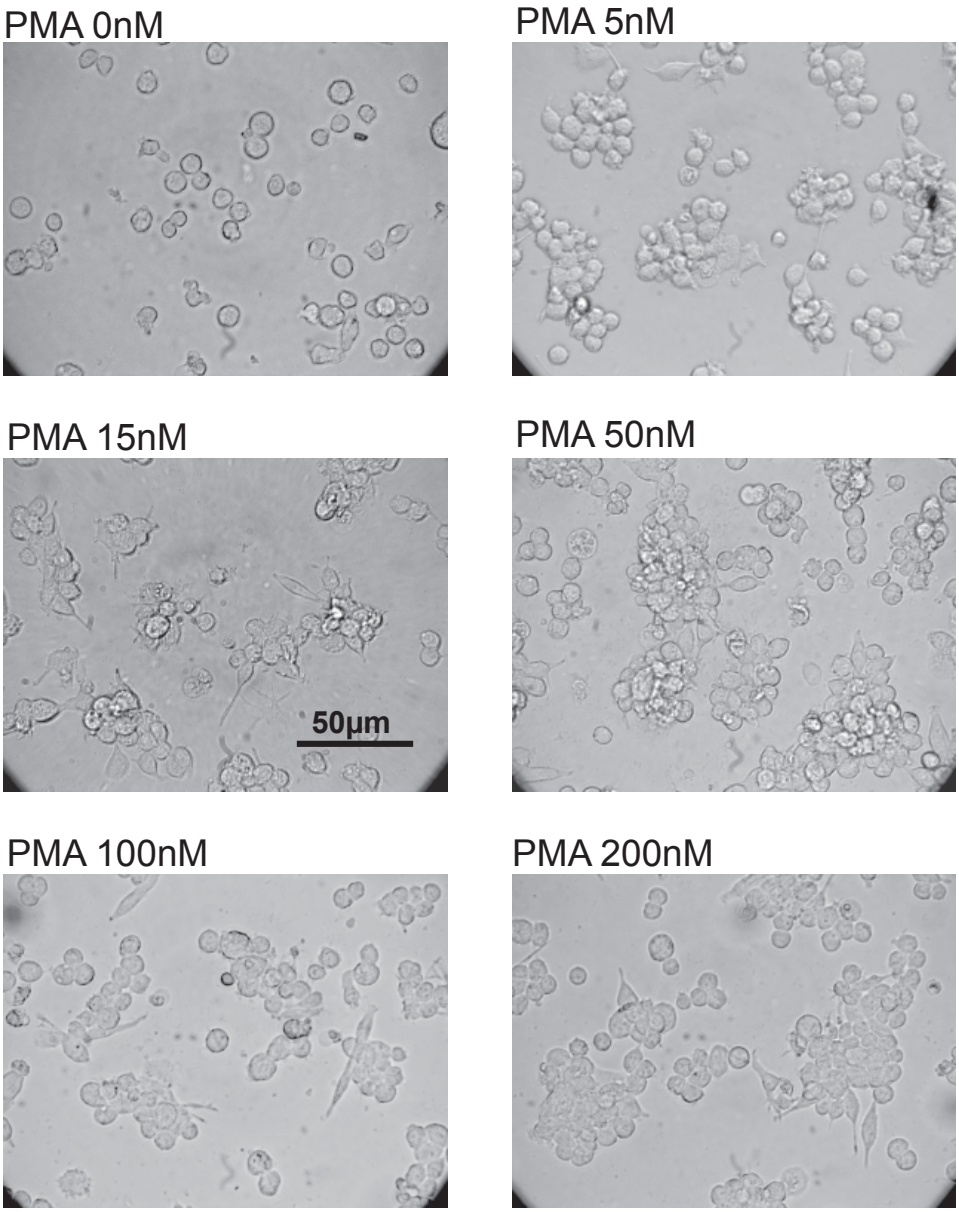

Figure 2.6: Morphology change in THP-1 resulting from different PMA concentrations. Cells were treated with PMA at corresponding concentration for 48 h. Images were acquired with Zeiss Axiovert 40CFL light microscope with 40× objective.

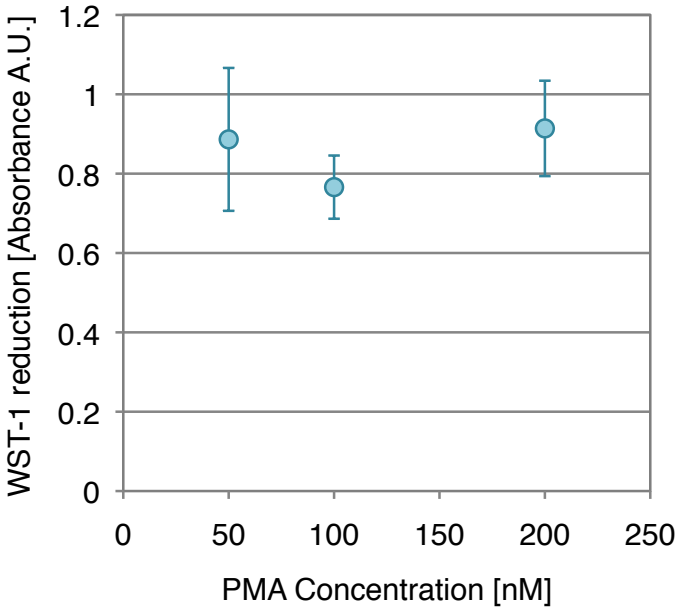

Figure 2.7: Effect of different PMA concentrations on THP-1 activation. The standardized procedure is described in Section 2.5.3. In brief, after cell stimulation with 300 ng/ml LPS, 20 ng/ml IFN-γ and 20 ng/ml TNF-α for 2 days, cells were incubated with PMA in HBSS containing 100 μM WST-1 for 4 hours. The superoxide anion production was measured by the absorbance of the supernatant. The PMA concentrations examined were 50, 100, 200 nM. Two independent experiments were carried out.

2.3 Detection of superoxide anion

Activity of NADPH oxidase can be detected by (i) oxygen consumption, (ii) superoxide anion production, or (iii) production of oxygen-derived radicals such as hydrogen peroxide.

Because oxygen is a substrate of NADPH oxidase, the level of oxygen consumption increases with the NADPH oxidase activity of the cells. However, any increase in consumption of oxygen by mitochondria would lead to inflated estimates of NADPH oxidase activity, which has caused large errors, especially in the measurement with monocytes [75].

Superoxide anion is negatively charged, non permeable through the plasma membrane, and unstable in aqueous solution. Hydrogen peroxide is membrane permeable and relatively stable, thus it is easy to measure. Though both radicals are detectable by chemiluminescence, this method is difficult to quantitate correctly. Furthermore, in a system with an electron donor such as NADPH or NADH, secondary generation of superoxide anion occurs through the reaction of the electron donor with reagents, inducing positive error in the measurement [130, 131].

A method to detect superoxide anion directly is using electron spin resonance (ESR). This spectroscopic method detects unpaired electrons excited by magnetic resonance and offers specificity and the sensitivity despite the brief life time of superoxide. However, it requires a rather expensive apparatus and complex experimental setup.

The colorimetric assay using chemical dyes that can be reduced by superoxide anion is facile, and therefore currently a popular method for superoxide anion detection. Since the reduction of these dyes by superoxide anion is not specific, superoxide dismutase (SOD) can be used as a control for the detection of superoxide anion [130]. The use of SOD automatically dismisses the method to detect hydrogen peroxide, since SOD is an enzyme that catalyzes the spontaneous reaction of superoxide anion to hydrogen peroxide.

The common colorimetric assay is using ferricytochrome c [132].

Cytochrome c $(Fe^{3+}) + O_2^- \cdot \longrightarrow$ cytochrome c $(Fe^{2+}) + O_2$

This method takes advantage of the enhanced absorption of cytochrome c at 550 nm when reduced. The sensitivity of this method suffers from the narrow bandwidth of the absorbance peak of reduced cytochrome c [133] and the poor signal to noise ratio due to high background absorbance of the oxidized state (Fig.2.9). Interference is also known from redox cycling reactions which themselves generate superoxide anion [130] or reoxidization of reduced cytochrome c

via derivatives of superoxide anion, hydrogen peroixde or peroxynitrite [134].

Another widely used reagent is nitro blue tetrazolium (NBT). NBT is reduced to a corresponding formazan which exhibits high absorbance in 560 nm [131]. However, the reduced product is insoluble and the intermediate product, a radical, may reduce oxygen to superoxide anion that disturbs accurate measurements [130].

Although newer synthesized tetrazolium salt, XTT (2,3-bis(2-methoxy-4-nitro-5-sulfophenyl)-5-((phenylamino)carbonyl)-2H- tetrazolium hydroxide), yields water soluble formazan in reduced form [135], this method loses the sensitivity with lowering pH by SOD inhibition and in the physiological pH their sensitivity is less than NBT [131].

WST-1 (2-(4-Iodophenyl)-3-(4-nitrophenyl)-5-(2,4-disulfophenyl)-2H- tetrazolium, monosodium salt) is membrane-impermeable, therefore can be reduced to its soluble formazan extracellularly by plasma membrane NADPH oxidase [135]. Compared to cytochrome c, it exhibits extremely low background (Fig. 2.9) and high sensitivity due to its low molecular mass and the high molar extinction coefficient of the reduced formazan [136]. Moreover, unlike cytochrome c, WST-1 does not interfere with hydrogen peroxide, a derivative of superoxide anion after its spontaneous dismutation [136].

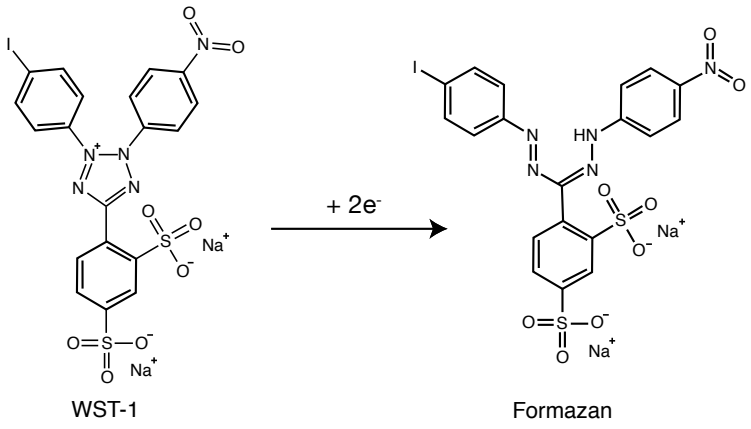

Figure 2.8: WST-1 can be converted to a water-soluble formazan through two electron reductions.

To observe NADPH oxidase activity via superoxide anion production, we employed a colorimetric assay using WST-1.

The concentration of WST-1 used in the assay was determined by testing the absorbance when WST-1 was completely reduced (Fig. 2.10). WST-1 diluted in UHQ water and HBSS in different concentrations was completely reduced

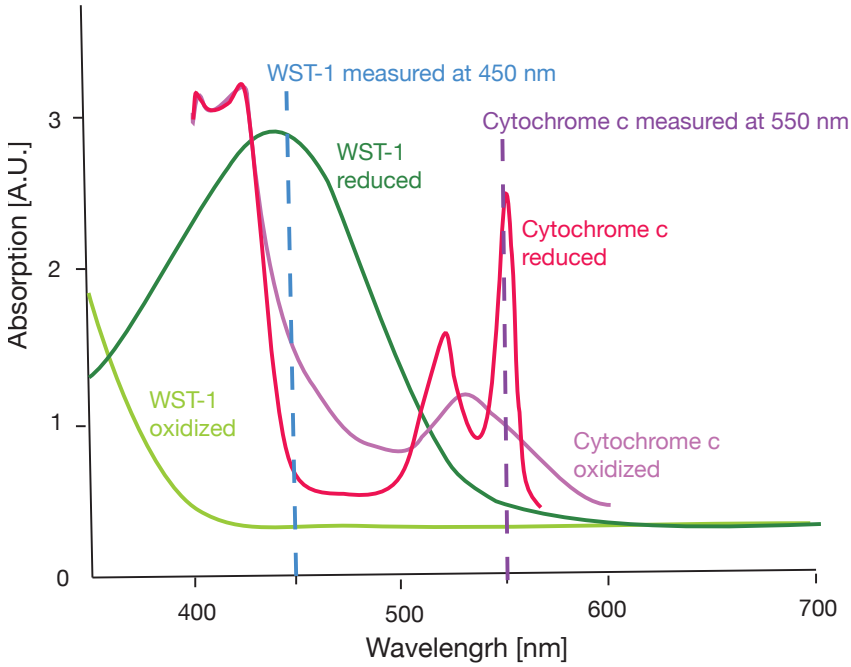

Figure 2.9: Spectral scan of WST-1 and cytochrome c both in oxidized and reduced form. 100 μM WST-1 or 33μM cytochrome c diluted in HBSS was reduced by sodium dithionite completely. Schematic diagram based on measurements.

by sodium dithionite and the absorbance of the solution was measured with spectrophotometer at 450 nm.

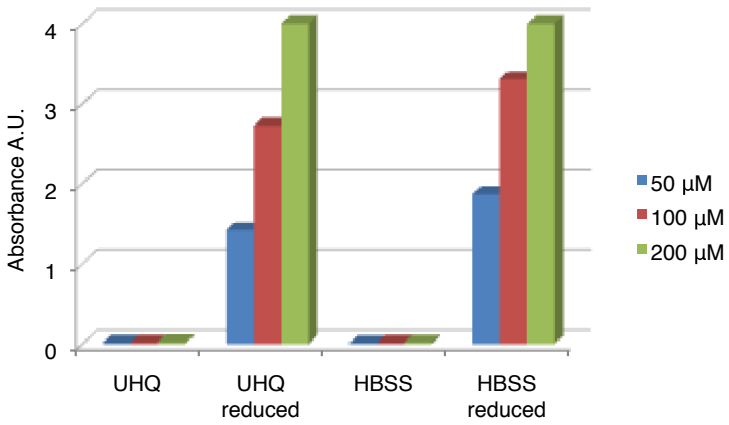

Figure 2.10: Absorbance of reduced WST-1 in different concentrations. WST-1 diluted in UHQ water and HBSS at the concentration of 50 μM, 100 μM, and 200μM, was fully reduced by sodium dithionite and the absorbance was measured.

As a control, the reduction of both WST-1 and cytochrome c by superoxide anion produced from activated THP-1 was compared. The procedure is precisely described in Section 2.5.3, except that cytochrome c was also employed parallel to WST-1 as a detector in the same manner.

Although the absorbance of cytochrome c in the oxidized state caused high background as expected, both the reduction of WST-1 and cytochrome c showed the same tendencies between the activated cells with/without SOD, and non-activated cells (Fig. 2.11).

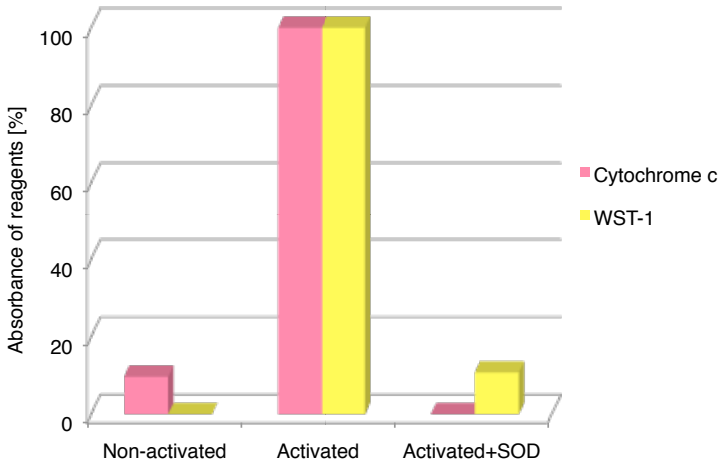

Figure 2.11: Comparison of superoxide anion detection using cytochrome c and WST-1. The reduction of reagents refers to the spectrophotometric absorbance normalized to the value of activated cells (vs. nonactivated cells). The stimulation of the cells is described in Section 2.5.3. The superoxide anion production was measured colorimetrically using either 33μM cytochrome c or 100 μM WST-1 at 550 nm or 450 nm, respectively. For inhibitory tests with SOD, the cells were pre-incubated with 118 U/ml SOD before activation.

Therefore, for our study, WST-1 provided us with a superoxide anion detection method comparable to other reports using cytochrome c.

Since WST-1 was slightly reduced when incubated in the culture media, the components in the culture media may have caused the reduction of WST-1 (Fig. 2.12). To avoid this interference, the incubation media used for cell stimulation was replaced with Hank's buffer salt solution (HBSS) before the measurement of NADPH oxidase activity by WST-1.

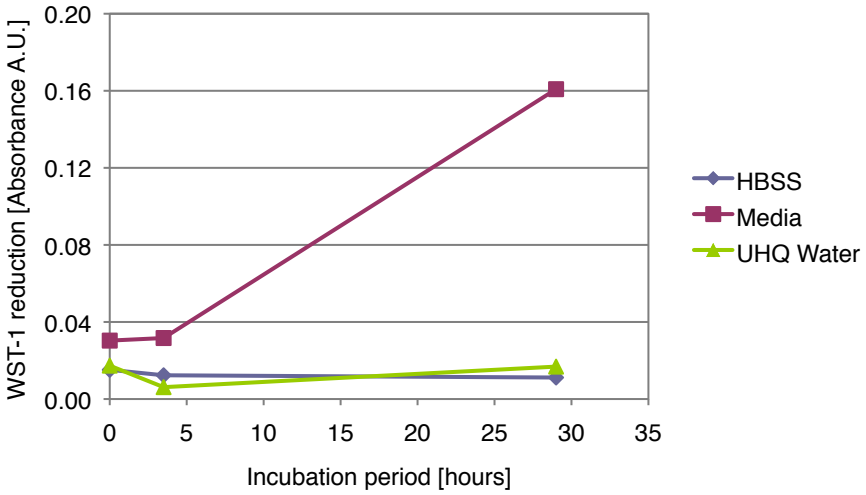

Figure 2.12: Effect of solvent on WST-1 reduction. Culture wells were filled with the RPMI1640 media (without phenol red), HBSS, and UHQ water. 200 μM WST-1 was added in each well. After 0h, 4h, and 29h of incubation, the absorbance of each fluid was measured with the spectrophotometer at 450 nm.

To examine the feasible range of WST-1 colorimetric assay for the superoxide anion production from activated cells, a preliminary test using hypoxanthine/xanthine oxidase was conducted[1]. Superoxide anion ($O_2^- \cdot$) was generated from the conversion of hypoxanthine to uric acid by xanthine oxidase [137]. From 1 mol hypoxanthine the production of 2 mol superoxide anion is expected (Table 2.1, *B*).

$$\text{Hypoxanthine} + O_2 + H_2O \longrightarrow \text{Xanthine} + O_2^- \cdot + H_2O_2$$

$$\text{Xanthine} + O_2 + H_2O \longrightarrow \text{Uricacid} + O_2^- \cdot + H_2O_2$$

For the measurements, hypoxanthine dissolved in UHQ water was diluted in PBS containing 100 μM WST-1 to a final volume of 1.5 ml. To initiate the reaction, 100 mU/ml xanthine oxidase was added and the solution was mixed by pipetting. After 60 min the absorbance of WST-1 formazan was measured with a spectrophotometer at 450 nm (Table 2.1, *C*).

The reduction of WST-1 increased with increasing the superoxide anion production in the system (Fig. 2.13). However, the linearity of the WST-1 reduction and the superoxide anion production was lost above the absorption value read on the spectrophotometer of 3. In the measurements of WST-1 reduction by superoxide anion released from activated macrophages, the absorption value

[1] I gratefully thank Claudia Küttel for her collaboration.

Hypoxanthine [μM] *(A)*	$O_2^- \cdot$ produced from hypoxanthine [nmol/1.5 ml] *(B)*	Absorbance [A.U.] *(C)*
10	30	0.127
50	150	0.574
100	300	1.212
200	600	2.66
500	1500	3.663

Table 2.1: Superoxide anion production from hypoxanthine and its detection by WST-1 reduction. Dissolved hypoxanthine was converted by xanthine oxidase into uric acid producing superoxide anion in UHQ containing 100 μM WST-1. After 60 min of reaction time, the reduction of WST-1 was measured with a spectrophotometer at 450 nm.

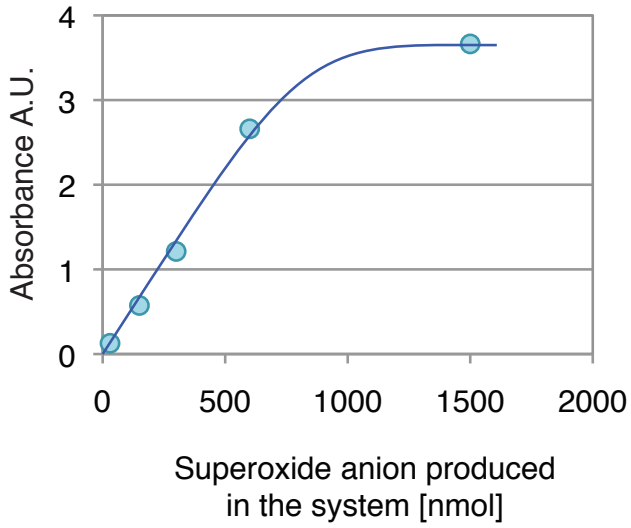

Figure 2.13: Absorbance of reduced WST-1 depending on the amount of superoxide anion production in hypoxanthine/xanthinoxidase system.

read on the spectrophotometer was consistently lower than 3 throughout this thesis, thus linearity between the spectrophotometric measurement value and superoxide anion production from cells was fulfilled.

2.4 Biofuel cell setup

2.4.1 Architecture of biofuel cell setup

To determine the architecture of the fuel cell setup, the designs of microbial fuel cells was studied. In microbial fuel cells a two-chamber system is widely used,

since this system does not require expensive catalysts. The characteristic feature of a two-chamber system is the membrane. The membrane serves as a separator of chambers and is usually a cation exchange membrane. The performance of such a membrane is evaluated by the rate of proton transfer. Good performance of the membrane, i.e. good proton transfer through the membrane, results in the low ohmic losses and raises the electrical yield of the whole system. Nafion is a sulfonated tetrafluoroethylene based fluoropolymer-copolymer developed by DuPont. Due to its unique ionic properties it permits effective hydrogen ion transport while preventing electron conduction. Therefore Nafion based cation exchange membranes are commonly used for conventional and microbial fuel cells. The drawback of Nafion relates to its excess of protons. A preliminary test with HBSS buffer with phenol red showed the immediate lowering of pH in the anodic fluid by Nafion. Moreover, the active protonated residue can easily be replaced by other positively charged species such as sodium or potassium ions, present at high concentration (10^5 times more than protons) in cell culture media or buffer. In this case, Nafion preferably transports these positively charged species instead of protons, affecting the performance of the whole setup. Thus the use of Nafion membrane for our experiment was excluded. Another cation exchange membrane examined is sold by BDH (BDH 55165, VWR International Ltd.). The technical data of this membrane is unfortunately not available. The performance test using a proton exchange fuel cell (the anodic compartment was filled with pressured hydrogen gas, the cathode was exposed to air for oxygen reduction) showed that the proton exchange of the BDH membrane was ca. 10 % of that of a Nafion membrane (Conductivity of BDH membrane was 0.01 S/cm, while that of Nafion membrane was 0.083 S/cm[2]). Nevertheless, the BDH membrane did not exhibit acidification of the anodic fluid. Thus this membrane was used for the current measurement throughout this thesis.

In the cathodic compartment the protons transferred through the membrane react with dissolved oxygen, the final electron acceptor in the cathodic compartment. The electron flowing from the anode through an external resistor to the cathode participate in this reaction [138].

$$H^+ + O_2 + e^- \longrightarrow H_2O$$

To promote this reaction, oxygen has been purged in the cathodic compartment [139, 140], or the graphite electrode has been modified with platinum for better catalytic activity [141].

[2]I gratefully thank Xun Wei for the measurement and the Paul Scherrer Institut for providing the experimental equipment.

Instead of using dissolved oxygen in the cathodic fluid, the cathode can be placed in direct contact with air. This replacement of the oxygen source increased the power density in microbial fuel cells [142]. The use of the membrane for air cathode system prevents the oxygen diffusion into the anodic compartment, increasing the Coulomb yield at the anode as well [6].

Ferricyanide $[Fe(CN)_6]^{-3}$ is also commonly used as an electron acceptor in the cathodic chamber.

$[Fe(CN)_6]^{-3} + e^- \longrightarrow [Fe(CN)_6]^{-4}$

The reduced product ferrocyanide is reoxidized to ferricyanide. Since the regeneration of the ferricyanide is very slow limiting the sustainability of the cathodic compartment, the use of ferricyanide is not useful in practice. Nonetheless the highest power densities so far in microbial fuel cells have been reported using ferricyanide in the laboratory use [6], due to its good performance lowering the internal resistance in the system [19]. Thus, the current measurements in this thesis were conducted in a two-compartment fuel cell system using ferricyanide as an electron acceptor in the cathodic compartment.

2.4.2 Selection of electrode material

The electrode for a biofuel cell should fulfill certain conditions regarding conductivity and biocompatibility. Additionally, as discussed in Section 2.2.2, obtaining higher signal from cells is preferred.

For microbial fuel cells carbon electrodes in diverse form, such as glassy carbon, woven graphite, plain graphite, graphite foam, granular graphite or carbon paper, are used [138] owing to their low-cost and ease of modification. However, compared to metals, the electrical conductivity of carbon is rather low.

For this thesis, four different electrode materials, platinum, gold, indium tin oxide (ITO), and carbon, were examined. These were the materials which can easily be prepared with the accessible apparatus. Since these materials, except ITO, are non-transparent, they were deposited as thin as possible on glass coverslip to allow the observation of cells under the light microscope. The deposition method and the thickness of materials deposited on glass are shown in Table 2.2.

The biocompatibility of these materials with THP-1 cells was tested via (i) cell survival, and (ii) cell adherence.

Cell survival was tested by seeding cells in culture wells containing electrode substrates. 5×10^5cells/ml were seeded in the culture media and incubated for

Material	Platinum	Gold	ITO	Carbon
Deposition method	E-beam evaporation	Resistive evaporation	Sputtering	Resistive evaporation
Layer thickness	5 nm	5 nm	200 nm	7 nm
Adhesive layer	no	chrome 1nm	no	no

Table 2.2: Electrode materials deposited on glass coverslips.

24 hours. The number of cells counted after incubation on each substrate was in all cases between 8.5×10^5cells/ml and 1.3×10^6cells/ml and no significant differences in the proliferation of the cells on each substrate was observed.

Cell adherence was tested by stimulating cells with PMA. When THP-1 cells are incubated with PMA, the morphology of the cells changes into macrophage like form, elongating and spreading their lamellipodia, and then cells adhere to the substrate, obtaining maximum contact with the substrate surface. 5×10^5cells/ml were seeded in the culture wells containing electrode materials and incubated for 24 hours with PMA. The morphology change was observed with all substrates and there was no visible difference between different substrates. The number of the cells also did not differ significantly (Fig. 2.14). Thus the materials used for this test were all acceptable with respect to biocompatibility with THP-1 cells.

The activity of the cells on each substrate was evaluated by superoxide anion production from the cells seeded on the substrates. The protocol is based on the procedure in Section 2.5.3. THP-1 cells suspended in the culture media were seeded on the substrate in the culture wells. After 2 days stimulation, the activator was added and the superoxide anion production from the cells was measured colorimetrically using WST-1. Here, a plain glass coverslip was also tested as a substrate. On ITO and glass substrates the cells always showed enhanced superoxide anion production as on the cell culture treated polystyrene substrate. On platinum and carbon the cells were less active, whereas on carbon the activity of the cells showed large variability.

Material	Platinum	Gold	ITO	Carbon (Graphite)
Specific resistance [Ωm]	10.6×10^{-8}	2.3×10^{-8}	1×10^{-3}	5-33$\times10^{-6}$

Table 2.3: Electrical resistivity of the electrode materials [143, 144]

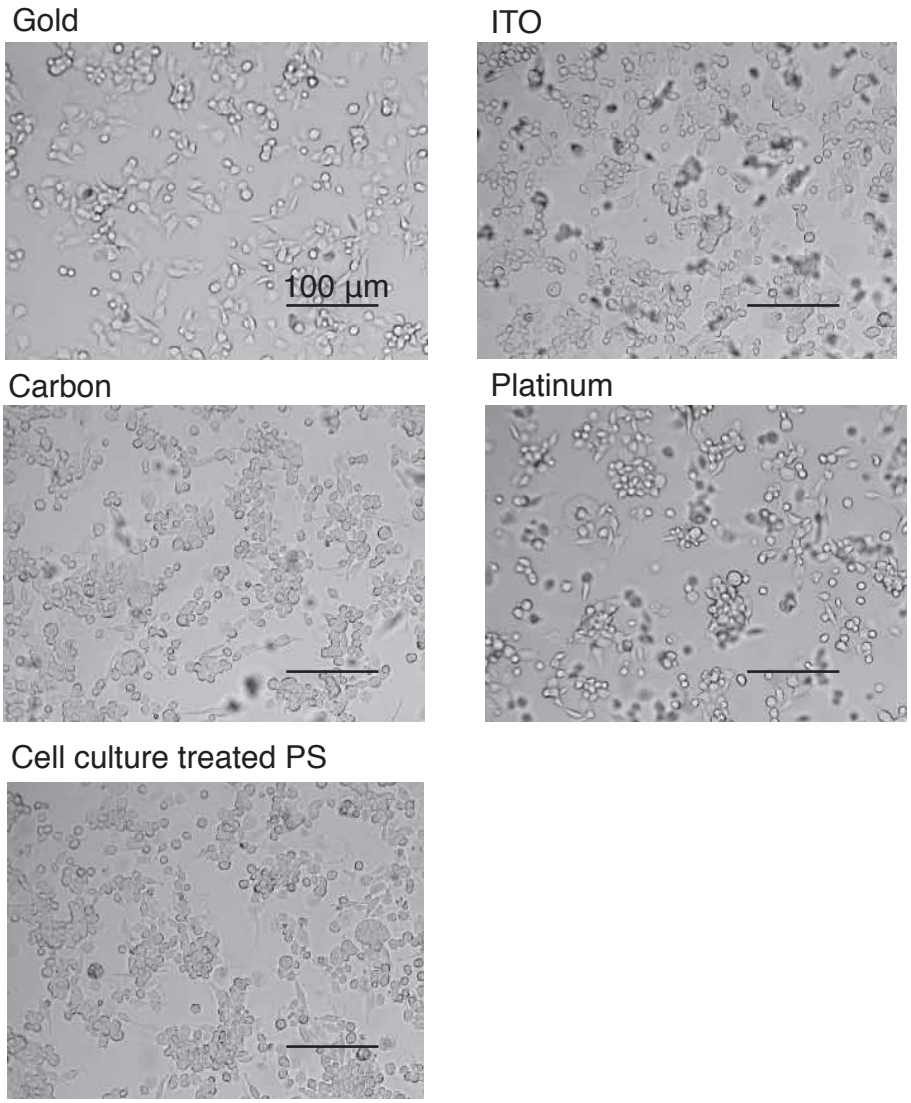

Figure 2.14: Adhesion of THP-1 cells on different substrates upon PMA stimulation for 24h. Images were obtained with Zeiss Axiovert 40CFL light microscope with 10× objective.

In view of the application in a biofuel cell, in addition to cell activity on the electrode material, the conductivity of the electrode itself has to be considered. The activity of the cells on ITO was higher than on other materials, however electrical conductivity of ITO is rather low. Gold exhibits high electrical conductivity, and the activity of the cells on gold was stable and not too low. Thus gold electrodes were employed for the experiments in this thesis.

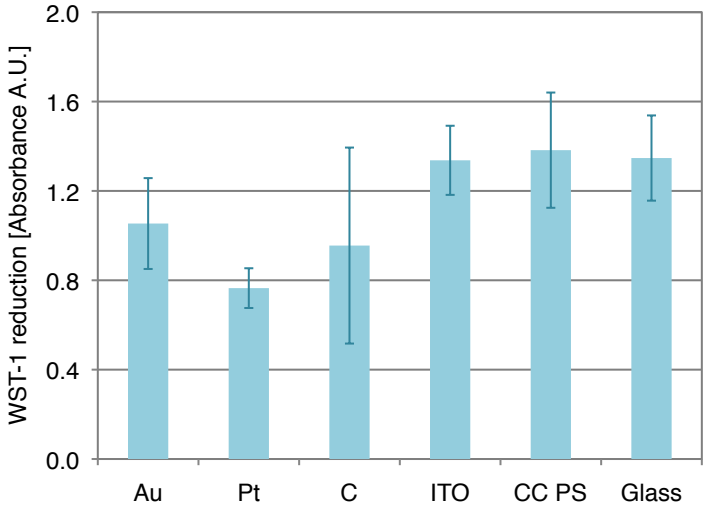

Figure 2.15: Superoxide anion production from the cells on different substrates. CC PS refers to cell culture treated polystyrene well. THP-1 cells were seeded and differentiated in culture wells containing different materials deposited on glass coverslips. The stimulation procedure was as described in Section 2.5.3. After 2 days, the superoxide anion production from the cells upon activation was measured by colorimetric assay with WST-1. The experiments were performed once in single and twice in duplicate.

2.5 Materials and Methods

In this section the materials and methods commonly employed throughout the experiments are described. Special techniques and materials will be mentioned later in the respective chapters and sections.

2.5.1 Cell culture

Human THP-1 monocytes were purchased from DSMZ (Braunschweig, Germany) and maintained in RPMI1640 Media with Glutamax (Invitrogen) supplemented with 10% fetal calf serum (FCS; Invitrogen) in a humidified atmosphere of 5% CO_2 at 37°C. The cells were passaged twice a week to maintain 0.1-1$\times 10^6$ cells/ml.

2.5.2 Analysis of the expression of NADPH oxidase subunits

The expression of three NADPH oxidase subunits, namely p22phox, p47phox, and p67phox, upon stimulation was examined by Western blot[3].

4×10^5 THP-1 cells/ml were seeded in culture wells in FCS containing media. To differentiate the cells 300 ng/ml LPS (Sigma-Aldrich), 20 ng/ml Recombinant Human TNF-α and 20 ng/ml Recombinant Human IFN-γ (both Invitrogen) were added. After 2-day incubation, the cells were activated with 50 nM PMA for 4 hours, and then collected and homogenized in a 2$\times$ SDS loading buffer (160 mM Tris-HCl (pH 6.8), 20% Glycerol, 4% SDS, 10% β-mercaptoethanol, 0.04% Bromophenol blue). The cells for negative control (non-stimulated) were seeded simultaneously with the cells to be stimulated. When the treated cells were collected, the un-stimulated cells were also collected for lysis. Samples were separated by 12% SDS-PAGE and subsequently transferred to a PVDF membrane. The blots were blocked by incubation for 1 h in PBS-T (1x PBS, 0.2% Tween 20) containing 5% nonfat milk then incubated at 4°C overnight with the appropriate primary antibody in PBS-T at the following dilutions: anti-p22phox and anti-p47phox (both Santa Cruz Biotechnology, Inc.) at 1:1000, anti-p67phox (BD Biosciences) at 1:500. The same blots were probed with anti-glyceraldehyde-3-phosphate dehydrogenase (GAPDH) (HyTest Ltd., 1:20000) for loading control. The blots were washed with TBS-T (1x TBS, 0.2% Tween 20), then incubated for 1.5 h with the appropriate horseradish peroxidase-conjugated and alkaline phosphatase-conjugated secondary antibody (Promega) at a 1:10000 dilution. After washing with TBS-T, the blots were visualized either with ECL Western blotting detection reagents (Amersham Bioscience) or CDP-Star chemiluminescence substrate (Roche Diagnostics) and exposed to Super RX X-ray film (Fujifilm).

2.5.3 Detection of superoxide anion production from cells

The superoxide anion production from THP-1 cells was detected colorimetrically using 2-(4-iodophenyl)-3-(4-nitrophenyl)-5-(2,4-dis-ulfophenyl)-2H tetrazolium, monosodium salt (WST-1) (Dojindo Laboratories) (see section 2.3).

4×10^5 THP-1 cells/ml were seeded in culture wells in FCS containing media. To differentiate the cells 300 ng/ml LPS, 20 ng/ml TNF-α and 20 ng/ml IFN-

[3]I gratefully thank the members of the group of Prof. Ari Helenius at the Institute of Biochemistry, ETH Zurich and Dr. Axel Niemann of the group of Prof. Ueli Suter at the Institute of Cell Biology, ETH Zurich for providing support and experimental equipment

γ were added, followed by a 2-day incubation. After cell differentiation the media were replaced with HBSS. Then 100 μM WST-1, 300 ng/ml LPS, 20 ng/ml TNF-α and 20 ng/ml IFN-γ (equivalent concentrations as for cell differentiation), and subsequently 50 nM PMA were added. After 4 hours of incubation, the supernatant was collected, and then was spun down to remove cellular debris. The supernatant was used for determining superoxide anion production from the cells by measuring the amount of reduced WST-1 with a spectrophotometer (Bio-Rad Laboratories, Inc.) at 450 nm.

2.5.4 Current measurement in biofuel cell setup

The current generated from the cells was measured in a custom-made two-compartment fuel cell setup.

The two-compartment fuel cell was constructed with plexiglass elements that were bolted together. The anodic and the cathodic compartment had a volume of 6 ml each. The compartments were separated by a cation exchange membrane (BDH 55165, VWR International Ltd.) that was soaked in HBSS prior to use. Electrodes were fabricated by depositing a 100 nm thick gold layer (with a 10 nm chromium adhesion layer) on glass slides by e-beam evaporation. The surface area of the electrodes for cell seeding was 4 cm^2.

3 ml of THP-1 cell suspension at a concentration of 4×10^5 cells/ml was seeded on a gold electrode in custom-made incubation containers in FCS-containing media. To differentiate the cells 300 ng/ml LPS, 20 ng/ml TNF-α and 20 ng/ml IFN-γ were added.

After 2 days of incubation, the cells were differentiated and adhered to the electrode. This electrode was rinsed with PBS and transferred into the anodic compartment just before the current measurement. The fluid in the anode compartment was HBSS with LPS, TNF-α and IFN-γ in equivalent concentrations as for cell differentiation, while the cathode compartment was filled with HBSS containing 0.1 M potassium ferricyanide. The electric circuit was closed with copper cables that had been attached to the electrodes with silver paint, with the junctions being sealed with silicone paste. To prevent evaporation of fluid from the fuel cell, the setup was covered with an aluminum foil housing with a wet paper towel placed inside. The measurements were carried out at room temperature. The current was calculated from the voltage drop measured across a resistor with a digital multimeter (2000, Keithley Instruments Inc.) (Fig. 2.16). The activator PMA was added after the current stabilized and the change in the current signal was observed.

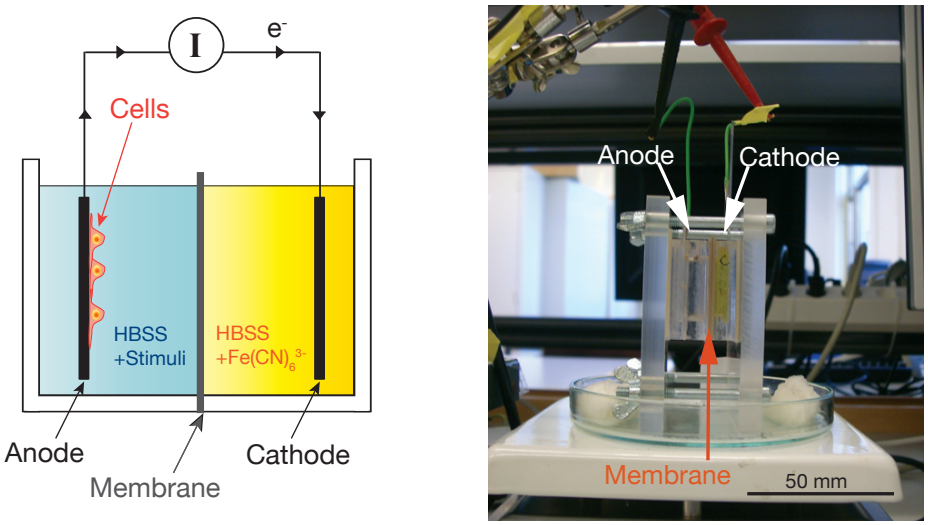

(a) Schematic of the current measurement

(b) Custum-made fuelcell setup

Figure 2.16: Current measurement in the biofuel cell

2.5.5 Potential measurement of the electrodes in biofuel cell

In addition to the current in the biofuel cell, the individual electrode potentials were determined using an Ag/AgCl and a calomel reference electrode for the anode and the cathode, respectively, which had been connected via salt bridges (Fig. 2.17).

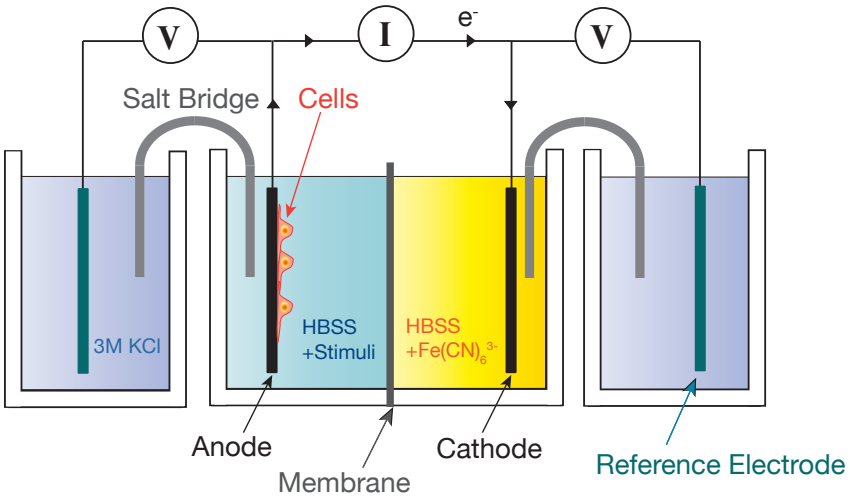

Figure 2.17: Schematic of the measurement of electrode potentials in the biofuel cell.

Chapter 3

Current Generation in Fuel Cell and NADPH Oxidase Activity

To investigate the correlation between current generation and NADPH oxidase activity, first the superoxide anion release from the cells and the protein expression in the cells during differentiation/activation were examined. Secondly these results were compared with the current generation in the fuel cell.

All experiments were repeated several times using THP-1 cells of different passage numbers. Due to the state of cells, variations in performance were unavoidable. Nevertheless, the data presented here are representative for the experiments conducted, if not stated otherwise.

3.1 Cell stimulation and NADPH oxidase activity

As detailed in Section 2.2.2, THP-1 cells had first to differentiate into macrophages and then get activated. Now the correlation between the expression of NADPH oxidase subunits and the superoxide anion release from THP-1 cells is examined by comparing different cell-differentiation/activation stages.

NADPH oxidase consists of two membrane-bound subunits, gp91phox and p22phox, and four cytosolic subunits, p67phox, p47phox, p40phox and RacGTP [93, 145, 146]. Upon macrophage activation, the cytosolic subunits translocate to the plasma membrane and bind to the membrane-bound subunits to form the NADPH oxidase complex [147] (page 10, Fig. 1.2). In this thesis, the expression of p22phox, a membrane-bound subunit, and two cytosolic subunits, p47phox and p67phox on the differentiation/activation stages was analyzed by Western blot.

THP-1 cells were stimulated in two steps for superoxide anion production

(detailed protocol in Section 2.5.2). As differentiation stimuli LPS, TNF-α, and IFN-γ were used (below, these substances are called differentiation stimuli). Monocytes were further activated by PMA (below this chemical is called activator). Here, cells treated with 4 different methods were investigated; (i) non-stimulated cells as negative control, (ii) cells stimulated only with the activator, (iii) cells stimulated only with the differentiation stimuli, (iv) cells stimulated with the differentiation stimuli and subsequently the activator.

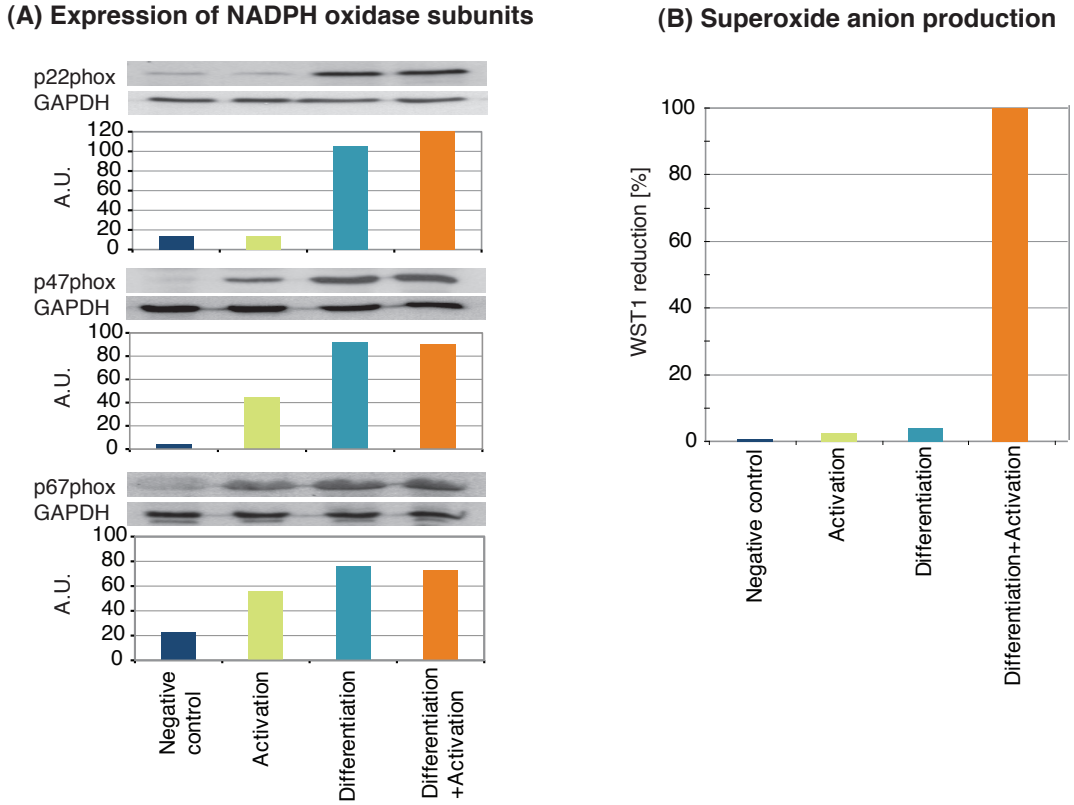

Figure 3.1: Expression of NADPH oxidase subunits and WST-1 reduction by superoxide anion at differentiation/activation stages of THP-1 cells. (A) From top to bottom; p22phox, p47phox, p67phox. Immunodetection of GAPDH serves as loading control. Bar graphs represent the band intensity of immunoblots, normalized to GAPDH. (B) WST-1 reduction refers to the spectrophotometric absorbance normalized to the value of fully stimulated (differentiated and activated) cells in each experiment. (A), (B) From left: Untreated cells as negative control; Activation with 50 nM PMA; Differentiation with 300 ng/ml LPS, 20 ng/ml TNF-α, and 20 ng/ml IFN-γ; Differentiation+Activation sequentially at same concentration as before.

All subunits analyzed were expressed in low levels in resting cells (Fig. 3.1 (A)■). When the cells were only exposed to the activator PMA, the expression of both cytosolic subunits increased, whereas this activator did not have any effect

on the p22phox synthesis (Fig. 3.1 (A)■). In both cases the percentage of WST 1 reduction was small, reflecting the low superoxide anion production from the cells (Fig. 3.1 (B)■■). This can be explained as a result of the small amount of NADPH oxidase due to low expression of subunits.

The cells exposed to the differentiation stimuli (Fig. 3.1 (A) ■) and the cells exposed to the differentiation stimuli plus the activator in sequential order (Fig. 3.1 (A)■) both expressed an enhanced level of all three NADPH oxidase subunits investigated. Although the addition of the activator to the cells treated with differentiation stimuli did not change the amount of NADPH oxidase subunits expressed, it increased the WST-1 reduction abundantly (Fig. 3.1 (B)■→■). This result confirmed that the differentiation of THP-1 cells promotes the expression of NADPH oxidase subunits, and the complex of these molecules were assembled only when the cells were further activated by PMA. The detail of the assembly mechanism of the NADPH oxidase subunits will be discussed later in Section 4.2.2.

3.2 Current Generation on Cell Stimulation

3.2.1 Background current from the system

To determine the background current induced by the fluid and the chemicals in the fuel cell, current generation in the absence of cells on the electrode was examined employing the same procedure as the current measurement with cells on the electrode (Section 2.5.4). Briefly, the anodic compartment was filled with HBSS containing differentiation stimuli, while the cathodic compartment was filled with HBSS containing potassium ferricyanide. After the current stabilized, the activator PMA was added to the anodic compartment (Fig. 3.2 (A), solid arrows). The addition of the activator to the anodic compartment induced no obvious current change. This indicates that none of the substances used in the system, i.e., the differentiation and the activation stimuli, potassium ferricyanide and the buffer, generate a substantial electrical current.

Since homeostatic cellular function could influence the redox reaction at the electrode surface. THP-1 cells are suspension cells and do not adhere on the electrode without stimulation, thus these cells cannot be used as example of intact cells. Therefore, Vero cells were used to examine the current generation when seeded on the electrode.

Vero cells[1] were derived from kidney epithelial cells of the African Green Monkey and possess an adherent growth property. The cells were seeded in MEM media with GlutaMAX-I containing 1× non essential amino acid and 10% FCS (all Invitrogen) into the culture wells and after 1 day incubation the medium was replaced with HBSS and the superoxide anion production in the following period was measured. In one well, a gold-coated glass cover slip was contained, which was used as anode in the fuel cell for the current measurement. No superoxide anion production from the Vero cells was detected (data not shown). The result of the current measurement (Fig. 3.2 (B)) clearly showed that Vero cells did not produce any electron flow in the fuel cell. This implies that the constitutive cellular function of intact cells may not cause any electron flow to the electrode.

Thus the effect of a possible background current can be neglected in the experiments reported below.

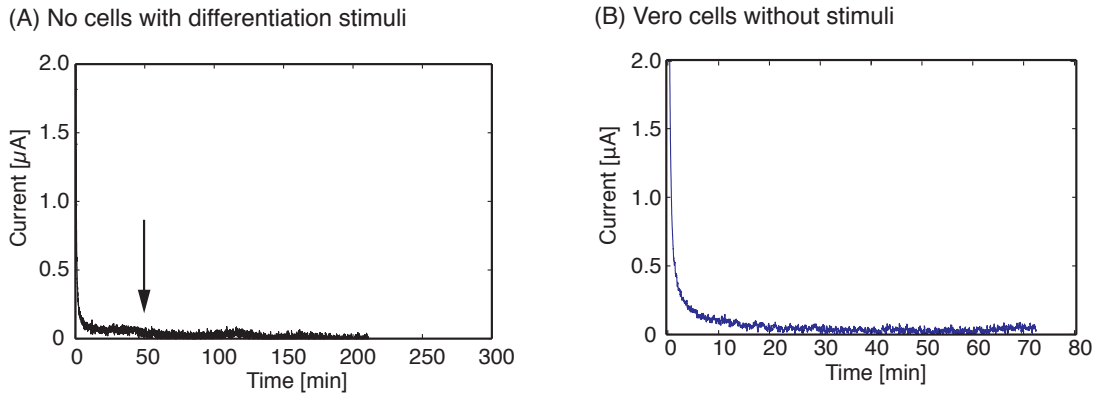

Figure 3.2: Current flow in the fuel cell (A) without cells on electrode, and (B) with Vero cells adhering to electrode. (A) The measurement was started with HBSS already containing LPS, TNF-α and IFN-γ in the anodic compartment. At the time point of the solid arrow, the activator PMA was added to the anodic compartment. (B) The measurement was conducted with HBSS in the anodic compartment without stimuli.

The current dropped in the beginning due to the equilibration between the two compartments (Fig. 3.2). This first current decay was faster compared to that in the measurement with THP-1 cells on the electrode (Fig. 3.2 (A), on page 50, Fig. 3.3 (A-C)), which was possibly due to the lower impedance of the cell-free electrode. The fast decay of the current measurement with Vero cells on the electrode (Fig. 3.2 (B)) cannot be compared due to the differences in the electrode's size and the amount of the cells seeded.

[1]Vero cells were kindly provided by the group of Prof. Ari Helenius, the Institute of Biochemistry, ETH Zurich.

3.2.2 Current generation correlates to superoxide anion production by NADPH oxidase

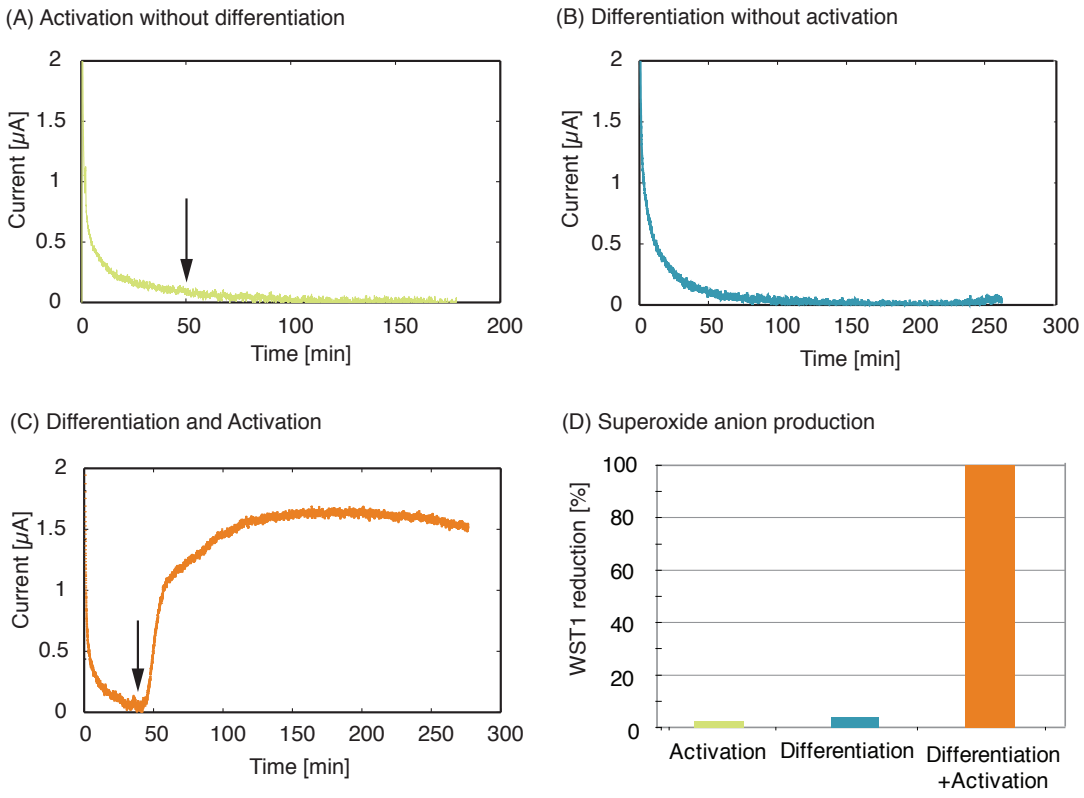

Figure 3.3: Current generation in the fuel cell (A-C) and WST-1 reduction upon differentiation/activation of THP-1 cells (D). (A-C) the measurement was started with HBSS already containing LPS, TNF-α and IFN-γ in the anodic compartment. (D) WST-1 reduction refers to the spectrophotometric absorbance normalized to the value of fully stimulated (differentiated and activated) cells in each experiment. (A) and (D) cells only activated with 50 nM PMA; (B) and (D) only differentiated with 300 ng/ml LPS, 20 ng/ml TNF-α and 20 ng/ml IFN-γ; (C) and (D) cells differentiated and activated sequentially. At the time point of the solid arrow, the activator PMA was added to the anodic compartment.

In the previous Section 3.1, the correlation between the expression of NADPH oxidase subunits and the superoxide anion production from activated THP-1 cells was examined. Applying the same method of distinguished cell stimulation, the current generation in the fuel cell was monitored.

Cells not treated with any chemical stimuli did not adhere to the electrode. Hence we did not measure current from these cells in the fuel cell system. When the cells were activated by PMA without differentiation treatment, they adhered to the electrode, however, no current was generated (Fig. 3.3 (A)). When the

cells were exposed to the differentiators, the cells adhered onto the electrode as well and no current increase was observed (Fig. 3.3 (B)) unless the activator PMA was added into the anodic compartment (Fig. 3.3 (C)). These results were in excellent agreement with the superoxide anion produced by the cells each in differentiation/activation stage (Fig. 3.3 (D)).

Together with the correlation of superoxide anion production and NADPH oxidase activity discussed in Section 3.1, it is obvious that the NADPH oxidase activity and the current generation in the fuel cell are strongly linked.

3.3 Validity of the measurement using THP-1 cells

The difference between primary cells and cell line is a delicate issue since the two types do not necessarily posses the same characteristics, often regarding reaction on stimuli, signal pathway, or expression of molecules [58]. To verify the reliability of the experimental concept, the superoxide anion production and the current generation of primary cells upon the stimulation were examined.

3.3.1 Superoxide anion production of mouse macrophages

First, the superoxide anion release from mouse macrophages was compared to that from THP-1 cells.

The mouse macrophages[2] were isolated from mouse peritoneum and cultured in RPMI 1640 media containing 1% PS (penicillin and streptomycin) and 10% FCS for 1 day. The cells were trypsinized and resuspended for experimental use.

Both THP-1 cells and the purified mouse macrophages were seeded in the culture wells in the concentration of 5×10^5/ml. The cells were incubated for 2 days with (i) no stimuli, (ii) with LPS, (iii) with TNF-α and IFN-γ, (iv) (v) with the differentiation stimuli (LPS, TNF-α and IFN-γ). The protocol is based on the experimental procedure described in Section 2.5.3. After replacing the media with HBSS, all samples got the same stimuli at the same concentration for the WST-1 colorimetric experiment, and in (v) additionally activator was added. Due to the limited number of cells the test with macrophages stimulated only with activator failed.

Since macrophages exhibit already adherent characteristic, no difference in morphology between stimulations was observed.

[2]The purified mouse macropages were kindly provided by the group of Prof. Romeo Ricci, the Institute of Cell Biology, ETH Zurich.

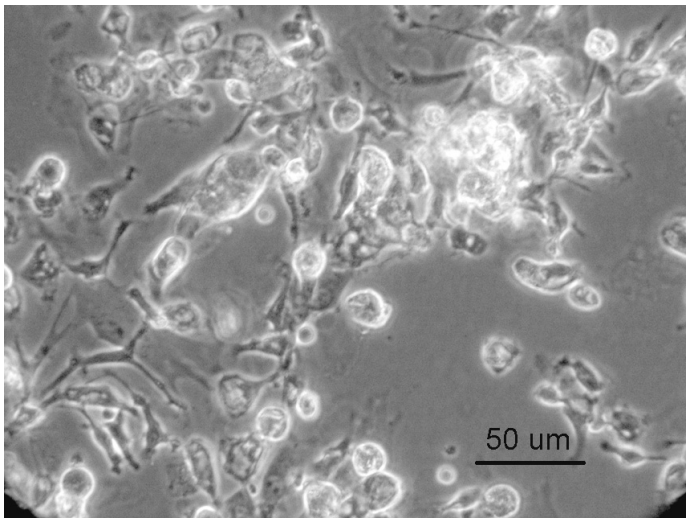

Figure 3.4: Mouse macrophages purified and seeded in culture well.

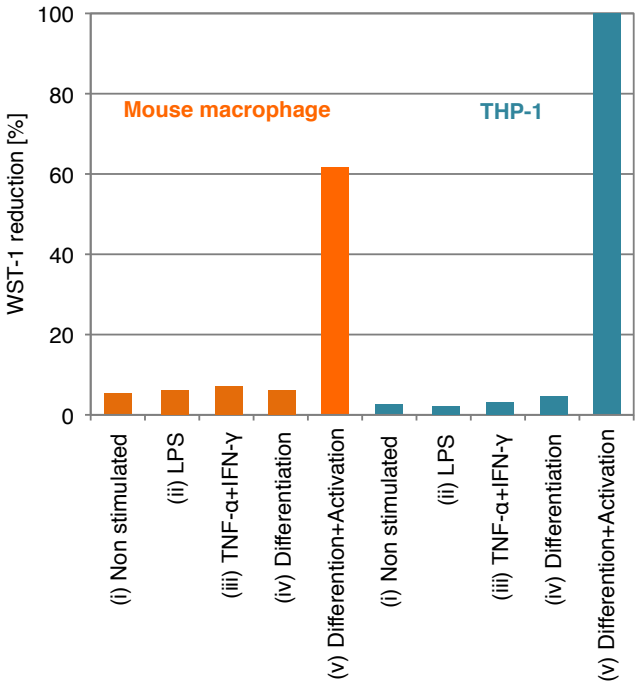

Figure 3.5: Superoxide anion production by mouse macrophages■ and THP-1 cells■ on different stimulation. The cell stimulation was based on the standardized protocol described in Section 2.5.3. From left: Untreated cells as negative control; Activation with 50 nM PMA; Differentiation with 300 ng/ml LPS, 20 ng/ml TNF-α, and 20 ng/ml IFN-γ; Differentiation+Activation with sequential stimuli of same concentration as before. The experiment was carried out once.

The macrophages treated with the differentiation stimuli and activator sequentially produced superoxide anion, while other stimulation methods did not cause any superoxide anion production (Fig. 3.5). This result is in good agreement with the superoxide anion production by THP-1 cells on corresponding stimulation.

3.3.2 Current generation measured with primary mononuclear leukocytes

It has been reported that the superoxide anion production from blood monocytes activated by PMA is maintained at the high levels observed when the cells were pretreated with IFN-γ or TNF-α [148]. This suggests reliability of the experimental procedure used throughout the thesis. However, some regulatory systems of THP-1 cells might be slightly different from those of primary monocytes in the blood [149]. Thus, the superoxide anion release and the current generation from primary monocytes were compared with the results obtained with THP-1 cells[3].

Mononuclear leukocytes were isolated from heparinized peripheral blood of a healthy female adult volunteer by Ficoll-Paque (Amersham Biosciences) density gradient centrifugation. The cells were suspended in RPMI 1640 media with 10 % FCS in culture wells and used for the superoxide anion detection test as described in Section 2.5.3, whereas the incubation period was shortened to 1 day.

The superoxide anion production from primary mononuclear blood cells showed the same tendency as THP-1 cells (Fig. 3.6 (A)). Additionally the mononuclear leukocytes were seeded on a gold electrode as described in Section 2.5.4 and the current generation from the cells was measuered. A marked increase in the current was seen after the PMA activation (Fig. 3.6 (B)). Both results are in an excellent agreement with the experimental data using THP-1 cells (Section 3.2.2.

The experiments with THP-1 cells exhibited similar tendencies as those with primary mouse peritoneal macrophages and primary blood mononuclear leukocytes. Consequently, the use of THP-1 as a model for the experiments is well justified.

By Ficoll-Paque blood separation and subsequent washing with medium, not only monocytes but also other mononuclear leukocytes (lymphocytes) were obtained. However, the exact number of monocytes and whether lymphocytes

[3]The experiment was carried out in collaboration with the group of Prof. Ehlert, the Institute of Clinical Psychology and Psychotherapy, University Zurich.

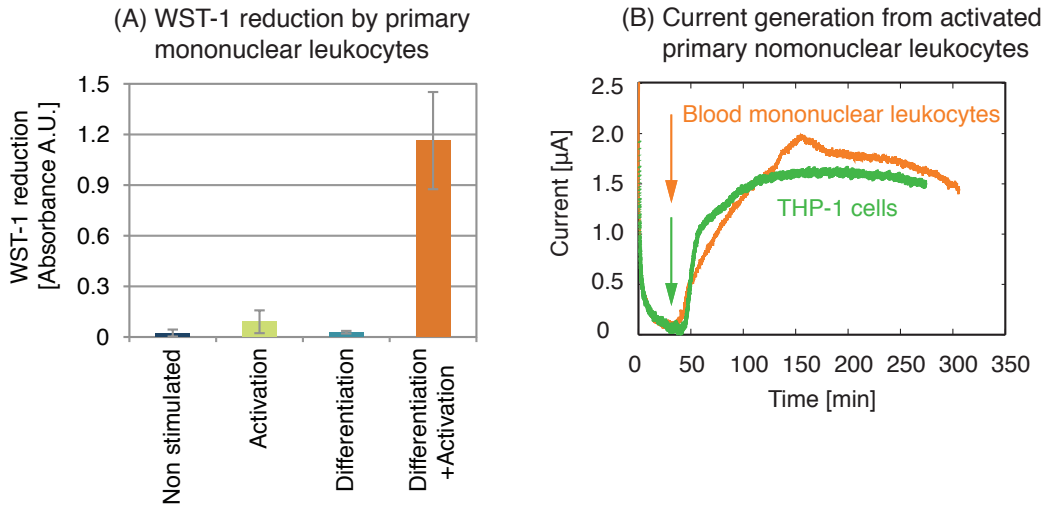

Figure 3.6: Detection of superoxide anion production and current generation from purified human mononuclear leukocytes. (A)Cell stimulation was based on the protocol in Section 2.5.3. WST-1 reduction refers to the spectrophotometric absorbance. From left: Untreated cells as negative control; Activation with 50 nM PMA; Differentiation with 300 ng/ml LPS, 20 ng/ml TNF-α, and 20 ng/ml IFN-γ; Differentiation+Activation with sequential stimuli of same concentration as before. Three independent experiments were carried out. (B) Current flow in the fuel cell was measured as described in Section 2.5.4, using primary mononuclear leukocytes■ and THP-1 cells■. At the time point of the solid arrow, the activator PMA was added to the anodic compartment.

are also influenced by the stimuli have not been analyzed yet.

Chapter 4

Analysis of the source of current generation

In this chapter, the source of electrons for current generation is discussed. The chemicals used for cell stimulation and the constitutive cellular function did not cause any change in the current generation in the fuel cell (Section 3.2.1). The current was generated only when the cells were properly stimulated. Through this stimulation, NADPH oxidase in the plasma membrane was activated to release superoxide anion. To validate whether a current production can be attributed to active NADPH oxidase in macrophages, first the potential change of each electrode during the NADPH oxidase activation was monitored, and then the effect of different NADPH oxidase inhibitors on the superoxide anion detection and the current generation in the biofuel cell were examined.

4.1 Electrode potentials

The current flowing through the fuel cell is driven by the potential difference between the anode and the cathode. Thus, a change of the potential of the cathode via redox reaction in the cathodic compartment could cause a change in the current measured in the fuel cell. To investigate the influence of each compartment on the current production, the potential of the anode and the cathode were determined independently with reference electrodes during the current measurement. As shown in Fig. 4.1, the potential of the anode corresponded to the change in current after stimulation by PMA and inhibition by diphenylene iodonium (DPI) (see Section 4.2.1), while the cathode potential changed insignificantly (the variation is less than 10% of the anode). This observation indicates that the current production is not substantially driven by

the cathodic chemical reaction, but by the potential change at the anode through the activation of macrophages.

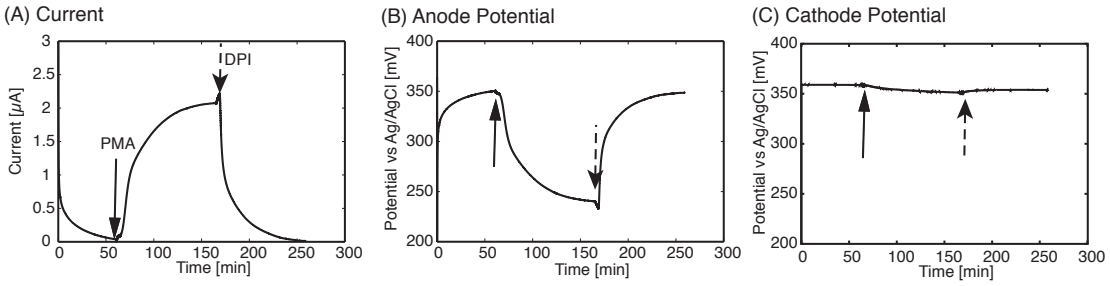

Figure 4.1: Current generation and the potential of the electrodes in the fuel cell. The differentiated cells were activated with PMA (solid arrows) during the current measurement as described in Section 2.5.4. After a clear increase in current the NADPH oxidase inhibitor DPI was added to the anodic compartment (dashed arrows). The anode potential (B) and the cathode potential (C) were measured using an Ag/AgCl reference electrode and a calomel reference electrode, respectively. The potential value of the cathode was converted to.Ag/AgCl reference scale.

4.2 Effect of Inhibition of NADPH oxidase on current generation

Stimulation of one cell function may cause chain reactions in the signal cascade, through which secondary effects on other cellular functions are induced. The activation of NADPH oxidase in THP-1 cells was suppressed by different inhibitors and the superoxide anion production from the cells and the current generation in the fuel cell were analyzed.

4.2.1 Assay development with different inhibitors

Apocynin Apocynin (4'-hydroxy-3'methoxy-acetophenone) is a compound isolated from a variety of plant sources and a potent inhibitor of reactive oxygen species production by activated human phagocytes [102]. Abolition of the production of oxygen radical species from activated phagocytes by apocynin alone or in combination with other inhibitors has been reported [87, 150, 151]. Apocynin is a small molecule (molecular weight of 166.17 Da) and penetrates through the cell membrane, where it forms its active derivative. This active metabolite impedes the translocation of cytoplasmic subunits of NADPH oxidase

to the membrane [63, 152, 153] by interfering with the binding of p47phox to gp91phox [154].

To examine the inhibitory effect of apocynin (Sigma-Aldrich), superoxide anion release from activated THP-1 cells depending on different concentration of apocynin was measured.

The cell stimulation was based on the protocol described in Section 2.5.3, except for the addition of the inhibitor. Apocynin was added to the differentiated THP-1 cells in HBSS 1 hour before cell activation. 5 hours after cell activation, the superoxide anion production from the cells was determined using WST-1 colorimetric assay.

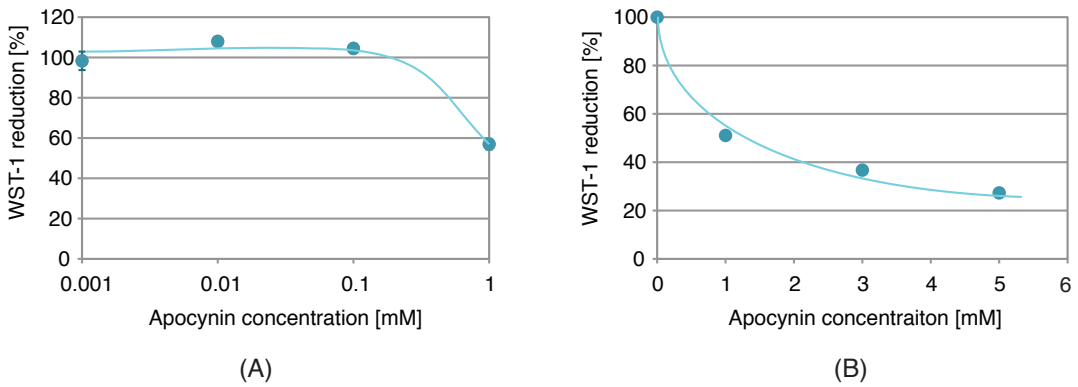

Figure 4.2: Inhibition of superoxide anion production from activated THP-1 cells using apocynin at different concentrations. The cells were differentiated as described in Section 2.5.3. Apocynin was added after the differentiation in HBSS. After 1 hour incubation, the cells were activated and the amount of superoxide anion produced from the cells for the following 4 hours was measured colorimetrically using WST-1. WST-1 reduction refers to the spectrophotometric absorbance normalized to the value of stimulated cells without the inhibitor in each experiment. Apocynin added was 0, 0.001, 0.01, 0.1, 1 mM in (A), 0, 1, 3, 5 mM in (B). The experiments were performed (A) once in duplicate, and (B) once.

No decrease of superoxide anion production was detected until a high concentration (1 mM) of apocynin (Fig. 4.2 (A)). This concentration is rather high compared to the literature values ($\leq$100 μM [87, 102]). This may be due to the use of PMA as the cell activator. The conversion of apocynin to its active metabolite may require the abundant presence of myeloperoxidase (MPO) [152,155,156]. Since the stimulation of phagocytes with PMA results in little or no myeloperoxidease release [157], only littel amounts of apocynin were assumably be activated under our experimental condition. Thus, no apocynin test was

further conducted.

DPI Diphenylene iodonium (DPI) binds covalently to flavoproteins and suppresses reactions in which these proteins are involved [63]. The inhibition by DPI is therefore not limited to NADPH oxidase activity, but includes other flavin-containing enzymes such as nitric oxide synthase, NADH dehydrogenase [158], or cytochrome P450s [154]. The suppression of superoxide anion production from macrophages [154, 159, 160] or neutrophils [161, 162] has been reported. The suppression of superoxide anion production is caused by DPI blocking the reduction of flavin adenine dinucleotide (FAD) in the plasma membrane component of NADPH oxidase [163], thereby inhibiting electron transport to the extracellular space.

To examine the inhibitory effect of DPI (Sigma-Aldrich), superoxide anion release from activated THP-1 cells depending on different inhibitory timing and concentrations was compared. The cell stimulation was based on the protocol described in Section 2.5.3, except for the addition of the inhibitor.

First, the timing of the addition of the inhibitor was examined. THP-1 cells were differentiated with/without DPI at different concentrations. After 2 days of incubation, both samples were treated with DPI for 1 hour in HBSS before the cell activation by PMA. The cells pretreated with 10 μM DPI did not form clusters seen after the usual differentiation (page 25, Fig. 2.1(C)) and higher roughness on the cell membrane was observed. As a result of its inhibitory effect on NADPH oxidase-mediated generation of reactive oxygen species, DPI affects signaling pathways involved in mitogenesis and cell proliferation [164]. This disturbance in the cellular function may cause the change in the cell morphology.

The superoxide anion production from the cells was dependent on the concentration of DPI, but not on the timing of addition of DPI (Fig. 4.3 (A)). The addition before the PMA activation was sufficient to inhibit superoxide anion production and the cells did not need to be preincubated with DPI in advance.

Next, the optimal concentration of the inhibitor was investigated. THP-1 cells were differentiated and treated with DPI at different concentrations in HBSS for 1 hour before the PMA activation. The superoxide anion release from the cells was measured with WST-1 colorimetric method.

As shown in Fig.4.3(B), full inhibition of superoxide anion production from the cells was observed with DPI $\geq$5 μM. Thus the inhibitory test in the current measurement was conducted with 5 μM DPI.

Additionally, the timing of inhibition of superoxide anion production by DPI

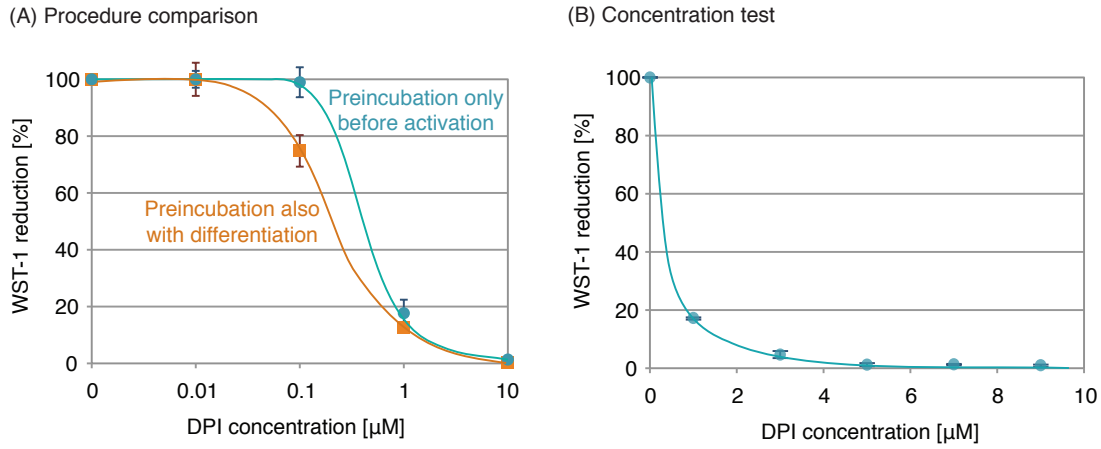

Figure 4.3: Inhibition of superoxide anion production from activated THP-1 cells using DPI at different concentrations. The cells were differentiated as described in Section 2.5.3 with DPI (A) ■ or without DPI (A, B) ■. In both cases, DPI was added after the differentiation in HBSS. After 1 hour incubation, the cells were activated and the amount of superoxide anion produced from the cells for the following 4 hours was measured colorimetrically using WST-1. WST-1 reduction refers to the spectrophotometric absorbance normalized to the value of stimulated cells without the inhibitor in each experiment. DPI added was 0, 0.01, 0.1, 1, 10 μM in (A), 0, 1, 3, 5, 7, 9 μM in (B). The experiments (A) and (B) were carried out once in duplicate and twice in duplicate, respectively.

was examined by adding DPI after the cell activation. After differentiation, the cells were activated in HBSS for the subsequent superoxide anion detection. After the cell activation, 5 μM DPI was added at different time points and the total superoxide anion production in 4 hours after the activation was measured. As shown in Fig. 4.4 addition of DPI had an immediate effect on superoxide anion production from the activated cells. Therefore, addition of DPI in the anodic compartment of the fuel cell during the current measurement may causes an immediate change in the superoxide anion release from activated cells.

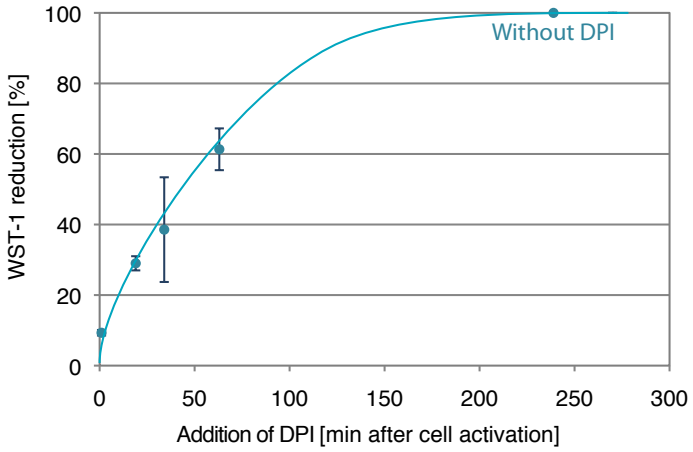

Figure 4.4: Addition of DPI at different time points after cell activation. To the differentiated cells according to Section 2.5.3, 5 μM DPI was added in HBSS simultaneously with the activator, or at 20, 35, 65 minutes after the activation. One well remained without DPI. Following by 4 hours incubation of each well, the samples were collected for colorimetric assay using WST-1. WST-1 reduction refers to the spectrophotometric absorbance normalized to the value of stimulated cells without the inhibitor. The experiment was conducted once in duplicate.

SOD The electron transferred by NADPH oxidase is usually captured by oxygen to form superoxide anion [67]. Superoxide dismutase (SOD) catalyzes the reaction of superoxide anion to hydrogen peroxide ($2\,O_2^- \cdot + 2\,H^+ \longrightarrow O_2 + H_2O_2$) and decreases the amount of superoxide anion in the system rapidly. Therefore SOD is commonly used to confirm superoxide anion production. At physiologic pH the rate constant of the reaction mentioned above with SOD is $\approx 2 \times 10^9$ $M^{-1}sec^{-1}$ [165], whereas the rate constant of the reaction between superoxide anion and WST-1 is about five orders of magnitude lower ($\approx$3-4 $\times 10^4$ $M^{-1}sec^{-1}$ [131]). Thus the addition of SOD shortens the lifetime of superoxide anion and prevents almost all WST-1 reduction by the superoxide anion.

To investigate the optimal concentration of SOD for the inhibition of superoxide anion, SOD at different concentrations was added in HBSS after the THP-1 differentiation. Followed by 1 hour incubation, the cells were activated with PMA and the superoxide anion release from the cells was measured with WST-1 colorimetric method. The amount of superoxide anion was drastically lowered with SOD in low concentration (Fig. 4.5). The decrease of superoxide anion in the system reached a plateau after 100 U/ml. Thus the inhibitory test in the current measurement was conducted with 100 U/ml SOD.

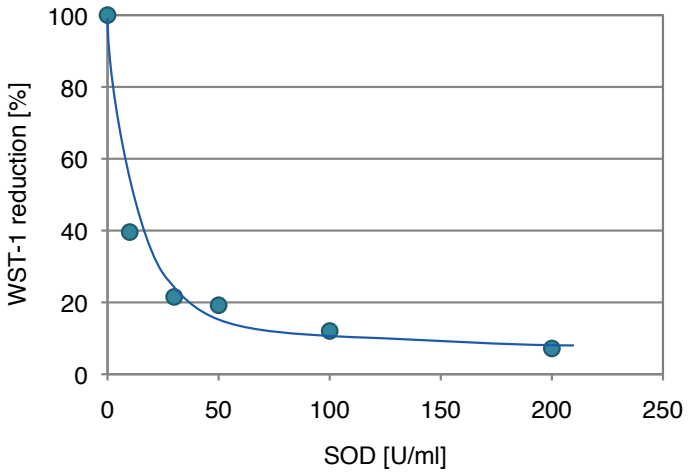

Figure 4.5: Inhibition of superoxide anion production from activated THP-1 cells using SOD at different concentrations. The cells were differentiated as described in Section 2.5.3. SOD was added after the differentiation in HBSS. After 1 hour incubation, the cells were activated and the amount of superoxide anion produced from the cells for the following 4 hours was measured colorimetrically using WST-1. WST-1 reduction refers to the spectrophotometric absorbance normalized to the value of stimulated cells without the inhibitor. SOD added was 0, 10, 30, 50, 100, 200 U/ml. The experiment was carried out once.

$ZnCl_2$ $ZnCl_2$ is known as a blocker of H^+ channel [106,166] and simultaneously reduces superoxide anion production in phagocytes [106, 167, 168]. Due to the charge compensation, the proton efflux may be functionally conjugated to the exocytic electron transport by NADPH oxidase [106, 169] through the concomitant regulation by PKC [170, 171]. If the proton channels are blocked, the lack of electrogenic compensation induces intensified polarization and accumulation of protons at the inner membrane surface, attenuating the NADPH oxidase activity [167, 169].

To investigate the optimal concentration of $ZnCl_2$ for the inhibition of superoxide anion release from activated THP-1 cells, $ZnCl_2$ at different concentrations was added in HBSS after the THP-1 differentiation according to the standardized protocol in Section 2.5.3. After 1 hour of incubation, the cells were activated and the superoxide anion production from the cells was determined using WST-1 colorimetric assay. Since many salt crystals were observed in the sample well with 1 mM $ZnCl_2$, this WST-1 reduction value was disregarded. The decrease of WST-1 reduction damped at a concentration above 40 μM (Fig. 4.6 (B)).

Therefore, for the inhibitory test of the current measurement with $ZnCl_2$, the concentration of 40 μM was employed.

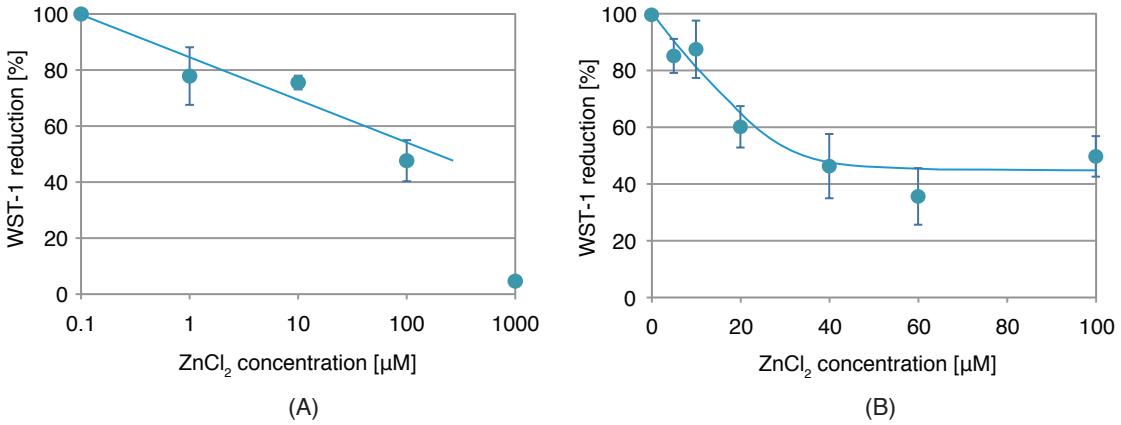

Figure 4.6: Inhibition of superoxide anion production from activated THP-1 cells using $ZnCl_2$ at different concentrations. The cells were differentiated as described in Section 2.5.3. $ZnCl_2$ was added after the differentiation in HBSS. After 1 hour of incubation, the cells were activated and the amount of superoxide anion produced from the cells for the following 4 hours was measured colorimetrically using WST-1. WST-1 reduction refers to the spectrophotometric absorbance normalized to the value of stimulated cells without the inhibitor in each experiment. $ZnCl_2$ added was (A) 0, 1, 10, 100, 1000 μM, (B) 0, 5, 10, 20, 40, 60, 100 μM. Two independent experiments were carried out in (A), and the experiment in (B) was carried out once in triplicate.

Inhibitors of nitric oxide production and its derivative Production of superoxide anion via the activated NADPH oxidase is linked to the production of nitric oxide through inducible nitric oxide synthase (iNOS), which is expressed in response to proinflammatory cytokines or LPS [172–174]. The regulation of superoxide anion and nitric oxide release occur independently via PKC activation [82]. Catalyzed by NOS, nitric oxide is produced via the conversion of L-arginine to L-citrulline [175]. Nitric oxide can bind with superoxide anion to form another reactive species, peroxynitrite [176] and contributes to the regulation of wide range of physiological processes including blood flow. Since these species are reactive and could also influence the current in the fuel cell, an inhibitory test of the current measurement was intended. Some NOS inhibitors may interfere with the concurrent superoxide anion production [173], therefore not only the effects of NOS inhibitors on the production of nitric oxide and its derivatives, but also the effect of these inhibitors on the superoxide anion production were examined. In this thesis three commonly used iNOS inhibitors were selected, namely N^G-nitro-l-arginine methyl ester (L-NAME), N^{ω} -monomethyl-L-arginine (L-NMMA), and aminoguanidine.

L-NAME is chaperoned across the plasma membrane and hydrolyzed by

esterases to form N(G)-nitro-L-arginine (L-MA), a structural analog of L-arginine. This product L-NA interacts with NOS competing against L-arginine, and as a result nitric oxide synthesis is suppressed [177, 178].

L-NMMA is one of the most commonly used inhibitors of NOS which inhibits NOS in the same manner as L-NAME, by competing against L-arginine. This inhibitor is also known as a potent vasoconstrictor, therefore it has been examined in various types of shock [179, 180]. The effect of L-NMMA is relatively non-selective.

Aminoguanidine incorporates the guanide group of L-arginine [181] and also inhibits NOS activity. It is relatively selective for iNOS and thus widely used to investigate the role of iNOS in host defense against infections caused by various pathogens [182].

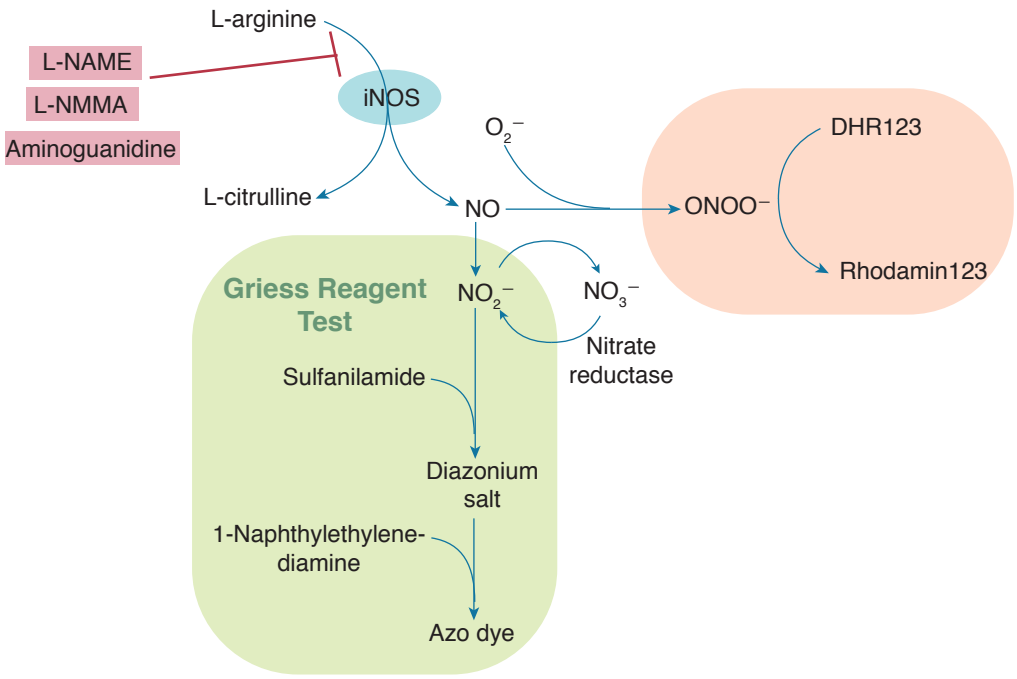

Figure 4.7: Schematic diagram of nitric oxide and its detection methods.

The concentrations of the inhibitors used for the experiments properly covered the known literature values [173, 175, 183].

Since the chemical structure of nitric oxide changes immediately after it is released from NOS, the production of nitric oxide from activated THP-1 cells was determined indirectly. Griess reagent method is a common assay of nitric oxide by detecting nitrite (NO_2^-) spectrophotometrically, which is a product of spontaneous oxidization of nitric oxide under physiological conditions. The

conversion of nitric oxide and superoxide anion to peroxynitrite is a diffusion controlled rapid reaction (k=1.9-$\times 10^{10}\mathrm{M}^{-1}\mathrm{s}-1$). Peroxynitrite production can be determined by measuring the fluorescence properties of the oxidation of dihydrorhodamine 123 (DHR) to rhodamine.

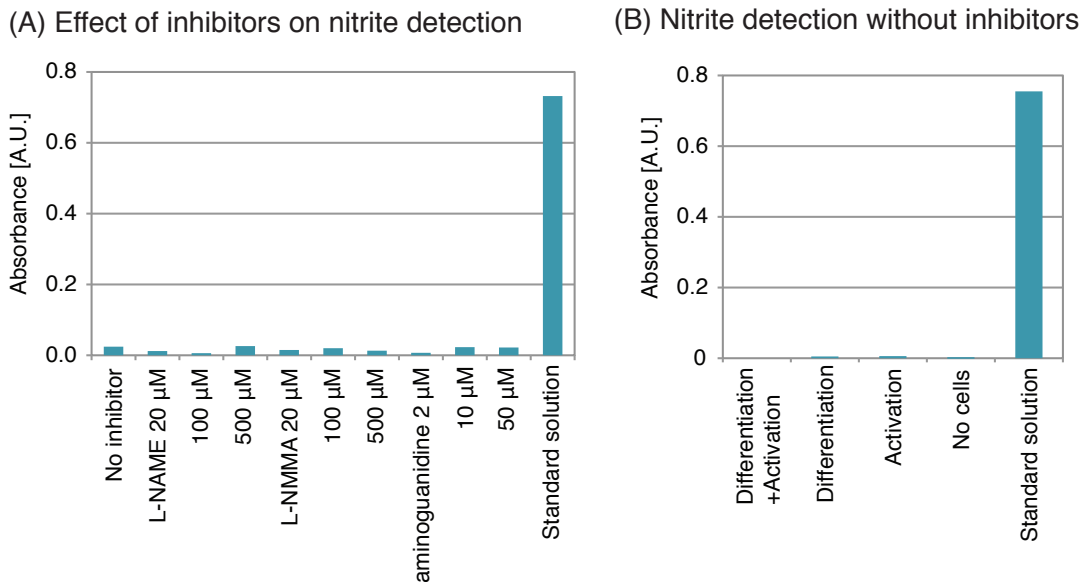

Figure 4.8: Inhibitory test of nitric oxide production from activated THP-1 cells. The cell stimulation procedure was as described in Section 2.5.3. (A) 30 minutes before the addition of the differentiation stimuli, the cells were pretreated with inhibitors. After changing the medium to HBSS, the inhibitors were added for 30 minutes before the activation. After 4 hours, the supernatants were collected for the nitrite detection using Griess reagent kit (Molecular Probes). (B) The same test was conducted without the inhibitors. From left: the cells were differentiated and activated, only differentiated, only activated, not stimulated. After the reduction of nitrate by incubation with nitrate reductase (Sigma-Aldrich) for 100 minutes in 37°C, the samples were mixed with the reagents, followed by another 30 minutes incubation in ambient. The amount of nitrite was measured with a spectrophotometer at 548 nm. In both (A) and (B) the rightmost sample is the standard solution (sodium nitrite) provided by the supplier. Both (A) and (B) experiments were performed once.

The positive control with the activated cells showed negligible amount of nitrite (Fig. 4.8 (B) Differentiation+Activation), thus the effect of the inhibitors was not detectable. The detection limit for the Griess reagent method is 1.0 μM. Thus, the amount of nitrite produced in the system was likely less than 1.0 μM.

The amount of peroxynitrite detected in the system was also invariant (Fig. 4.9). Since this method may be suitable for the detection of intracellular species rather than extracellular species [184] due to the accumulative characteristic of

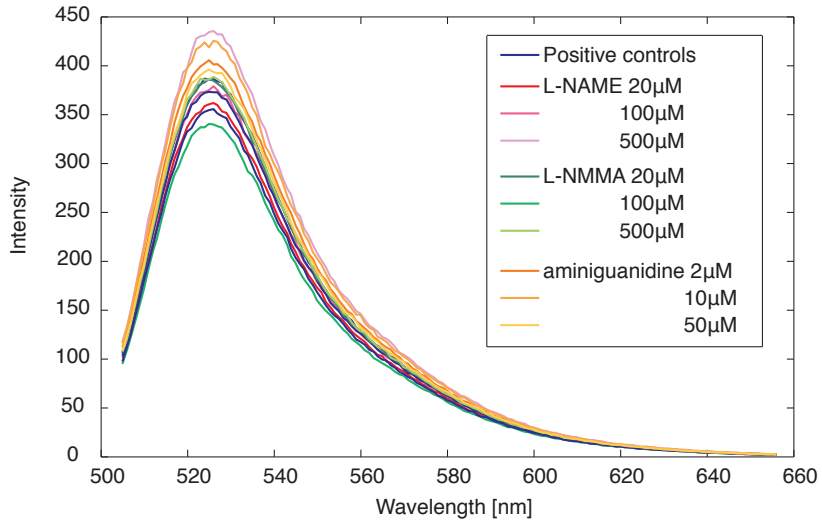

Figure 4.9: Inhibitory test of peroxynitrite production from activated THP-1 cells. The cell stimulation procedure was as described in Section 2.5.3. (A) 30 minutes before the addition of the differentiation stimuli, the cells were pretreated with inhibitors. After changing the medium to HBSS, the inhibitors were added for 30 minutes before the activation. After 1.5 hours, 100 μM DHR123 was added followed by another 1 hours incubation. The supernatants were collected and the amount of peroxynitrite was detected on a spectrophotometer with excitation and emission wavelengths of 500 nm and 536 nm respectively, and excitation and emission slit widths of 2.5 nm and 3.0 nm, respectively. The experiment was performed once.

rhodamine 123 in mitochondria [185], the amount of peroxynitrite exposed to the extracellular space was possibly negligible.

No effect of the NOS inhibitors on the superoxide anion production from activated cells was observed (Fig. 4.10) in single use of the inhibitors or in combination.

Consequently, the superoxide anion production was not influenced by nitric oxide or peroxynitrite under our experimental conditions.

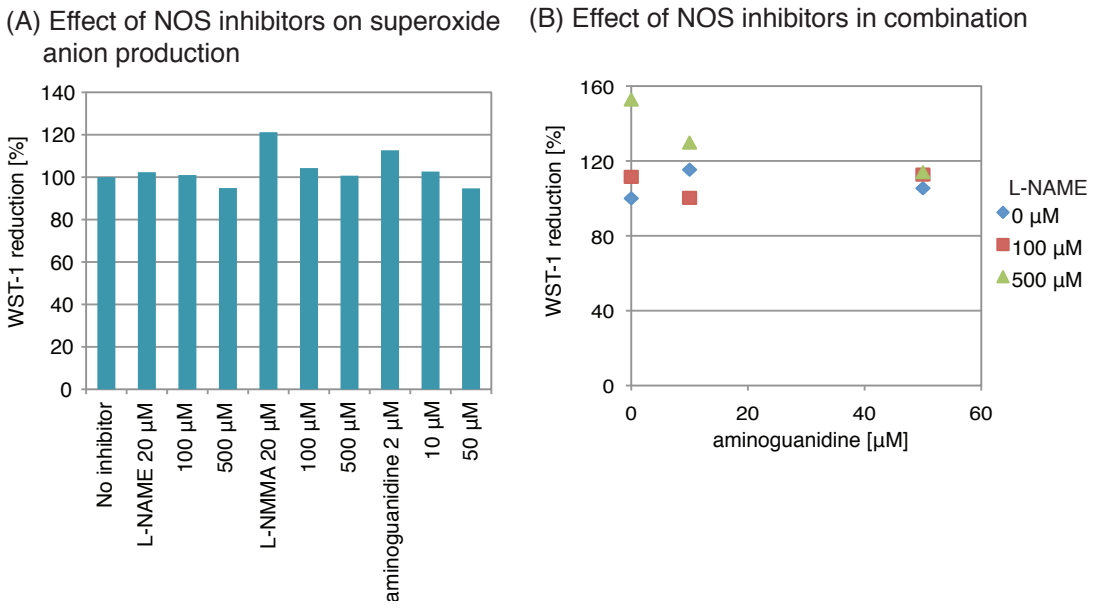

Figure 4.10: Effect of NOS inhibitors on superoxide anion production from activated THP-1 cells. The cell stimulation procedure was as described in Section 2.5.3. 30 minutes before the addition of the differentiation stimuli, the cells were pretreated with inhibitors. After changing the medium to HBSS, the inhibitors were added for 30 minutes before the activation. After 4 hours, the supernatants were collected for superoxide anion production assay using WST-1 colorimetric method. (A) Single use of the inhibitors, (B) L-NAME and aminoguanidine were used in combination. WST-1 reduction refers to the spectrophotometric absorbance normalized to the value of stimulated cells without the inhibitor in each experiment. Both (A) and (B) experiments were carried out once.

PI3K and PKCβ inhibitor For the activation of THP-1 cells, PMA is employed to activate protein kinase C (PKC) which promotes the phosphorylation of cytosolic NADPH oxidase subunits [89]. Since this activation of PKC by PMA occurs via phosphotidyl inositol-3 kinase (PI3K) signaling pathway [63, 66], the effect of PI3K inhibitors, wortmannin and LY294002, on cell activity was examined.

Wortmannin is a fungal metabolite originally identified as an antifungal agent [186] and inhibits PI3K, mitogen-activated protein kinase (MAPK) (which can be activated by TNF-α or IFN-γ and is involved in one of the important pathway for the activation of NADPH oxidase [124, 149]) and myosin light-chain kinase (MLCK) [187]. Thereby wortmannin inhibits the respiratory burst [188–190] and the stimulated locomotion of phagocytes [191].

LY294002 is a specific inhibitor of PI3K. Although the inhibitory effect of

LY294002 is weaker compared to that of wortmannin, LY294002 is still widely used due to its stability [192].

50 μM LY294002 inhibited constantly the cell adhesion to the substrate, agreeing with the reported fact that this inhibitor prevents IFN-induced adhesion of THP-1 cells and human monocytes [149, 193]. Therefore the measurement of superoxide anion production with the inhibition by LY294002 was not carried out.

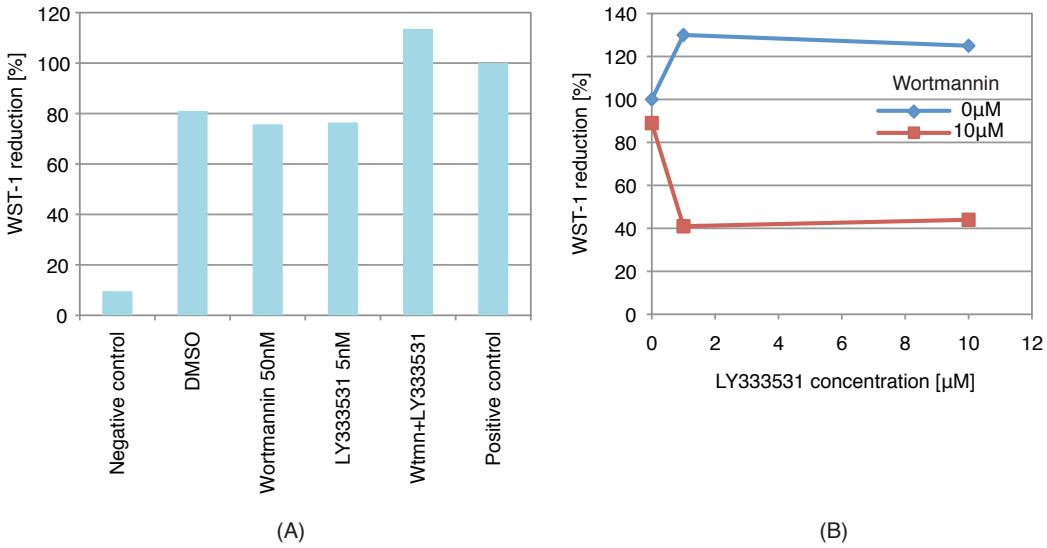

Figure 4.11: Effect of wortmannin and LY333531 on superoxide anion production from activated THP-1 cells. The cell stimulation procedure was as described in Section 2.5.3. 30 minutes before the addition of the differentiation stimuli, the cells were pretreated with inhibitors. After changing the medium to HBSS, the inhibitors were added for 30 minutes before the activation. After 4 hours, the supernatants were collected for superoxide anion production assay using WST-1 colorimetric method. (A) Single and combined use of the inhibitors at low concentration, (B) concurrent use of both inhibitors at high concentrations. WST-1 reduction refers to the spectrophotometric absorbance normalized to the value of stimulated cells without the inhibitor in each experiment. The experiments in (A) and (B) were carried out once.

LY333531 is a specific PKCβ inhibitor. The contribution of the PKCβ activation to phosphorylation of cytosolic NADPH oxidase subunits in THP-1 cells is disturbed by LY333531 [154, 194], thereby this inhibitor reduces NADPH oxidase activity [195].

The single use of wortmannin or LY333531 exhibited little inhibitory effect. This may due to the addition of their solvent DMSO (Fig. 4.11(A)) since the levels of these inhibitions were comparable. The concurrent use of wortmannin and

LY333531 in low dose did not show any inhibitory effect. Thus, the effect of these inhibitors at these concentrations were negligible.

Wortmannin at high concentration (10 μM) showed slight inhibitory effect on superoxide anion production in combination with LY333531 (1μM or 10μM) (Fig. 4.11(B)) .

It has been reported that wortmannin of high concentration (100 nM or 1280 nM) was necessary for inhibition of MAPK or superoxide anion production induced by PMA [187, 196]. However, the concentrations of these inhibitors, at which the superoxide anion production decreased in our experiments, were much too high compared to the reported concentrations in literatures [149, 187, 194, 196]. Excess of these inhibitors may evoke side effects in cellular function. Therefore the current measurements with these inhibitors were not carried out.

Staurosporine Staurosporine is known as a protein kinase inhibitor. Though it may inhibit different protein kinases, staurosporine works as a selective protein kinase C inhibitor at lower concentration [197]. Superoxide anion production from activated phagocytes is inhibited by staurosporine [197–199]. Since protein kinase C induces the phosphorylation of cytosolic NADPH oxidase subunits, p47phox [146,197] and p67phox [72], the presence of staurosporine prevents these proteins from binding to each other and translocating to the plasma membrane, resulting in blocking of the assembly of NADPH oxidase.

To examine the inhibitory effect of staurosporine (Sigma-Aldrich), superoxide anion release from activated THP-1 cells depending on different timing of the addition was compared. The cell stimulation was based on the protocol described in Section 2.5.3, except for the addition of the inhibitor.

THP-1 cells were differentiated with/without staurosporine at different concentrations. In both cases, the samples were pretreated with staurosporine for 1 hour in HBSS before the cell activation by PMA. The cells exposed to staurosporine during the differentiation showed the increase of lamellipodia and the loss of cluster formation for elevated staurosporine concentration (Fig. 4.12).

The superoxide anion production from the cells was dependent on the concentration of staurosporine, but not on whether cells were preincubated with staurosporine during differentiation (Fig. 4.13). The addition of this inhibitor before the PMA activation was sufficient to inhibit superoxide anion production.

The WST-1 reduction upon the inhibition of staurosporine reached asymptote for concentrations $\geq$10 nM. Thus the inhibitory test in the current measurement was conducted with 10 nM staurosporine.

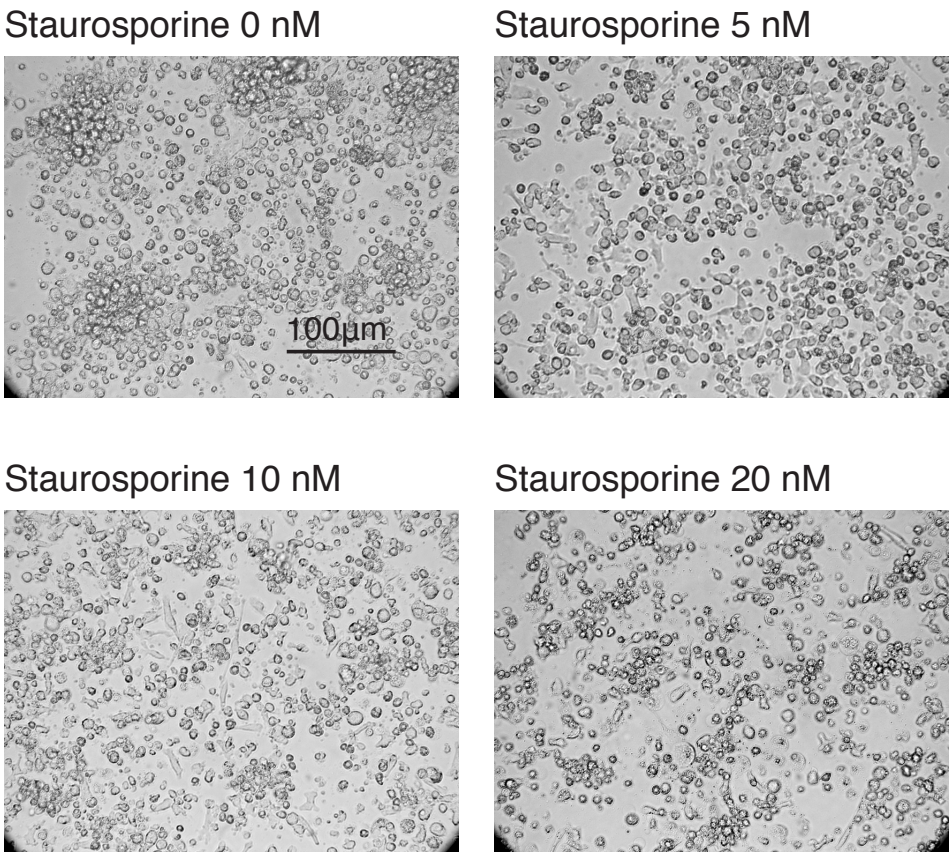

Figure 4.12: Morphology change in THP-1 on effect of different staurosporine concentrations. The cells were treated with staurosporine during the differentiation for 2 days. Images were acquired with Zeiss Axiovert 40CFL light microscope with 20× objective.

Additionally, the timing of the inhibitory effect of staurosporine was examined by adding the inhibitor after the cell activation. After the differentiation, the cells were activated in HBSS for the subsequent superoxide anion detection. After the cell activation, 10 nM staurosporine was added at different time points and the total superoxide anion production over 4 hours after the activation was measured. As shown in Fig. 4.14 staurosporine exhibited an immediate effect on superoxide anion production from the activated cells.

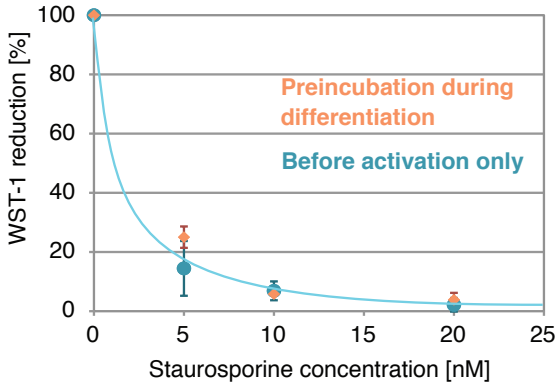

Figure 4.13: Inhibition of superoxide anion production from activated THP-1 cells using staurosporine at different concentrations. The cells were differentiated as described in Section 2.5.3 with ■, or without staurosporine ■. In both cases, staurosporine was added after the cell differentiation in HBSS. After 1 hour incubation, the cells were activated and the amount of superoxide anion produced from the cells for the following 4 hours was measured colorimetrically using WST-1. WST-1 reduction refers to the spectrophotometric absorbance normalized to the value of stimulated cells without the inhibitor. Staurosporine added was 0, 5, 10, 20 nM. The experiments were performed twice in duplicate.

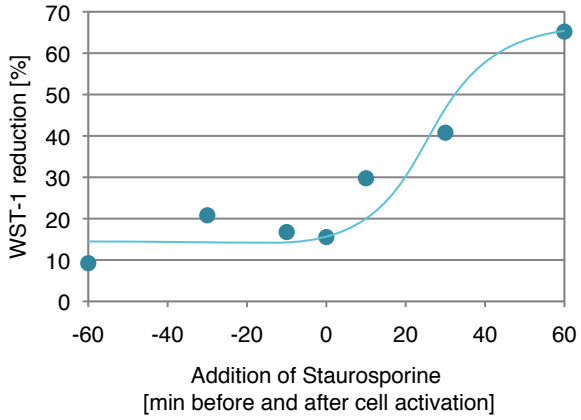

Figure 4.14: Addition of staurosporine at different time points before and after cell activation. To the cells differentiated according to the protocol in Section 2.5.3, 10 nM staurosporine was added in HBSS at 60, 30, 10 minutes before the activation, simultaneously with the activator, and 10, 30, 60 minutes after the activation. Following by 4 hours incubation of each well, the samples were collected for colorimetric assay using WST-1. WST-1 reduction refers to the spectrophotometric absorbance normalized to the value of stimulated cells without the inhibitor. The experiment was conducted once.

4.2.2 Inhibition studies on current measurement in fuel cell

To investigate the source of the current generation, using the NADPH oxidase inhibitors discussed in Section 4.2.1, the effect of these inhibitors on the current generation in the biofuel cell was examined. The concentration of inhibitors represented the effective amount necessary for maximum inhibition of WST-1 reduction by superoxide anion produced by activated THP-1 cells. The NADPH oxidase inhibitors used for the experiments were 100 U/ml superoxide dismutase (SOD), 5 μM diphenylene iodonium (DPI), 10 nM Staurosporine, and 40 μM $ZnCl_2$ (all Sigma-Aldrich). Additionaly the effect of 100 μM iNOS inhibitor L-NAME (Sigma-Aldrich) on the current was verified. The standardized procedure was as described in Section 2.5.4. The differentiated THP-1 cells on the electrode were placed in the anodic compartment of the fuel cell. The activator PMA was added after the current stabilized and the inhibitors were added after a clear increase in current.

No background current induction by inhibitors

To determine the background current induced by the addition of inhibitors, current generation in the absence of cells on the electrode was examined in a same manner as in Section 3.2.1 (Fig. 4.16 grey lines). After the current stabilized, the activator PMA was added to the anodic compartment (Fig. 4.16, grey solid arrows) followed by the addition of inhibitors (Fig. 4.16, grey dashed arrows). The addition of the inhibitors to the anodic compartment induced no considerable current change, indicating that the inhibitors generate no substantial electrical current.

Inhibition of superoxide anion and its derivatives

SOD catalyzes the reaction of superoxide anion to hydrogen peroxide ($2\,O_2^- \cdot + 2\,H^+ \longrightarrow O_2 + H_2O_2$) and reduces the amount of superoxide anion in the system. The addition of SOD decreased the current in the fuel cell (Fig. 4.16(A)), indicating a participation of the superoxide anion in the current production. However, on the addition of SOD, the current only decreased to 50% of the maximum, whereas the amount of WST-1 reduction decreased to 10% of the maximum (Fig. 4.16(F)). Since hydrogen peroxide, the product of the catalytic reaction, can oxidize or reduce a variety of inorganic ions in aqueous solution, hydrogen peroxide could contribute to the remaining current. To examine the contribution of hydrogen peroxide to the current flow, catalase was added to the

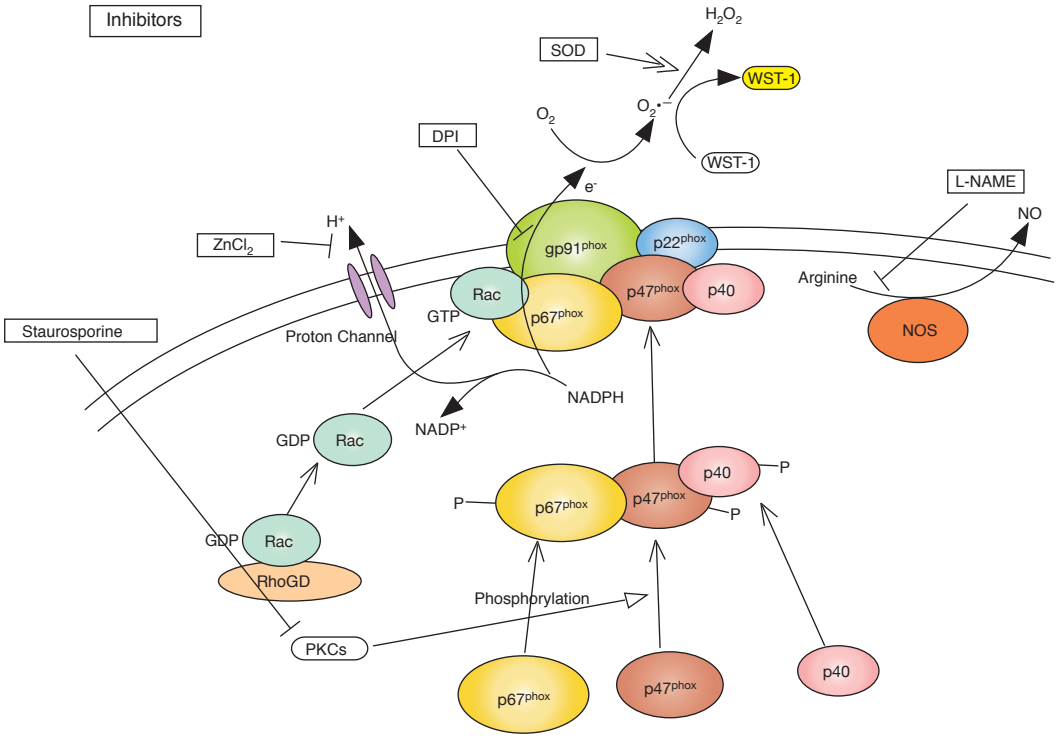

Figure 4.15: Schematic illustration of NADPH oxidase assembly and inhibition routes. Upon differentiation NADPH oxidase subunits are expressed abundantly. Upon activation the cytosolic subunits (p67phox, p47phox, p40phox and RacGTP) are phosphorylated, assemble, and translocate to the membrane-bound subunits (gp91phox, p22phox). Completely assembled NADPH oxidase oxidizes NADPH in the cytosol to $NADP^+$ and electrons are transported to the extracellular space. The action of inhibitors SOD, L-NAME, DPI, staurosporine, and $ZnCl_2$ is also indicated.

anodic compartment after SOD, to catalyze the reaction of hydrogen peroxide to water and oxygen. The addition of catalase did not cause any significant change in the current, thus we conclude that hydrogen peroxide does not contribute to the current production under our experimental conditions. The different inhibitory effect of SOD in the superoxide anion production and the current generation from the activated cells will be further discussed in Chapter 5.

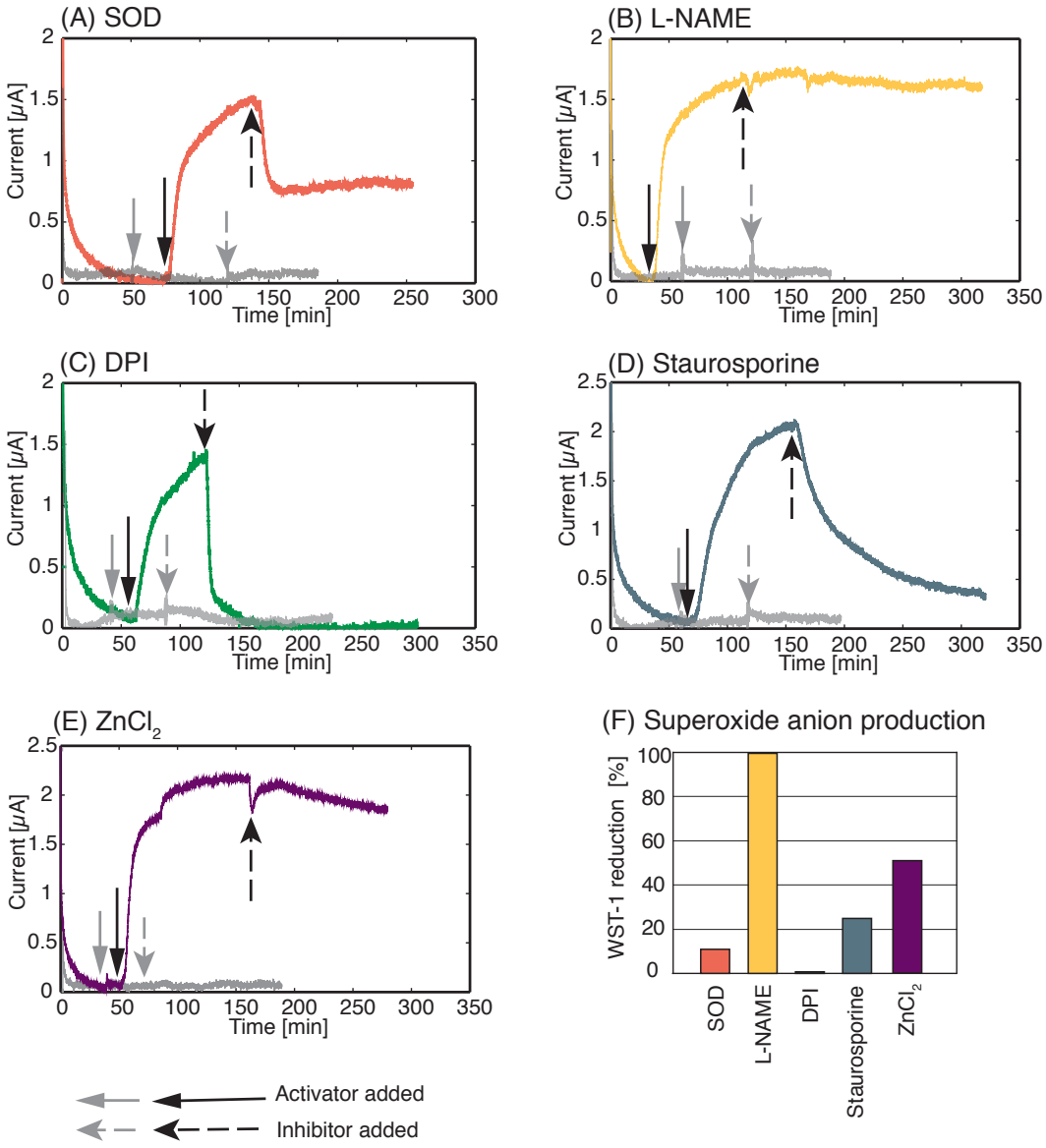

Figure 4.16: Inhibitory effects on current generation in the fuel cell. After cell differentiation and activation as in Section 2.5.4, inhibitors were added to the anode fluid. Inhibitors used were (A) 100 U/ml SOD, (B) 100 μM L-NAME, (C) 5 μM DPI, (D) 10 nM Staurosporine, and (E) 40 μM $ZnCl_2$. For each inhibitory test the current without cells on electrodes was measured ((A-E), grey lines). Solid arrows indicate addition of the activator PMA, dashed arrows indicate addition of inhibitors. (F) Parallel experiment in the culture well for superoxide anion detection from activated cells. After the differentiation, the cells were incubated with the inhibitors used above at the same concentration in HBSS for 1 hour. Then the activator was added and the superoxide anion production was measured colorimetrically using WST-1. WST-1 reduction refers to the spectrophotometric absorbance normalized to the value of stimulated cells without the inhibitor in each experiment.

Inhibition of nitric oxide and its derivatives

The activation of NADPH oxidase elicits not only superoxide anion release, but also the production of nitric oxide through inducible nitric oxide synthase [172], and thus the formation of another reactive species, peroxynitrite [176]. These species are reactive and could also influence the current. As described in Section 4.2.1, the nitric oxide production from THP-1 on stimulation was not observed and the NOS inhibitors did not influence superoxide anion production from the cells. The effect of NOS inhibitor on the current generation in the fuel cell was examined for confirmation.

Since the addition of L-NAME did not change the current (Fig. 4.16(B)), current production was not influenced by nitric oxide or peroxynitrite under our experimental conditions.

Inhibition of electron transfer by NADPH oxidase subunit

DPI binds to flavoproteins and suppresses reactions in which these proteins are involved. NADPH oxidase and iNOS [82] both possess flavoprotein within their structures, thus DPI suppresses the production of superoxide anion and nitric oxide in phagocytotic cells [158]. The suppression of superoxide anion production is caused by DPI blocking the reduction of FAD in the plasma membrane component of NADPH oxidase [163], thereby inhibiting electron transport to the extracellular space.

The addition of DPI suppressed the current generation by activated macrophages (Fig. 4.16(C), suggesting that superoxide anion and/or nitric oxide might take part in the current production in the fuel cell. However, according to our experimental results with L-NAME described above, nitric oxide does not have any influence on the current, which proved that neither nitric oxide nor peroxynitrite, the derivative of superoxide anion and nitric oxide, served as an electron mediator between the cells and the electrode. Hence, the current decrease upon inhibition by DPI supports an active role of an electron transfer of NADPH oxidase in the current production.

Inhibition of assembly of NADPH oxidase

Assembly of the NADPH oxidase complex in activated macrophages is necessary for current generation, as evidenced by the difference in the NADPH oxidase activity in each differentiation/activation stage as shown in Fig. 3.1 and 3.3. PMA is an activator of protein kinase C (PKC) known to phosphorylate

cytosolic NADPH oxidase subunits, p47phox and p67phox [146, 200]. Without phosphorylation these proteins do not build up a complex that is translocated together to the plasma membrane to assemble the NADPH oxidase complex. When cells were differentiated but not activated, no current production was observed although the NADPH oxidase subunits were sufficiently expressed (Fig. 3.1 and 3.3). This may be because the NADPH oxidase complex had not yet been assembled completely since the phosphorylation of p47phox and p67phox is possibly first triggered upon activation by PMA.

Staurosporine is one of the most potent and widely used inhibitors of protein kinases, and at low concentrations selectively inhibits the activity of PKC [201]. The presence of this inhibitor inactivates PKC, thus blocks the translocation of these subunits to the plasma membrane components by inhibiting their phosphorylations. The assembled NADPH oxidase complex is not permanently stable since cytosolic subunits dissociate from the membrane-bound components through hydrolyzation of GTP-bound Rac [82]. The addition of staurosporine gradually stops the assembly of NADPH oxidase and only dissociation of the complex continues. Thus the amount of electron transfer through the NADPH oxidase will drop with the decrease of fully assembled NADPH oxidase.

Staurosporine did not abolish the WST-1 reduction completely (Fig. 4.16(F)), and the current generated from activated macrophages decayed slowly on addition of staurosporine in the system (Fig. 4.16(D)). This gradual change in the current reflected the successive change in the rate of asssembly and disassembly of NADPH oxidase. These findings prove again that the assembled NADPH oxidase is essential for current production in the fuel cell.

Inactivation of NADPH oxidase via depolarization

$ZnCl_2$ inhibits NADPH oxidase activity indirectly by blocking the proton channel, whose activity is coupled with NADPH oxidase activity due to the charge compensation. The inhibition of proton efflux during the activation of NADPH oxidase induces a transient depolarization of membrane potential [92], that reduces gradually NADPH activity. Indeed the addition of $ZnCl_2$ decreased the current slowly (Fig. 4.16(E)).

This fact supports that NADPH oxidase is the source of the current generation.

If the differentiated cells were first pretreated with $ZnCl_2$ for 2 hours in HBSS before cell activation, the current did not increase as without pretreatment with $ZnCl_2$ (Fig. 4.17). 2 hours preincubation is presumed to be long enough to block most of the proton channels. However, the increase of the current on PMA

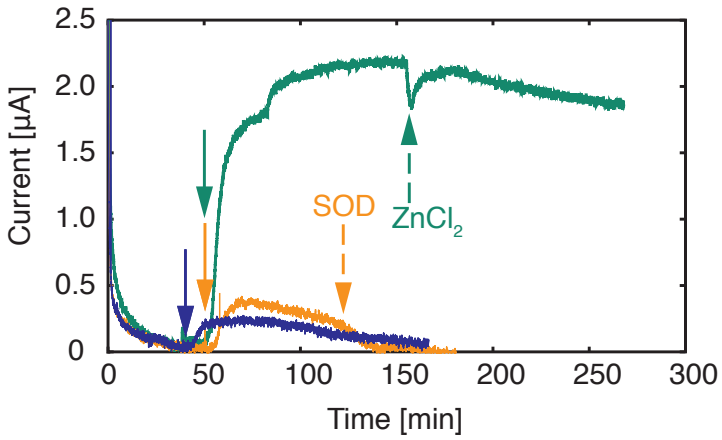

Figure 4.17: Effect of preincubation of $ZnCl_2$ before the cell activation. In the experiment ■ and ■, after cell differentiation according to Section 2.5.4, 40 μM $ZnCl_2$ was added in HBSS followed by 2 hours incubation. The cells on the electrode were then placed in the fuel cell and the current was measured. In the experiment ■, 100 U/ml SOD was added after the current increase on activation stabilized. In the experiment ■, the differentiated cells were placed directly in the fuel cell setup without preincubation with $ZnCl_2$. After the current increase on PMA activation stabilized, 40 μM $ZnCl_2$ was added.

activation was obvious. Together with the non-complete reduction of WST-1 by $ZnCl_2$ (Fig. 4.16(F)), this fact may support a model with potentially alternative charge compensation by potassium channels [169, 202, 203].

4.3 Summary

In the previous chapter, the link between the current generation in the fuel cell and NADPH oxidase activity has been substantiated. To investigate whether electron transfer by NADPH oxidase to extracellular space is the source of the current flow, chemicals with different inhibitory effects were applied during current measurement in the fuel cell. After optimizing the concentration and the timing of addition of the inhibitors by verifying the effects on superoxide anion production from activated THP-1 cells, these inhibitors were added to the anodic compartment while activated cells generated the current.

The current change upon addition of each inhibitors corresponded to the expected inhibition mechanism. Consequently, the activated NADPH oxidase was proven to be the origin of the electrons transferred to the electrode.

Chapter 5

Analysis of Electron Transfer between Cells and Electrode

In the previous chapter, the current generated in the fuel cell was proved to originate from the electron transfer through NADPH oxidase in activated THP-1 cells. Here, possible electron paths between activated cells are the anode is analyzed by the results of inhibitory tests, the estimation of the amount of superoxide anion produced from activated cells, and the difference in WST-1 reduction in the anodic compartment during the current measurement.

Between the cell membrane and the electrode there are several conceivable electron pathways; (i) direct electron transfer, (ii) indirect electron transfer through (a) superoxide anion, (b) derivatives of superoxide anion, (c) other molecules mediating electron transfer.

The inhibitory test using SOD showed that the current decreased to 50% of the maximum on the addition of this inhibitor (Fig. 4.16(A)), whereas the superoxide anion production decreased to 10% of the maximum (Fig. 4.16(F)). The possibility of an influence of hydrogen peroxide, a derivative of superoxide anion, was excluded under our experimental condition (Section 4.2.2). This fact suggests an additional route of electron flow besides superoxide anion.

The contribution of superoxide anion to the current flow was demonstrated in Section 4.2.2. Although both SOD and DPI reduced the superoxide anion production (Fig. 4.16), current suppression upon inhibition by DPI was stronger than that by SOD. SOD prevents the electron flow mediated by superoxide anion, whereas DPI is cell-permeable and inhibits the electron flow through the plasma membrane by binding to a NADPH oxidase subunit. This suggests the existence

of an additional route of electron flow different from superoxide anion.

To evaluate the contribution of superoxide anion and its derivatives to the current production, the amount of current measured in our biofuel cell (1.5-2 μA/10^6 cells seeded) was compared to the expected amount of current based on the superoxide anion produced from activated cells. The amount of superoxide anion produced can be estimated from the spectrophotometrical measurement of WST-1 reduction.

WST-1 reduction by superoxide anion was calibrated using hypoxanthine/ xanthine oxidase as described in Section 2.3. Superoxide anion ($O_2^- \cdot$) was generated from the conversion of hypoxanthine to uric acid by xanthine oxidase [137]. From 1 mol hypoxanthine the production of 2 mol superoxide anion is expected (Table 5.1, *(B)*). After 60 min the reaction was completed, and the absorbance of WST-1 formazan was measured with a spectrophotometer at 450 nm (Table 5.1, *(C)*). The reduction of WST-1 to WST-1 formazan requires two electrons [204], i.e. two superoxide anions. The amount of superoxide anion used for the WST-1 reduction for a specific amount of hypoxanthine was estimated (Table 5.1, *(D)*)by Lambert-Beer's law; $E_\lambda = c\epsilon l$ [132], where E_λ is the extinction absorption, c is the concentration of WST-1 formazan, ϵ is the extinction coefficient (WST-1 formazan, 37000 at 438 nm) and l is the optical path length (10 mm). The ratio of superoxide anion detected by WST-1 reduction to the superoxide anion produced from hypoxanthine was calculated (Table 5.1, the rightmost column). This value was plotted in Fig. 5.1.

Hypoxanthine [μM] *(A)*	$O_2^- \cdot$ produced from hypoxanthine [nmol/1.5 ml] *(B)*	Absorbance [A.U.] *(C)*	O_2^- detected by WST-1 reduction [nmol/1.5 ml] *(D)*	The ratio of *(C)/(A)* [%]
10	30	0.127	10.3	34.3
50	150	0.574	46.5	31.0
100	300	1.212	98.3	32.8
200	600	2.660	215.7	35.9
500	1500	3.663	297.0	19.8

Table 5.1: Calibration of the rate of superoxide anion used for WST-1 reduction. As described in Section 2.3, dissolved hypoxanthine *(A)* was converted by xanthine oxidase into uric acid producing superoxide anion *(B)* in UHQ containing 100 μM WST-1. After 60 min reaction time, the reduction of WST-1 was measured with a spectrophotometer at 450 nm *(C)*.

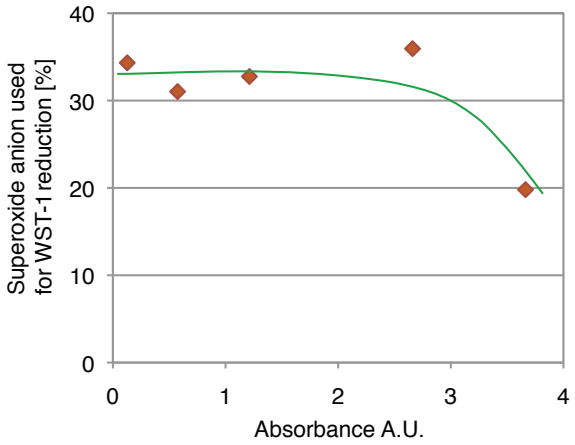

Figure 5.1: Fraction of superoxide anion detected by WST-1 reduction in hypoxanthine/xanthinoxidase system, normalized to the superoxide anion produced from hypoxanthine.

The amount of the superoxide anion detected by WST-1 reduction was about one third of the amount of superoxide anion produced in the system in the linear range. Since our measurements with cells were in the linear range throughout this thesis, we assume that one third of the superoxide anion produced from activated cells was used for WST-1 reduction as well. This is plausible since the rate constant of the reaction of WST-1 with superoxide anion ($\approx$3-4$\times10^4$ $M^{-1}sec^{-1}$) is expected to be lower than that of spontaneous conversion of superoxide anion to hydrogen peroxide ($\approx1\times10^5$ $M^{-1}sec^{-1}$) [131].

Calculating with a representative spectrophotometric absorption value of the reduced WST-1 (1-1.5) and accounting for the control measurement, the superoxide anion production of THP-1 cells in our experiments was estimated to be 1.4-2 nmol/min/10^6 cells.

This value is higher than the superoxide anion production of THP-1 cells reported in literature (0.05-0.5 nmol/min/10^6 cells) [120,205,206]. The superoxide anion detection methods using cytochrome c, chemiluminescence, or WST-1 are indirect measurements and due to the non-specificity of indicators and the reoxidation of indicators the reliability of these detection methods is an issue [207]. Moreover, due to the complexity of signal pathways within cells and the difference in cell activation stimuli employed in each study the activation degree of the cells responding to various stimuli has not been well-examined. Therefore, the direct comparison of superoxide anion release between different reports is

difficult. In our experiments, if all electrons flowing from cells to superoxide anions were caught and transferred to the electrode, a current of 1.6-2.4 μA/10^6 cells seeded would be produced in the biofuel cell, which matches roughly the current measured with activated macrophages in our setup (1.5-2 μA/10^6 cells seeded).

Whole-cell patch-clamp experiments showed that the amount of current flow from NADPH oxidase corresponds to the amount of superoxide anion release from granulocytes (10-20 pA per cell current measured, 10 nmol/min/10^6 cells superoxide anion produced) [106, 208]. In patch clamp experiments NADPH, oxidase substrate, or GTP-γS, nonhydrolyzable analogue of GTP, was added to stabilize the measurements. Without adding these chemicals, less electron flow from cells was detected. Furthermore, the yield of electron transfer from cells in patch clamp experiments should be in any case better than that between cells and the anode in our biofuel cell due to lower system impedance. Thus, for our experimental condition, the contribution of superoxide anion to the current generation is expected to be much lower. However, the current measured in the biofuel cell is larger than expected, indicating also the existence of an additional route of electron flow from the cell to the electrode independent of superoxide anions.

The current measurement with THP-1 cells was performed as described in Section 2.5.4, except the anodic fluid contained 100 μM WST-1 (Fig. 5.2(A)).

The presence of WST-1 in the anodic fluid during the current measurement did not change the current increase after the cell activation. The scavenging of superoxide anion for the WST-1 reduction did not cause substantial difference in the current generation in the fuel cell. In this experiment, slightly higher current was observed when the anodic fluid contained WST-1. This is assumed to be a variation in the cell activity upon the stimulation, however, the possibility that WST-1 can serve as a mediator in the fuel cell can not be excluded.

The WST-1 reduction by superoxide anion produced from activated cells were measured in the anodic compartment of the fuel cell setup both with open and closed circuit conditions (Fig. 5.2(B)).

The reason for the lower amount of WST-1 reduction in the fuel cell setup compared to that in culture wells may be a difference in the amount of cells on the substrates. Since the electrode was placed vertically in the fuel cell, the rinsing of non-adherent cells after differentiation was more effective than for the sample in the culture well.

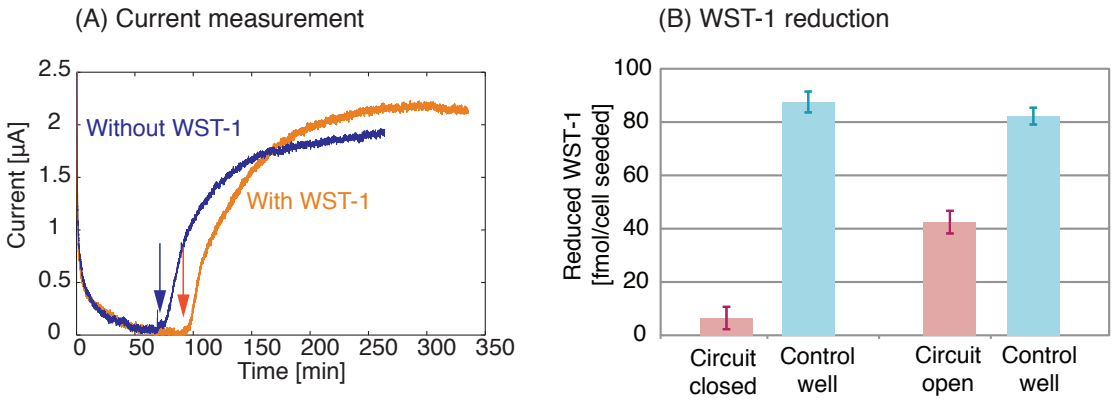

Figure 5.2: Current measurement with WST-1 in anodic compartment. (A) THP-1 cells were differentiated and the current generation in the fuel cell upon the activation was measured as described in Section 2.5.4. In the experiment of ■, the anodic fluid contained 100 μM WST-1 additional to the differentiation stimuli from the beginning of the current measurement. The experiment ■ refers to the ordinary current measurement without WST-1 addition in the anodic compartment. At the time point of the solid arrow, the activator PMA was added to the anodic compartment. (B) WST-1 reduction in the anodic compartment in the fuel cell. Either after the current measurement with closed circuit as in (A) or after 4 hours with open circuit condition, the reduction of WST-1 in the anodic fluid was examined. ■ refer to the absorbance of reduced WST-1 from the fuel cell sample. ■ were control measurement conducted simultaneously in culture wells. During the fuel cell measurement, the electrical circuit was; left: closed, right: open. The independent experiments with closed circuit and with open circuit were conducted three times and twice, respectively.

When the electric circuit was closed, less WST-1 reduction was observed. The electrons not used for the WST-1 reduction might be available for the current generation.

The difference in the amount of WST-1 reduced in the anodic compartment between the open and closed circuit was ≈45 nmol (calculated from Fig. 5.2(B)), thus ≈90 nmol electrons vanished by closing the electrical circuit. Meanwhile, the amount of electrons generating the current during the measurement with WST-1 in the anodic compartment was ≈220 nmol (integrated current signal after the activation in Fig. 5.2(A)).

Considering the change in the reaction kinetics due to the different conditions in both cases, evidence is provided that superoxide anion did not suffice to generate the current measured in the fuel cell. Thus, this analysis reinforces the hypothesis of an additional route of electron flow apart from superoxide anion.

Chapter 6

Optimization of Current Measurement

In previous chapters a biofuel cell whose current flow was driven by activated macrophages has been demonstrated. The experiments in this thesis focused mostly on the investigation of the source of the current generated. Thus, some materials and parameters should be further optimized for improving the measurement system and the performance of the biofuel cell.

To allow one to compare results of modification of the fuel cell such as changing materials, constancy of components including cells is desired. Under the constant conditions, maximum yield of the current generation in the fuel cell can be explored. Moreover, lifetime of the fuel cell has to be extended.

In this chapter, requirements for stabilizing current measurements, improving the performance of the fuel cell, and prolonged lifetime of the fuel cell are discussed, and some experiments carried out to examine their influence on the measurements are presented.

6.1 Stabilization of performance of biofuel cell

The variation of the current generated by activated THP-1 cells and measured in the fuel cell was high, therefore precise quantitative comparison of each experiment was difficult. Variations may be due to (i) the amount of cells adhering to the electrode, (ii) unspecific protein adsorption on the electrode, (iii) variation of parameters during the deposition of gold on the electrodes, and (iv) deterioration of the membrane of the fuel cell. Here, we discuss how one could control cell adherence and protein adsorption on the electrode.

6.1.1 Controlled cell adherence

Substrate coating

To reduce the variation in cell adhesion, coating of electrodes with a cell adhesion molecule may help. Fibronectin is an extracellular matrix glycoprotein used as a general cell adhesion molecule to anchor cells. Thin coatings of fibronectin are widely applied in various experiments to promote cell attachment [58], thus the attachment of THP-1 cells on fibronectin coating was examined. Culture wells were coated with 1 ml of 10 μg/ml fibronectin (Sigma-Aldrich) in PBS overnight. THP-1 cells were seeded in wells with and without fibronectin coating and were differentiated. After 2 days, the culture wells were washed with PBS to rinse off non-adherent cells, and then the attachment of the cells was investigated under the light microscope.

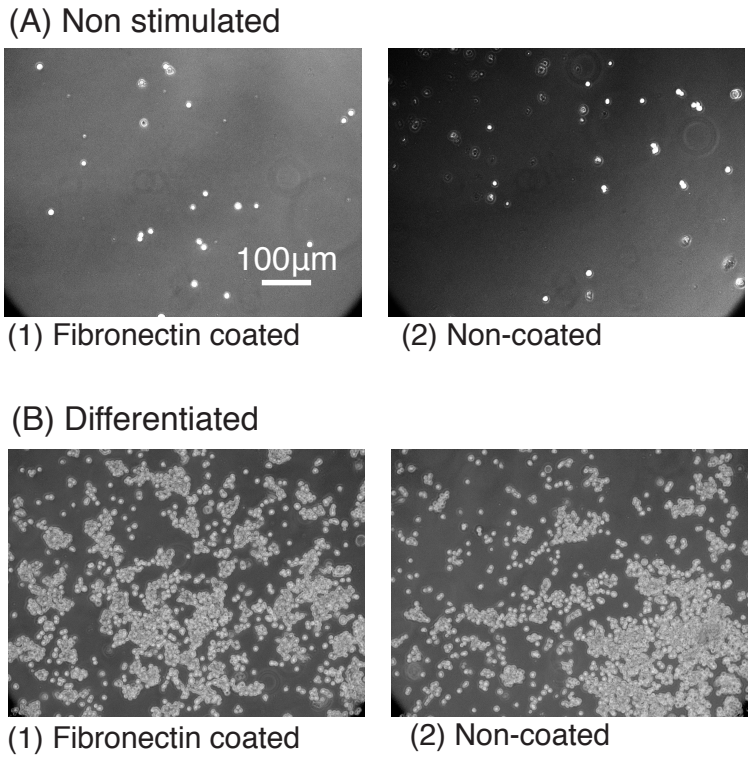

Figure 6.1: THP-1 cells seeded on (1) fibronectin coated and (2) non-coated culture wells. The cells were incubated (A) without stimuli, or (B) with differentiation stimuli, for 2 days and the wells were washed with PBS twice. The phase contrast images were acquired with Zeiss Axiovert 40 CFL light microscope with a 10X objective.

No substantial change in cell attachment between coated and non-coated substrates was observed during cell differentiation (Fig. 6.1).

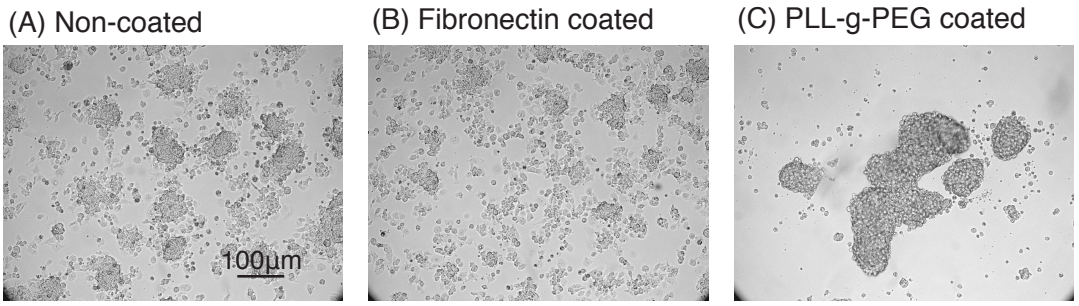

Figure 6.2: THP-1 cells seeded in culture wells with (A) no coating, (B) fibronectin coating, and (C) PLL-g-PEG coating, and incubated for 1 day with 50 nM PMA. Images were acquired with Zeiss Axiovert 40CFL light microscope with a 10X objective.

To confirm that the adherence of THP-1 cells may differ depending on the substrate, the cells were stimulated with only PMA in culture wells with different surface coating. Non-treated, fibronectin coated, and poly(L-lysine)-g-poly(ethylene glycol) (PLL-g-PEG) coated culture wells were examined. PLL-g-PEG is a comb-like graft copolymer and monomolecular PLL-g-PEG coatings are highly effective in reducing the adsorption of various proteins such as blood serum, heparinized blood plasma, fibrinogen and albumin [209]. A PLL-g-PEG coated culture well was prepared by incubating with 0.5 mg/ml PLL-g-PEG in Hepes[1] buffer overnight. THP-1 cells were seeded in culture wells with different coatings and 50 nM PMA was added. After 1 day incubation, the effects of these coatings were examined under the light microscope (Fig. 6.2). Although the cells activated by PMA showed adhesive feature, the attachment of the cells to the substrate was prevented by the PLL-g-PEG coating. Therefore the cells formed a big colony, binding each other. This result verified that THP-1 cells react to the chemical property of substrates, thus potential enhancement of cell activity via chemical surface modification should be further investigated.

Use of adherent cells

The use of the human monocytic cell line THP-1 allowed us to investigate the electron source of the current generation in the biofuel cell by inhibiting diverse differentiation phase. However, THP-1 cells become adherent only when differentiated. Cell differentiation is regulated by complex signal pathways, thus the level of cell adhesion varies in each experiment. Constant cell number may

[1]PLL-g-PEG solution was kindly provided by the group of Prof. Vörös, the Laboratory of Biosensors and Bioelectronics at ETH Zurich.

be realized by using already adherent cells. Therefore use of a macrophage cell line for the optimization of the system might be a good option.

6.1.2 Controlled protein adsorption on the electrode surface

When cells to be differentiated are seeded on a plain gold electrode, the unspecific adsorption of different proteins on the electrode is inevitable due to the high fraction of proteins in serum. The loss of sensitivity of biosensors utilizing enzymes due to low molecular weight serum components has been reported [53]. Especially biomolecules of $\leq$ 15 kDa cause apparent decrease in sensitivity [48]. Fibronectin, a cell adhesion molecule, has high molecular weight ($\approx$440 kDa), thus a homogeneous coating of the electrode may be obtained using this protein without impeding the electrical signal during the current measurement. THP-1 cells were seeded on two different electrodes. One electrode was a plain gold electrode fabricated as described in Section 2.5.4, another gold-coated electrode was further coated with fibronectin as described in Section 6.1.1. After 2 days differentiation, the current production upon activation was measured.

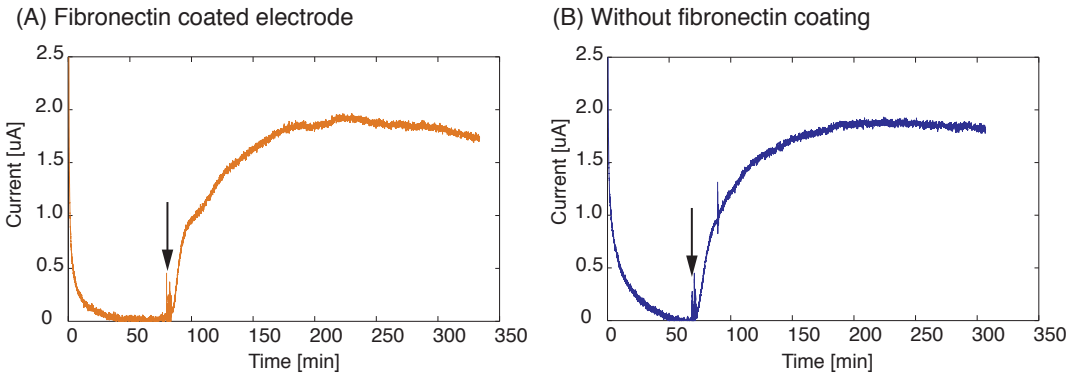

Figure 6.3: Current generation from THP-1 cells seeded in culture wells (A) with and (B) without fibronectin coating. The measurement was started with HBSS already containing LPS, TNF-α and IFN-γ in the anodic compartment. At the time point of the solid arrow, the activator PMA was added to the anodic compartment.

The current change with the cells on the fibronectin coated gold electrode resembled that of the non-coated gold electrode and no reduction in current was observed (Fig. 6.3). Thus an electrode coating with fibronectin is recommended for further experiments. However, a slight decay of the current was seen at the end of the measurement with the cells seeded on the fibronectin coating. The effect of this coating on the duration of cell activity has to be further investigated.

6.2 Improving performance of biofuel cell

6.2.1 Enhancement of cell activity

Glucose concentration

Glucose is a primary fuel for heterotrophs. Energy derived from glucose is stored mainly in the form of high-energy phosphate bonds in ATP, or other nucleotide triphosphates [58]. Various metabolic pathways are involved in the production and utilization of these high-energy intermediates.

The concentration of glucose influences also inflammatory responses of cells. High glucose treatment of THP-1 cells induced changes in the expression and secretion level of cytokines, chemokines and related molecules, such as IL-1β or IL-6 [210–212]. The level of p47phox translocation to the membrane has been shown to increase [213]. Consequently, increased superoxide anion production and induction of iNOS were observed in macrophages with high glucose concentration [214]. On the contrary, the inhibition of superoxide anion production from neutrophils with high glucose concentration has been reported [215].

Thus THP-1 cells were differentiated at different glucose concentrations, and superoxide anion production from the cells after activation was compared.

The measurement was based on the standardized protocol described as in Section 2.5.3. During the differentiation of the cells, 1, 2.5, 5, 10, 20 mM D(+)-glucose (Sigma Aldrich) was given to RPMI1640 media which contains 11.10 mM glucose. Superoxide anion production was measured at different time points following activation.

No tendency of any dependence on the glucose concentration was observed (Fig. 6.4). The normal turnover time for monocytes in vivo is 3 days [210], thus the 2 days incubation of cells with glucose should be long enough for the cells to exhibit reactions. Therefore we concluded that the glucose concentration had no effect on NADPH oxidase activation of THP-1 cells under our experimental conditions.

Chemical surface modification of substrate

Adhesion to extracellular matrices is known to modulate leukocyte activation [216, 217]. The presence of binding sites on the membrane is an indication of infection, at the same time these binding sites elicit signals that are transmitted into the cell (outside-in signaling) [216] and synergize to initiate phagocytotic

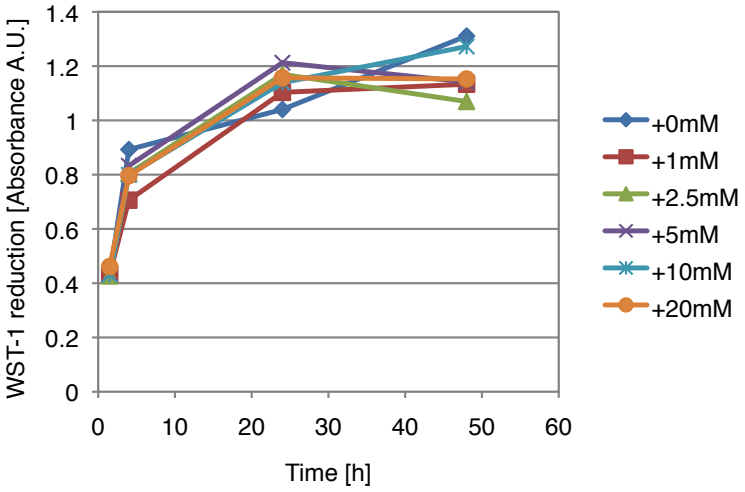

Figure 6.4: Superoxide anion production from THP-1 cells differentiated with higher glucose concentrations. The cells were differentiated as described in Section 2.5.3 with additional D(+)-glucose of 0 mM, 1 mM, 2.5 mM, 5 mM, 10 mM, and 20 mM. After 2 days incubation, the cells were activated and the superoxide anion production was measured using WST-1 colorimetric assay. Superoxide anion production was measured at 1.5, 4, 24, 48 hours after the cell activation. The experiment was performed once.

actions [218].

For instance, the enhancement of the phagocytic activity of leukocytes via fibronectin attachment has been reported [219]. Thus, the effect of substrate coating with fibronectin on superoxide anion production from activated THP-1 cells was examined.

Cell culture plate was coated with 1 ml of 10 μg/ml fibronectin in PBS overnight. THP-1 cells were seeded in wells with and without fibronectin coating and were stimulated differently as shown in Fig. 6.5. The superoxide anion production from the cells was detected as described in Section 2.5.3.

The superoxide anion production from the cells seeded on fibronectin coated wells was in same manner as that on non-coated wells and the level of superoxide anion production from the activated cells did not alter due to the fibronectin coating (Fig. 6.5). The fibronectin coating also did not change the current intensity (Fig. 6.3). Thus, the fibronectin coating did not enhance cell activity under our experimental condition.

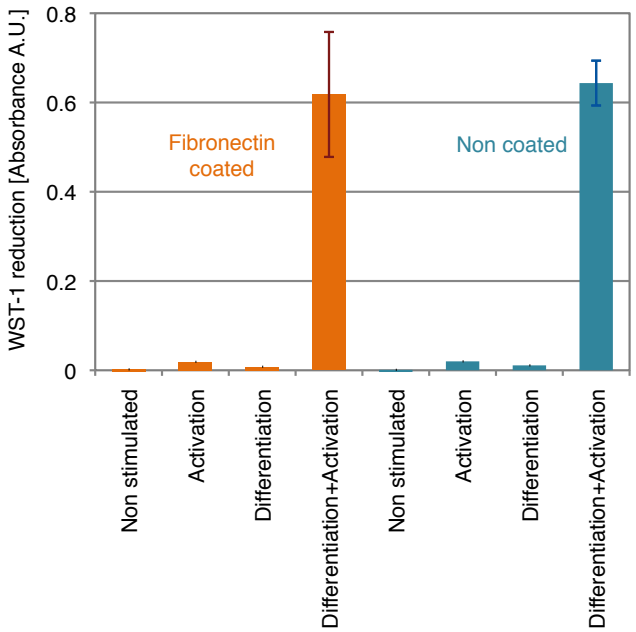

Figure 6.5: Superoxide anion production from THP-1 cells seeded in culture wells with ■ and without ■ fibronectin coating. From left: Untreated cells as negative control; Activation with 50 nM PMA; Differentiation with 300 ng/ml LPS, 20 ng/ml TNF-α, and 20 ng/ml IFN-γ; Differentiation+Activation in sequential order. Three independent experiments were carried out.

Environmental factors

pH change in the anodic compartment As mentioned in Section 2.4.1, the BDH membrane used in the experiments possesses a poor performance regarding to proton transfer. If the cell activity is higher than the capacity of proton transfer through the membrane, the proton release from the cells, which is coupled with the electron release via NADPH oxidase, may exceed the buffering capacity of the anodic fluid, causing acidification of the anodic fluid. Lowering pH induces an unfavourable environment for cell physiology and suppresses NADPH oxidase activity [220, 221].

To evaluate whether the membrane performance and the buffering capacity of the solution tolerate the proton release from activated cells, pH in the anodic fluid was examined during the current measurement. To determine if the pH change was acceptable for cell activity, phenol red was used as an indicator of the acidity of the fluid, since this method is facile and widely used in cell culturing. The differentiated cells on the anode were placed in the anodic compartment of the fuel cell, containing HBSS with phenol red (Invitrogen). The current generation

from the cells was measured as usual according to the regular protocol described in Section 2.5.4.

After 3 hours of current measurement, the color of HBSS was unchanged, suggesting the change in proton concentration was either within the proton transport capacity of the membrane or the buffering capacity of HBSS. Thus, the change in pH during the current measurement was assumed to be negligible.

Temperature and CO_2 concentration All experiments were carried out in ambient condition. Since cells are supposed to be maintained best at 37°C and 5% CO_2, the decline in the current (Fig. 3.3(C)) might be due to either a loss of cell activity or cell viability after a few hours under the experimental conditions. It is also reported that the superoxide anion production gradually increase between 25 °C and 32 °C with a sharp increases between 32-37 °C [222]. Therefore, the experimental environment could be further improved to prolong cell activity.

6.2.2 Improvement of electron transfer to/from electrodes

Oxygen in anodic compartment In our current setup the buffer in the anodic compartment had contact with ambient air and thus contained a certain amount of dissolved oxygen (≈8 mg/l) [223]. Generally, the anolyte should be deoxygenated, since oxygen is a very strong electron acceptor that reacts against the anode. However, mammalian cells need aerobic condition to survive. Therefore, maximization of the electron flow from cells to the anode has to be achieved in the presence of oxygen.

Mediators Throughout this thesis no mediator was intentionally employed in the system. However, to facilitate the electron transport from the electron donor to the electron acceptor, mediators may be introduced. Improved current yield in microbial biofuel cells and enzymatic fuel cells was successfully demonstrated by employing mediators in solution [13, 224] or immobilized on electrode surfaces [14, 225, 226]. For the optimal selection of mediators, more detailed electrochemical analysis would be necessary.

6.2.3 Improvement of electron transfer through electrical circuit

Selection of load resistance

The maximum power of a battery can be achieved when the external resistance and the internal resistance are equal (Jacobi's theorem). Our current measure-

ment in the fuel cell was conducted with an external load of 51 kΩ. The selection of this resistance value was validated by plotting power versus resistance (Fig. 6.6).

THP-1 cells were stimulated according to the standard protocol described in Section 2.5.4. Current and voltage between the electrodes were measured for different load resistances and the power was calculated according to $P = IV$.

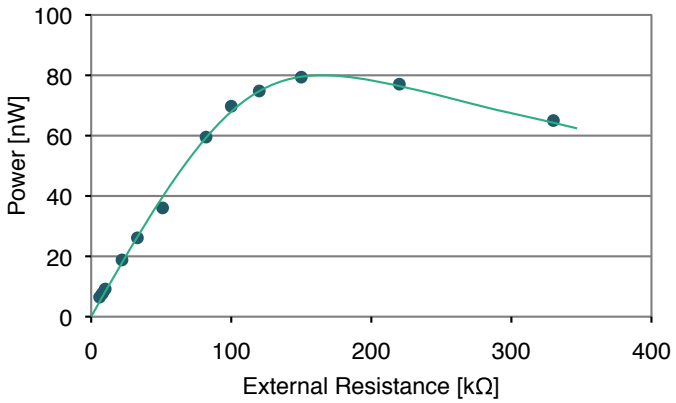

Figure 6.6: Power against load resistance in the fuel cell. The anode with THP-1 cells was prepared as described in Section 2.5.4. After the current stabilized following the rise upon PMA activation, the load resistance was varied and the corresponding current and voltage were measured to calculate the power.

Since maximum power was obtained around 150 kΩ, ideally the load resistance had to be selected at this value. However, the change in the current on cell activation was not easily observable due to low signal to noise ratio in the current measured. Therefore the load resistance was lowered to 51 kΩ and this resistor was used for the measurements throughout this thesis.

6.3 Lifetime of biofuel cell

Duration of cell activity

Without nutrition the cells cannot sustain their activity. Thus the addition of glucose may prolong the cell survival and thereby the NADPH oxidase activity of activated THP-1 cells. As described in Section 6.2.1, high glucose concentration did not enhance the NADPH oxidase activity in our experiments. No difference in the duration of superoxide anion production was observed as well (Fig.

6.4). Glucose is not membrane permeable without the assistance of transporter proteins and glucose has to be converted to its metabolite, pyruvate, to enter the mitochondria as a potential energy source. Hence adding pyruvate would be an alternative strategy to be investigated.

Cathodic compartment

In the cathodic compartment, oxygen is the final electron acceptor. In our setup, electrons were first captured by ferricyanide ions since the oxygen reduction rate in the absence of a catalyst is quite low relative to the reactivity of the ferricyanide solution [227]. In this case, oxygen is reduced when ferrocyanide is reoxidized to ferricyanide. The dissolved oxygen concentration controls the rate of the reoxidation, thus, in microbial fuel cells, the cathodic solution was aerated to promote this reaction [20]. However, the reoxidation rate of ferrocyanide by oxygen is low [12], thus this slow reaction may act as a limiting factor of current generation. In this thesis, the concentration of ferricyanide solution was high enough for the amount of current generated, consequently the slow reoxidation of ferricyanide did not hinder the current generation. However, considering the long term use, this low reoxidation rate of ferricyanide becomes a limiting factor of current generation. The replacement of the cathodic system with an air cathode would decrease the rate of electron flow from the electrode to the electron acceptor due to slower reduction rate of oxygen compared to ferricyanide as discussed above, but would overcome the sustainability problem. Concomitantly, this option fulfills the biocompatibility requirement as well.

Summary

The feasibility of harvesting electricity from activated human macrophages was confirmed in this thesis. To this end, host defense mechanisms was used, where monocytes underwent differentiation into macrophages and adhered to the anode in a fuel cell setup. Activation of the macrophages induced the current generation in the fuel cell. The current generation correlated positively with the activity of NADPH oxidase, as validated by superoxide anion production from cells. Different stimulations of cells and inhibitions of cell activities elucidated that electron transfer through the plasma membrane via NADPH oxidase resulted in the current generation. The results of stimulation/inhibition tests provided evidence that superoxide anion contributed to the current flow. Furthermore, together with an estimate of the amount of superoxide anion production from activated macrophages, the results also indicated the existence of another electron pathway between cells and the electrode, independent of superoxide anion.

With plain gold electrodes the extracted current reached 1.5-2 μA per 10^6 cells seeded in the two compartment fuel cell system. The use of a mediator or modifying the surface of electrodes may facilitate the electron transport from the electron donor to the electron acceptor, increasing the current in the fuel cell. Since the size, shape, and chemical and physical properties of the materials used influence the intensity and time duration of the inflammatory processes [91], modification of the electrode materials and surfaces may also stabilize and improve the current generation, which is preferable for the further development of the device.

References

[1] U. Schroder. Anodic electron transfer mechanisms in microbial fuel cells and their energy efficiency. *Physical Chemistry Chemical Physics*, 9(21):2619–2629, 2007.

[2] M. C. Potter. Electrical Effects Accompanying the Decomposition of Organic Compounds. *Proceedings of the Royal Society of London. Series B, Containing Papers of a Biological Character*, 84(571):260–276, 1911.

[3] B. Cohen. The bacterial culture as an electrical half-cell. *Journal of Bacteriology*, 21(1):18–19, 1931.

[4] J. B. Davis and H. F. Yarbrough. Preliminary Experiments on a Microbial Fuel Cell. *Science*, 137(3530):615–616, 1962.

[5] K Lewis. Symposium on Bioelectrochemistry of Microorganisms. 4. Biochemical Fuel cells. *Bacteriological Reviews*, 30(1):101–103, 1966.

[6] B. E. Logan, B. Hamelers, R. Rozendal, U. Schroder, J. Keller, S. Freguia, P. Aelterman, W. Verstraete, and K. Rabaey. Microbial Fuel Cells: Methodology and Technology. *Environmental Science & Technology*, 40(17):5181–5192, 2006.

[7] J Menicucci, H Beyenal, E Marsili, RA Veluchamy, G Demir, and Z Lewandowski. Procedure for determining maximum sustainable power generated by microbial fuel cells. *Environmental Science & Technology*, 40(3):1062–1068, 2006.

[8] Uwe Schröder, Juliane Niessen, and Fritz Scholz. A generation of microbial fuel cells with current outputs boosted by more than one order of magnitude. *Angewandte Chemie International Edition*, 42(25):2880–2883, 2003.

[9] D. H. Park and J. G. Zeikus. Electricity generation in microbial fuel cells using neutral red as an electronophore. *Applied and Environmental Microbiology*, 66(4):1292–1297, 2000.

[10] Monica Höfte Willy Verstraete Korneel Rabaey, Nico Boon. Microbial phenazine production enhances electron transfer in biofuel cells. *Environmental Science and Technology*, 39(9):3401–3408, 2005.

[11] C.F. Thurston, H.P. Bennetto, G.M. Delaney, J.R. Mason, S.D. Roller, and JL Stirling. Glucose-metabolism in an microbial fuel-cell - Stoichiometry of product formation in thionine-mediated Proteus-vulgaris fuel-cell and its relation to coulombic yields. *Journal of General Microbiology*, 131:1393–1401, 1985.

[12] G. M. Delaney, H. P. Bennetto, J. R. Mason, S. D. Roller, J. L. Stirling, and C. F. Thurston. Electron-Transfer Coupling in Microbial Fuel-Cells. 2. Performance of Fuel-Cells Containing Selected Microorganism Mediator Substrate Combinations. *Journal of Chemical Technology and Biotechnology B-Biotechnology*, 34(1):13–27, 1984.

[13] Namjoon Kim, Youngjin Choi, Seunho Jung, and Sunghyun Kim. Effect of initial carbon sources on the performance of microbial fuel cells containing Proteus vulgaris. *Biotechnology and Bioengineering*, 70(1):109–114, 2000.

[14] E Katz, A.N. Shipway, and I. Willner. *Biochemical fuel cells, Handbook of Fuel cells - Fundamentals, Technology and Applications*. John Wiley & Sons, Ltd., 2003.

[15] R. M. Allen and H. P. Bennetto. Microbial Fuel-Cells - Electricity Production From Carbohydrates. *Applied Biochemistry and Biotechnology*, 39:27–40, 1993.

[16] H.J. Kim, H.S. Park, M.S. Hyun, I.S. Chang, M. Kim, and B.H. Kim. A mediator-less microbial fuel cell using a metal reducing bacterium, Shewanella putrefaciense. *Enzyme and Microbial Technology*, 30(2):145–152, 2002.

[17] H. P. Bennetto, G. M. Delaney, J. R. Mason, S. D. Roller, J. L. Stirling, and C. F. Thurston. The Sucrose Fuel-Cell - Efficient Biomass Conversion Using a Microbial Catalyst. *Biotechnology Letters*, 7(10):699–704, 1985.

[18] Y. Choi, E. Jung, H. Park, S. Jung, and S. Kim. Effect of initial carbon sources on the performance of a microbial fuel cell containing environmental

microorganism Micrococcus luteus. *Bulletin of The Korean Chemical Society*, 28(9):1591–1594, 2007.

[19] D.H. Park and J. G. Zeikus. Improved fuel cell and electrode designs for producing electricity from microbial degradation. *Biotechnology and Bioengineering*, 81(3):348–355, 2003.

[20] K. Rabaey, G. Lissens, S. D. Siciliano, and W. Verstraete. A microbial fuel cell capable of converting glucose to electricity at high rate and efficiency. *Biotechnology Letters*, 25(18):1531–1535, 2003.

[21] Seiya Tsujimura, Akira Wadano, Kenji Kano, and Tokuji Ikeda. Photosynthetic bioelectrochemical cell utilizing cyanobacteria and water-generating oxidase. *Enzyme and Microbial Technology*, 29(4-5):225 – 231, 2001.

[22] T Yagishita, S Sawayama, KI Tsukahara, and T Ogi. Effects of intensity of incident light and concentrations of Synechococcus sp. and 2-hydroxy-1,4-naphthoquinone on the current output of photosynthetic electrochemical cell. *Solar Energy*, 61(5):347–353, 1997.

[23] Derek R. Lovley. Microbial fuel cells: novel microbial physiologies and engineering approaches. *Current Opinion in Biotechnology*, 17(3):327–332, 2006.

[24] Daniel R Bond and Derek R Lovley. Electricity production by Geobacter sulfurreducens attached to electrodes. *Applied and Environmental Microbiology*, 69(3):1548–1555, 2003.

[25] Kevin T Finneran, Claudia V Johnsen, and Derek R Lovley. Rhodoferax ferrireducens sp. nov., a psychrotolerant, facultatively anaerobic bacterium that oxidizes acetate with the reduction of Fe(III). *International Journal of Systematic and Evolutionary Microbiology*, 53(Pt 3):669–673, 2003.

[26] Daniel R Bond and Derek R Lovley. Evidence for involvement of an electron shuttle in electricity generation by Geothrix fermentans. *Applied and Environmental Microbiology*, 71(4):2186–2189, 2005.

[27] Booki Min and Bruce E Logan. Continuous electricity generation from domestic wastewater and organic substrates in a flat plate microbial fuel cell. *Environmental Science & Technology*, 38(21):5809–5814, 2004.

[28] Korneel Rabaey, Nico Boon, Steven D. Siciliano, Marc Verhaege, and Willy Verstraete. Biofuel Cells Select for Microbial Consortia That Self-Mediate Electron Transfer. *Applied and Environmental Microbiology*, 70(9):5373–5382, 2004.

[29] L. M. Tender, C. E. Reimers, H. A. Stecher, D. E. Holmes, D. R. Bond, D. A. Lowy, K. Pilobello, S. J. Fertig, and D. R. Lovley. Harnessing microbially generated power on the seafloor. *Nature Biotechnology*, 20(8):821–825, 2002.

[30] A. L. Walker and C. W. Walker. Biological fuel cell and an application as a reserve power source. *Journal of Power Sources*, 160(1):123–129, 2006.

[31] D. Prasad, S. Arun, M. Murugesan, S. Padmanaban, R. S. Satyanarayanan, Sheela Berchmans, and V. Yegnaraman. Direct electron transfer with yeast cells and construction of a mediatorless microbial fuel cell. *Biosensors and Bioelectronics*, 22(11):2604–2610, 2007.

[32] N. Mano, F. Mao, and A. Heller. A miniature biofuel cell operating in a physiological buffer. *Journal of the American Chemical Society*, 124(44):12962–12963, 2002.

[33] A. T. Yahiro, S. M. Lee, and D. O. Kimble. Bioelectrochemistry. I. Enzyme Utilizing Bio-Fuel Cell Studies. *Biochimica et Biophysica Acta*, 88(2):375–&, 1964.

[34] C. M. Moore, N. L. Akers, A. D. Hill, Z. C. Johnson, and S. D. Minteer. Improving the environment for immobilized dehydrogenase enzymes by modifying Nafion with tetraalkylammonium bromides. *Biomacromolecules*, 5(4):1241–1247, 2004.

[35] B. Persson, L. Gorton, G. Johansson, and A. Torstensson. Biofuel Anode Based On D-Glucose Dehydrogenase, Nicotinamide Adenine-Dinucleotide And A Modified Electrode. *Enzyme and Microbial Technology*, 7(11):549–552, 1985.

[36] L. Gorton, A. Torstensson, H. Jaegfeldt, and G. JohanssonN. Electrocatalytic Oxidation Of Reduced Nicotinamide Coenzymes By Graphite-Electrodes Modified With An Adsorbed Phenoxazinium Salt, Meldola Blue. *Journal of Electroanalytical Chemistry*, 161(1):103–120, 1984.

[37] Nicolas Mano, Fei Mao, Woonsup Shin, Ting Chen, and Adam Heller. A miniature biofuel cell operating at 0.78 V. *Chemical communications (Cambridge, England)*, (4):518–519, 2003.

[38] T. Chen, S.C. Barton, G. Binyamin, Z.Q. Gao, Y.C. Zhang, H.H. Kim, and A. Heller. A miniature biofuel cell. *Journal of the American Chemical Society*, 123(35):8630–8631, 2001.

[39] S Tsujimura, K Kano, and T Ikeda. Glucose/O-2 biofuel cell operating at physiological conditions. *Electrochemistry*, 70(12):940–942, 2002.

[40] N. L. Akers, C. M. Moore, and S. D. Minteer. Development of alcohol/O-2 biofuel cells using salt-extracted tetrabutylammonium bromide/Nafion membranes to immobilize dehydrogenase enzymes. *Electrochimica Acta*, 50(12):2521–2525, 2005.

[41] F. Sato, M. Togo, M. K. Islam, T. Matsue, J. Kosuge, N. Fukasaku, S. Kurosawa, and M. Nishizawa. Enzyme-based glucose fuel cell using Vitamin K-3-immobilized polymer as an electron mediator. *Electrochemistry Communications*, 7(7):643–647, 2005.

[42] I. Willner, G. Arad, and E. Katz. A biofuel cell based on pyrroloquinoline quinone and microperoxidase-1 monolayer-functionalized electrodes. *Bioelectrochemistry and Bioenergetics*, 44(2):209–214, 1998.

[43] G. T. R. Palmore and H. H. Kim. Electro-enzymatic reduction of dioxygen to water in the cathode compartment of a biofuel cell. *Journal of Electroanalytical Chemistry*, 464(1):110–117, 1999.

[44] H. H. Kim, N. Mano, X. C. Zhang, and A. Heller. A miniature membrane-less biofuel cell operating under physiological conditions at 0.5 V. *Journal of The Electrochemical Society*, 150(2):A209–A213, 2003.

[45] E. Katz, B. Filanovsky, and I. Willner. A biofuel cell based on two immiscible solvents and glucose oxidase and microperoxidase-11 monolayer-functionalized electrodes. *New Journal of Chemistry*, 23(5):481–487, 1999.

[46] E. Katz, I. Willner, and A.B. Kotlyar. A non-compartmentalized glucose vertical bar O-2 biofuel cell by bioengineered electrode surfaces. *Journal of Electroanalytical Chemistry*, 479(1):64–68, 1999.

[47] Frank Davis and Séamus P J Higson. Biofuel cells–recent advances and applications. *Biosensors and Bioelectronics*, 22(7):1224–1235, 2007.

[48] G.S. Wilson and R. Gifford. Biosensors for real-time in vivo measurements. *Biosensors & Bioelectronics*, 20(12):2388–2403, 2005.

[49] Itamar Willner and Eugenii Katz, editors. *Bioelectronics: From Theory to Applications*. John Wiley & Sons, Ltd., 2005.

[50] C. A. Quinn, R. E. Connor, and A. Heller. Biocompatible, glucose-permeable hydrogel for in situ coating of implantable biosensors. *Biomaterials*, 18(24):1665–1670, 1997.

[51] J.M. Anderson. Mechanisms of inflammation and infection with implanted devices. *Cardiovasclar Pathology*, 2(3, Suppl. S):S33–S41, 1993.

[52] M. Balcells, D. Klee, M. Fabry, and H. Hocker. Quantitative assessment of protein adsorption by combination of the enzyme-linked immunosorbent assay with radioisotope-based studies. *Journal of Colloid and Interface Science*, 220(2):198–204, 1999.

[53] M. Gerritsen, J. A. Jansen, A. Kros, D. M. Vriezema, N. A. Sommerdijk, R. J. Nolte, J. A. Lutterman, S. W. Van Hövell, and A. Van der Gaag. Influence of inflammatory cells and serum on the performance of implantable glucose sensors. *Journal of Biomedial Materials Research*, 54(1):69–75, 2001.

[54] Adam Heller and Ben Feldman. Electrochemical glucose sensors and their applications in diabetes management. *Chemical Reviews*, 108(7):2482–2505, 2008.

[55] Takeo Kamada. Some Observations on Potential Differences Across the Ectoplasm Membrane of Paramecium. *Journal of Experimental Biology*, 11(1):94–102, 1934.

[56] A. L. Hodgkin and A. F. Huxley. A Quantitative Description of Membrane Current and Its Application to Conduction and Excitation in Nerve. *Journal of Physiology-London*, 117(4):500–544, 1952.

[57] P. Mitchell. Coupling of Phosphorylation to Electron and Hydrogen Transfer by a Chemi-Osmotic Type of Mechanism. *Nature*, 191(478):144–, 1961.

[58] B. Albert, A. Johnson, J. Lewis, M. Raff, K. Roberts, and P. Walter. *Molecular biology of the cell.* Garland Science, 4th edition, 2002.

[59] S. Terada. Bioichemistry basic, 2009. accessed Jun. 2009, http://133.100.212.50/ bc1/Biochem/index1.htm.

[60] F. L. Crane, I. L. Sun, R. Barr, and H. Low. Electron And Proton Transport Across The Plasma-Membrane. *Journal of Bioenergetics and Biomembranes*, 23(5):773–803, 1991.

[61] A. W. Segal. The NADPH oxidase and chronic granulomatous disease. *Molecular Medicine Today*, 2(3):129–135, 1996.

[62] A.W. Segal. How neutrophils kill microbes. *Annual Review of immunology*, 23:197–223, 2005.

[63] K. Bedard and K. H. Krause. The NOX family of ROS-generating NADPH oxidases: Physiology and pathophysiology. *Physiological Reviews*, 87(1):245–313, 2007.

[64] A. R. Cross and A. W. Segal. The NADPH oxidase of professional phagocytes - prototype of the NOX electron transport chain systems. *Biochimica et Biophysica Acta-Bioenergetics*, 1657(1):1–22, 2004.

[65] Gary M. Bokoch and Ulla G. Knaus. NADPH oxidases: not just for leukocytes anymore! *Trends in Biochemical Sciences*, 28(9):502–508, 2003.

[66] G. E. Brown, M. Q. Stewart, H. Liu, V. L. Ha, and M. B. Yaffe. A novel assay system implicates PtdIns(3,4)P(2), PtdIns(3)P, and PKC delta in intracellular production of reactive oxygen species by the NADPH oxidase. *Molecular Cell*, 11(1):35–47, 2003.

[67] Bernard M. Babior. NADPH Oxidase: An Update. *Blood*, 93(5):1464–1476, 1999.

[68] G. L. Petheo, N. C. Girardin, N. Goossens, G. Z. Molnar, and N. Demaurex. Role of nucleotides and phosphoinositides in the stability of electron and proton currents associated with the phagocytic NADPH oxidase. *Biochemical Journal*, 400:431–438, 2006.

[69] C. H. Han, J. L. Freeman, T. Lee, S. A. Motalebi, and J. D. Lambeth. Regulation of the neutrophil respiratory burst oxidase. Identification

of an activation domain in p67(phox). *Journal of Biological Chemistry*, 273(27):16663–16668, 1998.

[70] A. Grogan, E. Reeves, N. Keep, F. Wientjes, N. F. Totty, A. L. Burlingame, J. J. Hsuan, and A. W. Segal. Cytosolic phox proteins interact with and regulate the assembly of coronin in neutrophils. *Journal of Cell Science*, 110(24):3071–3081, 1997.

[71] Marie-Hélène Paclet, Sylvie Berthier, Lauriane Kuhn, Jérôme Garin, and Françoise Morel. Regulation of phagocyte NADPH oxidase activity: identification of two cytochrome b558 activation states. *FASEB Journal*, 21(4):1244–1255, 2007.

[72] Xiaoxian Zhao, Bo Xu, Ashish Bhattacharjee, Claudine M Oldfield, Frans B Wientjes, Gerald M Feldman, and Martha K Cathcart. Protein kinase Cdelta regulates p67phox phosphorylation in human monocytes. *Journal of Leukocyte Biology*, 77(3):414–420, Mar 2005.

[73] Juan D Matute, Andrés A Arias, Mary C Dinauer, and Pablo J Patiño. p40phox: the last NADPH oxidase subunit. *Blood Cells, Molecules, and Diseases*, 35(2):291–302, 2005.

[74] S Tsunawaki and K Yoshikawa. Relationships of p40(phox) withp67(phox) in the activation and expression of the human respiratory burst NADPH oxidase. *Journal of Biochemistry*, 128(5):777–783, 2000.

[75] T. E. Decoursey and E. Ligeti. Regulation and termination of NADPH oxidase activity. *Cellular and Molecular Life Sciences*, 62(19-20):2173–2193, 2005.

[76] M. T. Quinn, T. Evans, L. R. Loetterle, A. J. Jesaitis, and G. M. Bokoch. Translocation of Rac correlates with NADPH oxidase activation. Evidence for equimolar translocation of oxidase components. *Journal of Biological Chemistry*, 268(28):20983–20987, 1993.

[77] G. M. Bokoch and B. A. Diebold. Current molecular models for NADPH oxidase regulation by Rac GTPase. *Blood*, 100(8):2692–2696, 2002.

[78] William M Nauseef. Assembly of the phagocyte NADPH oxidase. *Histochemistry and Cell Biology*, 122(4):277–291, 2004.

[79] Gary M. Bokoch and Tieming Zhao. Regulation of the phagocyte NADPH oxidase by Rac GTPase. *Antioxidants & Redox Signaling*, 8(9-10):1533–1548, 2006.

[80] P. G. Heyworth, B. P. Bohl, G. M. Bokoch, and J. T. Curnutte. Rac translocates independently of the neutrophil NADPH oxidase components p47phox and p67phox. Evidence for its interaction with flavocytochrome b558. *Journal of Biological Chemistry*, 269(49):30749–30752, 1994.

[81] R. Takeya, N. Ueno, and H. Sumimoto. Regulation of superoxide-producing NADPH oxidases in nonphagocytic cells. *Methods In Enzymology*, 406:456–468, 2006.

[82] Neil R. Bastian and John B. Hibbs. Assembly and regulation of NADPH oxidase and nitric oxide synthase. *Current Opinion in Immunology*, 6(1):131–139, 1994.

[83] F. Kanai, H. Liu, S. J. Field, H. Akbary, T. Matsuo, G. E. Brown, L. C. Cantley, and M. B. Yaffe. The PX domains of p47phox and p40phox bind to lipid products of PI(3)K. *Nature Cell Biology*, 3(7):675–678, 2001.

[84] A. T Bäumer, H. T. Freyhaus, H. Sauer, M. Wartenberg, K. Kappert, P. Schnabel, C. Konkol, J. Hescheler, M. Vantler, and S. Rosenkranz. Phosphatidylinositol 3-kinase-dependent membrane recruitment of Rac-1 and p47phox is critical for alpha-platelet-derived growth factor receptor-induced production of reactive oxygen species. *Journal of Biological Chemistry*, 283(12):7864–7876, 2008.

[85] J. M. Li and A. M. Shah. ROS generation by nonphagocytic NADPH oxidase: Potential relevance in diabetic nephropathy. *Journal of The American Society of Nephrology*, 14:S221–S226, 2003.

[86] Mark T Quinn and Katherine A Gauss. Structure and regulation of the neutrophil respiratory burst oxidase: comparison with nonphagocyte oxidases. *Journal of Leukocyte Biology*, 76(4):760–781, 2004.

[87] Martin Vejrazka, Radan Mícek, and Stanislav Stípek. Apocynin inhibits NADPH oxidase in phagocytes but stimulates ROS production in non-phagocytic cells. *Biochimica et Biophysica Acta (BBA) - General Subjects*, 1722(2):143 – 147, 2005.

[88] M. Valko, D. Leibfritz, J. Moncol, M. T. D. Cronin, M. Mazur, and J. Telser. Free radicals and antioxidants in normal physiological functions and human disease. *International Journal of Biochemistry & Cell Biology*, 39(1):44–84, 2007.

[89] Maureen R Gwinn and Val Vallyathan. Respiratory burst: role in signal transduction in alveolar macrophages. *Journal of Toxicology & Environmental Health Part B: Critical Reviews*, 9(1):27–39, 2006.

[90] C. F. Nathan. Secretory Products of Macrophages. *Journal of Clinical Investigation*, 79(2):319–326, 1987.

[91] J.M. Anderson. Biological responses to materials. *Annual Review of Materials Research*, 31:81–110, 2001.

[92] Jatinder Ahluwalia. Characterisation of electron currents generated by the human neutrophil NADPH oxidase. *Biochemical and Biophysical Research Communications*, 368(3):656–661, 2008.

[93] M. K. Cathcart. Regulation of superoxide anion production by NADPH oxidase in monocytes/macrophages: contributions to atherosclerosis. *Arteriosclerosis, Thrombosis, and Vascular Biology*, 24(1):23–8, 2004.

[94] Jeremy S Duffield. The inflammatory macrophage: a story of Jekyll and Hyde. *Clinical Science (London)*, 104(1):27–38, 2003.

[95] Siamon Gordon and Philip R Taylor. Monocyte and macrophage heterogeneity. *Nature Reviews Immunology*, 5(12):953–964, Dec 2005.

[96] Sampath Parthasarathy and Nalini Santanam. Mechanisms of oxidation, antioxidants, and atherosclerosis. *Current Opinion in Lipidology*, 5(5):371–375, 1994.

[97] J Auwerx. The human leukemia-cell line, THP-1 - a multifaceted model for the study of monocytes-macrophage differentiation. *Experientia*, 47(1):22–31, 1991.

[98] P. Chomarat, J. Banchereau, J. Davoust, and A. K. Palucka. IL-6 switches the differentiation of monocytes from dendritic cells to macrophages. *Nature Immunology*, 1(6):510–514, 2000.

[99] J. Banchereau and R. M. Steinman. Dendritic cells and the control of immunity. *Nature*, 392(6673):245–252, 1998.

[100] S. Tsuchiya, M. Yamabe, Y. Yamaguchi, Y. Kobayashi, T. Konno, and K. Tada. Establishment and characterization of a human acute monocytic leukemia cell line (THP-1). *International Journal of Cancer*, 26(2):171–176, 1980.

[101] E. K. Park, H. S. Jung, H. I. Yang, M. C. Yoo, C. Kim, and K. S. Kim. Optimized THP-1 differentiation is required for the detection of responses to weak stimuli. *Inflammation Research*, 56(1):45–50, 2007.

[102] Edwin van den Worm. *Investigations on apocynin, a potent NADPH oxidase inhibitor*. PhD thesis, University Utrecht, 2001.

[103] D. S. Regier, D. G. Greene, S. Sergeant, A. J. Jesaitis, and L. C. McPhail. Phosphorylation of p22phox is mediated by phospholipase D-dependent and -independent mechanisms - Correlation of NADPH oxidase activity and p22phox phosphorylation. *Journal of Biological Chemistry*, 275(37):28406–28412, 2000.

[104] K. Vaddi and R. C. Newton. Comparison of biological responses of human monocetes and THP-1 cells to chemokines of the intercrine-beta family. *Journal of Leukocyte Biology*, 55(6):756–762, 1994.

[105] S. Sergeant and L. C. McPhail. Opsonized zymosan stimulates the redistribution of protein kinase C isoforms in human neutrophils. *Journal of Immunology*, 159(6):2877–2885, 1997.

[106] T. E. DeCoursey, D. Morgan, and V. V. Cherny. The voltage dependence of NADPH oxidase reveals why phagocytes need proton channels. *Nature*, 422(6931):531–4, 2003.

[107] Online mendelian inheritance in man, omim, johns hopking university, baltimore, md. mim number 136537. accessed July 2009, www.ncbi..nlm.nih.gov.

[108] A. I. Tauber. Protein-kinase-c and the Activation of the Human Neutrophil Nadph-oxidase. *Blood*, 69(3):711–720, 1987.

[109] H. P. Koeffler, T. Amatruda, N. Ikekawa, Y. Kobayashi, and H. F. DeLuca. Induction of macrophage differentiation of human normal and leukemic myeloid stem cells by 1,25-dihydroxyvitamin D3 and its fluorinated analogues. *Cancer Research*, 44(121):5624–5628, 1984.

[110] R. Goldman. Induction of a high phagocytic capability in P388D1, a macrophage-like tumor cell line, by 1 alpha, 25-dihydroxyvitamin D3. *Cancer Reserach*, 44(1):11–19, 1984.

[111] H. Schwende, E. Fitzke, P. Ambs, and P. Dieter. Differences in the state of differentiation of THP-1 cells induced by phorbol ester and 1,25-dihydroxyvitamin D-3. *Journal of Leukocyte Biology*, 59(4):555–561, 1996.

[112] H. Tanaka, K. A. Hruska, Y. Seino, J. D. Malone, Y. Nishii, and S. L. Teitelbaum. Disassociation of the Macrophage-maturational Effects of Vitamin-d From Respiratory Burst Priming. *Journal of Biological Chemistry*, 266(17):10888–10892, 1991.

[113] S. Takashiba, T. E. Van Dyke, S. Amar, Y. Murayama, A. W. Soskolne, and L. Shapira. Differentiation of monocytes to macrophages primes cells for lipopolysaccharide stimulation via accumulation of cytoplasmic nuclear factor kappa B. *Infection and Immunity*, 67(11):5573–5578, 1999.

[114] Dong-Hwan Kim, Matt T. Novak, Jamie Wilkins, Minkyu Kim, Anita Sawyer, and William M. Reichert. Response of monocytes exposed to phagocytosable particles and discs of comparable surface roughness. *Biomaterials*, 28(29):4231 – 4239, 2007.

[115] F. R. DeLeo, J. Renee, S. McCormick, M. Nakamura, M. Apicella, J. P. Weiss, and W. M. Nauseef. Neutrophils exposed to bacterial lipopolysaccharide upregulate NADPH oxidase assembly. *Journal of Clinical Investigation*, 101(2):455–463, 1998.

[116] J. L. Morgan and R. E. Singer. Cytokine differences in mature and immature human macrophata cell lines. *Journal of Dental Research*, 77:1814, 1998.

[117] E. S. Kimball, E. Kovacs, M. C. Clark, and C. R. Schneider. Activation of cytokine production and adhesion molecule expression on THP-1 myelomonocytic cells by macrophage colony-stimulating factor in combination with interferon-gamma. *Journal of Leukocyte Biology*, 58(5):585–594, 1995.

[118] Cytokines & cells online pathfinder encyclopaedia. accessed July 2009, www.copewithcytokines.de.

[119] Kate Schroder, Paul J. Hertzog, Timothy Ravasi, and David A. Hume. Interferon-gamma: an overview of signals, mechanisms and functions. *Journal of Leukocyte Biology*, 75(2):163–189, 2004.

[120] A. C. Almeida, J. Rehder, S. D. Severino, J. Martins-Filho, P. E. Newburger, and A. Condino-Neto. The effect of IFN-gamma and TNF-alpha on the NADPH oxidase system of human colostrum macrophages, blood monocytes, and THP-1 cells. *Journal of Interferon and Cytokine Research*, 25(9):540–6, 2005.

[121] J. B. McCarthy, B. V. Vachhani, S. M. Wahl, D. S. Finbloom, and G. M. Feldman. Human monocyte binding to fibronectin enhances IFN-gamma-induced early signaling events. *Journal of Immunology*, 159(5):2424–2430, 1997.

[122] M. A. Cassatella, F. Bazzoni, R. M. Flynn, S. Dusi, G. Trinchieri, and F. Rossi. Molecular basis of interferon-gamma and lipopolysaccharide enhancement of phagocyte respiratory burst capability. Studies on the gene expression of several NADPH oxidase components. *Journal of Biological Chemistry*, 265(33):20241–20246, 1990.

[123] Yong Huang, Peter M Krein, Daniel A Muruve, and Brent W Winston. Complement factor B gene regulation: synergistic effects of TNF-alpha and IFN-gamma in macrophages. *Journal of Immunology*, 169(5):2627–2635, 2002.

[124] K. A. Gauss, L. K. Nelson-Overton, D. W. Siemsen, Y. Gao, F. R. DeLeo, and M. T. Quinn. Role of NF-kappaB in transcriptional regulation of the phagocyte NADPH oxidase by tumor necrosis factor-alpha. *Journal of Leukocyte Biology*, 82(3):729–741, 2007.

[125] C. Bombara and R. A. Ignotz. TGF-beta inhibits proliferation of and promotes differentiation of human promonocytic leukemia cells. *Journal of Cellular Physiology*, 153(1):30–37, 1992.

[126] Y. Vodovotz, L. Chesler, H. Chong, S. J. Kim, J. T. Simpson, W. DeGraff, G. W. Cox, A. B. Roberts, D. A. Wink, and M. H. Barcellos-Hoff. Regulation of transforming growth factor beta1 by nitric oxide. *Cancer Research*, 59(9):2142–2149, 1999.

[127] A. Condino-Neto, C. Whitney, and P. E. Newburger. Dexamethasone but not indomethacin inhibits human phagocyte nicotinamide adenine

dinucleotide phosphate oxidase activity by down-regulating expression of genes encoding oxidase components. *Journal of Immunology*, 161(9):4960–4967, 1998.

[128] C. L. Leger, N. Kadiri-Hassani, and B. Descomps. Decreased superoxide anion production in cultured human promonocyte cells (THP-1) due to polyphenol mixtures from olive oil processing wastewaters. *Journal of Agricultural and Food Chemistry*, 48(10):5061–5067, 2000.

[129] S. K. Venugopal, S. Devaraj, T. Yang, and I. Jialal. Alpha-tocopherol decreases superoxide anion release in human monocytes under hyperglycemic conditions via inhibition of protein kinase C-alpha. *Diabetes*, 51(10):3049–3054, 2002.

[130] I. Fridovich. Superoxide anion radical (O2-.), superoxide dismutases, and related matters. *Journal of Biological Chemistry*, 272(30):18515–18517, 1997.

[131] Hiroyuki Ukeda. Detection of Superoxide Anion with WST-1 and its Application. *Dojin News*, 112:1, 2004.

[132] Richard B. Johnston and Packer Lester. Measurement of O2- secreted by monocytes and macrophages. *Methods in Enzymology*, 105:365–369, 1984.

[133] A. V. Peskin and C. C. Winterbourn. A microtiter plate assay for superoxide dismutase using a water-soluble tetrazolium salt (WST-1). *Clinica Chimica Acta*, 293(1-2):157–166, 2000.

[134] Ralf P Brandes and Mariano Janiszewski. Direct detection of reactive oxygen species ex vivo. *Kidney International*, 67(5):1662–1664, 2005.

[135] M. V. Berridge and A. S. Tan. Trans-plasma membrane electron transport: a cellular assay for NADH- and NADPH-oxidase based on extracellular, superoxide-mediated reduction of the sulfonated tetrazolium salt WST-1. *Protoplasma*, 205(1-4):74–82, 1998.

[136] A. S. Tan and M. V. Berridge. Superoxide produced by activated neutrophils efficiently reduces the tetrazolium salt, WST-1 to produce a soluble formazan: a simple colorimetric assay for measuring respiratory burst activation and for screening anti-inflammatory agents. *Journal of Immunological Methods*, 238(1-2):59–68, 2000.

[137] Charles Beauchamp and Irwin Fridovich. Superoxide dismutase: Improved assays and an assay applicable to acrylamide gels. *Analytical Biochemistry*, 44(1):276–287, 1971.

[138] K Rabaey and W Verstraete. Microbial fuel cells: novel biotechnology for energy generation. *Trends in Biotechnology*, 23(6):291–298, 2005.

[139] F. Zhao, F. Harnisch, U. Schrorder, F. Scholz, P. Bogdanoff, and I. Herrmann. Challenges and constraints of using oxygen cathodes in microbial fuel cells. *Environmental Science & Technology*, 40(17):5193–5199, 2006.

[140] H. Y. Gu, X. W. Zhang, Z. J. Li, and L. C. Lei. Studies on treatment of chlorophenol-containing wastewater by microbial fuel cell. *Chinese Science Bulletin*, 52(24):3448–3451, 2007.

[141] B. E. Logan, C. Murano, K. Scott, N. D. Gray, and I. M. Head. Electricity generation from cysteine in a microbial fuel cell. *Water Research*, 39(5):942–952, 2005.

[142] Hong Liu and Bruce E Logan. Electricity generation using an air-cathode single chamber microbial fuel cell in the presence and absence of a proton exchange membrane. *Environmental Science and Technology*, 38(14):4040–4046, 2004.

[143] Greg M. Swain. *Handbook of Electrochemistry: Solid Electrode Materials: Pretreatment and Activation*. Elsevier, 2007.

[144] W.D. Callister Jr., editor. *Materials science and Engineering: An Introduction*. John Wiley & Sons Inc., 2007.

[145] B. M. Babior, J. D. Lambeth, and W. Nauseef. The neutrophil NADPH oxidase. *Archives of Biochemistry and Biophysics*, 397(2):342–344, 2002.

[146] E. A. Bey, B. Xu, A. Bhattacharjee, C. M. Oldfield, X. Zhao, Q. Li, V. Subbulakshmi, G. M. Feldman, F. B. Wientjes, and M. K. Cathcart. Protein Kinase Cdelta Is Required for p47phox Phosphorylation and Translocation in Activated Human Monocytes. *The Journal of Immunology*, 173(9):5730–5738, 2004.

[147] R. A. Clark, B. D. Volpp, K. G. Leidal, and W. M. Nauseef. 2 cytosolic components of the human neutrophil respiratory burst oxidase translocate to the plasma-membrane during cell activation. *Journal of Clinical Investigation*, 85(3):714–721, 1990.

[148] S. Dusi, M. Donini, D. Lissandrini, P. Mazzi, V. D. Bianca, and F. Rossi. Mechanisms of expression of NADPH oxidase components in human cultured monocytes: role of cytokines and transcriptional regulators involved. *European Journal of Immunology*, 31(3):929–938, 2001.

[149] A. Navarro, B. Anand-Apte, Y. Tanabe, G. Feldman, and A. C. Larner. A PI-3 kinase-dependent, Stat1-independent signaling pathway regulates interferon-stimulated monocyte adhesion. *Journal of Leukocyte Biology*, 73(4):540–545, 2003.

[150] P. A. R. Juliet, T. Hayashi, S. Daigo, H. Matsui-Hirai, A. Miyazaki, A. Fukatsu, J. Funami, A. Iguchi, and L. J. Ignarro. Combined effect of testosterone and apocynin on nitric oxide and superoxide production in PMA-differentiated THP-1 cells. *Biochimica et Biophysica Acta*, 1693(3):185–191, 2004.

[151] E. Van den Worm, C. J. Beukelman, A. J. Van den Berg, B. H. Kroes, R. P. Labadie, and H. Van Dijk. Effects of methoxylation of apocynin and analogs on the inhibition of reactive oxygen species production by stimulated human neutrophils. *European Journal of Pharmacology*, 433(2-3):225–230, 2001.

[152] R. M. Touyz. Apocynin, NADPH oxidase, and vascular cells - A complex matter. *Hypertension*, 51(2):172–174, 2008.

[153] C. Henriette Q. van Ufford B.H. Kroes A.J.J. van den Berg C..J. Beukelman, E. van den Worm. Discovery of new anti-inflammatory drugs from plant origin. *Annals of Gastroenterology*, 15:320–323, 2002.

[154] Holly C Williams and Kathy K Griendling. NADPH oxidase inhibitors: new antihypertensive agents? *Journal of Cardiovascular Pharmacology*, 50(1):9–16, 2007.

[155] J. M. Simons, B. A. Thart, T. R. Ip Vai Ching, H. Vandijk, and R. P. Labadie. Metabolic-activation of Natural Phenols Into Selective Oxidative Burst Agonists By Activated Human Neutrophils. *Free Radical Biology and Medicine*, 8(3):251–258, 1990.

[156] V. F. Ximenes, M. P. P. Kanegae, S. R. Rissato, and M. S. Galhiane. The oxidation of apocynin catalyzed by myeloperoxidase: proposal for NADPH oxidase inhibition. *Archives of Biochemistry and Biophysics*, 457(2):134–141, 2007.

[157] H. W. M. Niessen, T. W. Kuijpers, D. Roos, and A. J. Verhoeven. Release of Azurophilic Granule Contents In Fmlp-stimulated Neutrophils Requires 2 Activation Signals, One of Which Is A Rise In Cytosolic Free Ca-2+. *Cellular Signalling*, 3(6):625–633, 1991.

[158] D. J. Stuehr, O. A. Fasehun, N. S. Kwon, S. S. Gross, J. A. Gonzalez, R. Levi, and C. F. Nathan. Inhibition of macrophage and endothelial cell nitric oxide synthase by diphenyleneiodonium and its analogs. *FASEB Journal*, 5(1):98–103, 1991.

[159] K. Traore, M. A. Trush, M. George, E. W. Spannhake, W. Anderson, and A. Asseffa. Signal transduction of phorbol 12-myristate 13-acetate (PMA)-induced growth inhibition of human monocytic leukemia THP-1 cells is reactive oxygen dependent. *Leukemia Research*, 29(8):863–879, 2005.

[160] J. T. Hancock and O. T. Jones. The inhibition by diphenyleneiodonium and its analogues of superoxide generation by macrophages. *Biochemical Journal*, 242(1):103–107, 1987.

[161] A. R. Cross and O. T. Jones. The effect of the inhibitor diphenylene iodonium on the superoxide-generating system of neutrophils. Specific labelling of a component polypeptide of the oxidase. *Biochemical Journal*, 237(1):111–116, 1986.

[162] J. A. Ellis, S. J. Mayer, and O. T. Jones. The effect of the NADPH oxidase inhibitor diphenyleneiodonium on aerobic and anaerobic microbicidal activities of human neutrophils. *Biochemical Journal*, 251(3):887–891, 1988.

[163] J. A. Ellis, A. R. Cross, and O. T. Jones. Studies on the electron-transfer mechanism of the human neutrophil NADPH oxidase. *Biochemical Journal*, 262(2):575–579, 1989.

[164] R. M. Scaife. Selective and irreversible cell cycle inhibition by diphenyleneiodonium. *Molecular Cancer Therapeutics*, 4(6):876–884, 2005.

[165] A. M. Michelson. Biological role of the superoxide anion radical and of superoxyde-dismutase in cellular metabolism. *Comptes Rendus des Seances de la Societe de Biologie et des ses Filiales (Paris)*, 170(6):1137–1146, 1976.

[166] V. V. Cherny and T. E. DeCoursey. pH-dependent Inhibition of Voltage-gated H+ Currents in Rat Alveolar Epithelial Cells by Zn2+ and Other Divalent Cations. *The Journal of General Physiology*, 114(6):819–838, 1999.

[167] Gleich Grady Bankers-Fulbright, Kita. Regulation of Human Eosinophil NADPH Oxidase Activity: A Central Role for PKC-delta. *Journal of Cellular Physiology*, 189:306, 2001.

[168] O. Nüsse D. P. Lew E. Ligeti K. H. Krause B. Bánfi, J. Schrenzel and N. Demaurexd. A novel H(+) conductance in eosinophils: unique characteristics and absence in chronic granulomatous disease. *The Journal of Experimental Medicine*, 190(2):183, 1999.

[169] J. B. Chappell L. M. Henderson and O. T. Jones. Superoxide generation by the electrogenic NADPH oxidase of human neutrophils is limited by the movement of a compensating charge. *Biochemical Journal*, 255:285, 1988.

[170] W. Xu L. L. Thomas V. V. Cherny, L. M. Henderson and T. E. DeCoursey. Interactions between NADPH oxidase-related proton and electron currents in human eosinophil. *Journal of Physiology*, 535(3):767, 2001.

[171] J. L. Bankers-Fulbright, G. J. Gleich, G. M. Kephart, H. Kita, and S. M. O'Grady. Regulation of eosinophil membrane depolarization during NADPH oxidase activation. *Journal of Cell Science*, 116:3221, 2003.

[172] G. M. Rosen, S. Pou, C. L. Ramos, M. S. Cohen, and B. E. Britigan. Free radicals and phagocytic cells. *FASEB Journal*, 9(2):200–209, 1995.

[173] P. A. R. Juliet, T. Hayashi, A. Iguchi, and L. J. Ignarro. Concomitant production of nitric oxide and superoxide in human macrophages. *Biochemical and Biophysical Research Communications*, 310(2):367–370, 2003.

[174] C. Nathan and Q. W. Xie. Regulation of biosynthesis of nitric oxide. *Journal of Biological Chemistry*, 269(19):13725–13728, 1994.

[175] L. B. Valdez and A. Boveris. Nitric oxide and superoxide radical production by human mononuclear leukocytes. *Antioxidants & Redox Signaling*, 3(3):505–513, 2001.

[176] R. E. Huie and S. Padmaja. The Reaction of No with Superoxide. *Free Radical Research Communications*, 18(4):195–199, 1993.

[177] D. D. Rees, R. M. J. Palmer, R. Schulz, H. F. Hodson, and S. Moncada. Characterization of three inhibitors of endothelial nitric oxide synthase in vitro and in vivo. *British Journal of Pharmacology*, 101(3):746–752, 1990.

[178] U. Frandsen, J. Bangsbo, M. Sander, L. Hoffner, A. Betak, B. Saltin, and Y. Hellsten. Exercise-induced hyperaemia and leg oxygen uptake are not altered during effective inhibition of nitric oxide synthase with N-G-nitro-L-arginine methyl ester in humans. *Journal of Physiology-London*, 531(1):257–264, 2001.

[179] G. Cotter, E. Kaluski, A. Blatt, O. Milovanov, Y. Moshkovitz, R. Zaidenstein, A. Salah, D. Alon, Y. Michovitz, M. Metzger, Z. Vered, and A. Golik. L-NMMA (a nitric oxide synthase inhibitor) is effective in the treatment of cardiogenic shock. *Circulation*, 101(12):1358–1361, 2000.

[180] Alberto Boveris, Silvia Alvarez, and Ana Navarro. The role of mitochondrial nitric oxide synthase in inflammation and septic shock. *Free Radical Biology & Medicine*, 33(9):1186–1193, 2002.

[181] M. J. Griffiths, M. Messent, R. J. MacAllister, and T. W. Evans. Aminoguanidine selectively inhibits inducible nitric oxide synthase. *British Journal of Pharmacology*, 110(3):963–968, 1993.

[182] C. Tümer, H. M. Bilgin, B. D. Obay, H. D., M. Atmaca, and M. Kelle. Effect of nitric oxide on phagocytic activity of lipopolysaccharide-induced macrophages: possible role of exogenous L-arginine. *Cell Biology International*, 31(6):565–569, 2007.

[183] K. J. Pendino, J. D. Laskin, R. L. Shuler, C. J. Punjabi, and D. L. Laskin. Enhanced production of nitric oxide by rat alveolar macrophages after inhalation of a pulmonary irritant is associated with increased expression of nitric oxide synthase. *The Journal of Immunology*, 151(12):7196–7205, 1993.

[184] H. Ischiropoulos, A. Gow, S. R. Thom, N. W. Kooy, J. A. Royall, and J. P. Crow. Detection of reactive nitrogen species using 2,7-dichlorodihydrofluorescein and dihydrorhodamine 123. *Methods in Enzymology*, 301:367–373, 1999.

[185] Barry Halliwell and Matthew Whiteman. Measuring reactive species and oxidative damage in vivo and in cell culture: how should you do it and what do the results mean? *British Journal of Pharmacology*, 142(2):231–255, 2004.

[186] T. Oikawa and M. Shimamura. Potent inhibition of angiogenesis by wortmannin, a fungal metabolite. *European Journal of Pharmacology*, 318(1):93–96, 1996.

[187] M. Yang, W. Wu, and C. J. Mirocha. Wortmannin inhibits the production of reactive oxygen and nitrogen intermediates and the killing of the Saccharomyces cerevisiae by isolated chicken macrophages. *Immunopharmacology and Immunotoxicology*, 18(4):597–608, 1996.

[188] R. W. Bonser, N. T. Thompson, R. W. Randall, J. E. Tateson, G. D. Spacey, H. F. Hodson, and L. G. Garland. Demethoxyviridin and wortmannin block phospholipase C and D activation in the human neutrophil. *British Journal of Pharmacology*, 103(1):1237–1241, 1991.

[189] L. H. Young, Y. Ikeda, R. Scalia, and A. M. Lefer. Wortmannin, a potent antineutrophil agent, exerts cardioprotective effects in myocardial ischemia/reperfusion. *The Journal of Pharmacology and Experimental Therapeutics*, 295(1):37–43, 2000.

[190] M. Baggiolini, B. Dewald, J. Schnyder, W. Ruch, P. H. Cooper, and T. G. Payne. Inhibition of the Phagocytosis-induced Respiratory Burst By the Fungal Metabolite Wortmannin and Some Analogs. *Experimental Cell Research*, 169(2):408–418, 1987.

[191] V. Niggli and H. Keller. The phosphatidylinositol 3-kinase inhibitor wortmannin markedly reduces chemotactic peptide-induced locomotion and increases in cytoskeletal actin in human neutrophils. *European Journal of Pharmacology*, 335(1):43–52, 1997.

[192] K. Hazeki, S. Kinoshita, T. Matsumura, K. Nigorikawa, H. Kubo, and O. Hazeki. Opposite effects of wortmannin and 2-(4-morpholinyl)-8-phenyl-1(4H)-benzopyran-4-one hydrochloride on toll-like receptor-mediated nitric oxide production: negative regulation of nuclear factor-kappaB by phosphoinositide 3-kinase. *Molecular Pharmacology*, 69(5):1717–1724, 2006.

[193] A. Gaurnier-Hausser, V. L. Rothman, S. Dimitrov, and G. P. Tuszynski. The novel angiogenic inhibitor, angiocidin, induces differentiation of monocytes to macrophages. *Cancer Reserach*, 68(14):5905–5914, 2008.

[194] Y. L. Siow, K. K. Au-Yeung, C. W. Woo, and K. O. Homocysteine stimulates phosphorylation of NADPH oxidase p47phox and p67phox subunits in monocytes via protein kinase Cbeta activation. *Biochemical Journal*, 398(1):73–82, 2006.

[195] L. V. Dekker, M. Leitges, G. Altschuler, N. Mistry, A. McDermott, J. Roes, and A. W. Segal. Protein kinase C-beta contributes to NADPH oxidase activation in neutrophils. *Biochemical Journal*, 347 Pt 1:285–289, 2000.

[196] A. K. Sue-A-Quan, L. Fialkow, C. J. Vlahos, J. A. Schelm, S. Grinstein, J. Butler, and G. P. Downey. Inhibition of neutrophil oxidative burst and granule secretion by wortmannin: potential role of MAP kinase and renaturable kinases. *Journal of Cellular Physiology*, 172(1):94–108, 1997.

[197] M. Yamaguchi, H. Oishi, S. Araki, S. Saeki, H. Yamane, N. Okamura, and S. Ishibashi. Respiratory burst and tyrosine phosphorylation by vanadate. *Archives of Biochemistry and Biophysics*, 323(2):382–386, 1995.

[198] F. Watson, J. Robinson, and S. W. Edwards. Protein kinase C-dependent and -independent activation of the NADPH oxidase of human neutrophils. *Journal of Biological Chemistry*, 266(12):7432–7439, 1991.

[199] B. Dewald, M. Thelen, M. P. Wymann, and M. Baggiolini. Staurosporine inhibits the respiratory burst and induces exocytosis in human neutrophils. *Biochemical Journal*, 264(3):879–884, 1989.

[200] W. M. Nauseef, B. D. Volpp, S. McCormick, K. G. Leidal, and R. A. Clark. Assembly of the neutrophil respiratory burst oxidase. Protein kinase C promotes cytoskeletal and membrane association of cytosolic oxidase components. *Journal of Biological Chemistry*, 266(9):5911–5917, 1991.

[201] M. Yamaguchi, S. Saeki, H. Yamane, N. Okamura, and S. Ishibashi. Involvement of Several Protein Kinases in the Phosphorylation of p47-phox. *Biochemical and Biophysical Research Communications*, 220(3):891–895, 1996.

[202] Thomas E. DeCoursey. During the Respiratory Burst, Do Phagocytes Need Proton Channels or Potassium Channels, or Both? *Science's STKE*, 2004(233):pe21, 2004.

[203] E. P. Reeves, H. Lu, H. L. Jacobs, C. G. M. Messina, S. Bolsover, G. Gabella, E. O. Potma, A. Warley, J. Roes, and A. W. Segal. Killing activity of neutrophils is mediated through activation of proteases by K+ flux. *Nature*, 416(6878):291–297, 2002.

[204] Tadato Oritani, Nobutaka Fukuhara, Takeyoshi Okajima, Fusao Kitamura, and Takeo Ohsaka. Electrochemical and spectroscopic studies on electron-transfer reaction between novel water-soluble tetrazolium salts and a superoxide ion. *Inorganica Chimica Acta*, 357(2):436–442, 2004.

[205] Mark L. Wang, Peter V. Hauschka, Rocky S. Tuan, and Marla J. Steinbeck. Exposure to particles stimulates superoxide production by human THP-1 macrophages and avian HD-11EM osteoclasts activated by tumor necrosis factor-[alpha] and PMA. *The Journal of Arthroplasty*, 17(3):335–346, 2002.

[206] Jimmy S. Lee, William M. Nauseef, Alireza Moeenrezakhanlou, Laura M. Sly, Sanaa Noubir, Kevin G. Leidal, Jamie M. Schlomann, Gerald Krystal, and Neil E. Reiner. Monocyte p110alpha phosphatidylinositol 3-kinase regulates phagocytosis, the phagocyte oxidase, and cytokine production. *Journal of Leukocyte Biology*, 81(6):1548–1561, 2007.

[207] M. M. Tarpey and I. Fridovich. Methods of detection of vascular reactive species - Nitric oxide, superoxide, hydrogen peroxide, and peroxynitrite. *Circulation Research*, 89(3):224–236, 2001.

[208] J. Schrenzel, L. Serrander, B. Banfi, O. Nüsse, R. Fouyouzi, D. P. Lew, N. Demaurex, and K. H. Krause. Electron currents generated by the human phagocyte NADPH oxidase. *Nature*, 392(6677):734–737, 1998.

[209] S. Tosatti, S. M. De Paul, A. Askendal, S. VandeVondele, J. A. Hubbell, P. Tengvall, and M. Textor. Peptide functionalized poly(L-lysine)-g-poly(ethylene glycol) on titanium: resistance to protein adsorption in full heparinized human blood plasma. *Biomaterials*, 24(27):4949–4958, 2003.

[210] Narkunaraja Shanmugam, Irene T Gaw Gonzalo, and Rama Natarajan. Molecular mechanisms of high glucose-induced cyclooxygenase-2 expression in monocytes. *Diabetes*, 53(3):795–802, 2004.

[211] Mohan R. Dasu, Sridevi Devaraj, Ling Zhao, Daniel H. Hwang, and Ishwarlal Jialal. High Glucose Induces Toll-Like Receptor Expression in Human Monocytes Mechanism of Activation. *Diabetes*, 57(11):3090–3098, 2008.

[212] S. Devaraj, S. K. Venugopal, U. Singh, and I. Jialal. Hyperglycemia induces monocytic release of interleukin-6 via induction of protein kinase C-alpha and -beta. *Diabetes*, 54(1):85–91, 2005.

[213] O. Cachia, J. E. Benna, E. Pedruzzi, B. Descomps, M. A. Gougerot-Pocidalo, and C. L. Leger. Alpha-tocopherol inhibits the respiratory burst in human monocytes. Attenuation of p47(phox) membrane translocation and phosphorylation. *Journal of Biological Chemistry*, 273(49):32801–32805, 1998.

[214] Toshio Hayashi, Packiasamy A R Juliet, Asaka Miyazaki, Louis J Ignarro, and Akihisa Iguchi. High glucose downregulates the number of caveolae in monocytes through oxidative stress from NADPH oxidase: implications for atherosclerosis. *Biochim Biophys Acta*, 1772(3):364–372, 2007.

[215] A. Perner, S. E. Nielsen, and J. Rask-Madsen. High glucose impairs superoxide production from isolated blood neutrophils. *Intensive Care Medicine*, 29(4):642–645, 2003.

[216] R. G. Sitrin, P. M. Pan, S. Srikanth, and R. F. Todd. Fibrinogen activates NF-kappa B transcription factors in mononuclear phagocytes. *The Journal of Immunology*, 161(3):1462–1470, 1998.

[217] S. T. Smiley, J. A. King, and W. W. Hancock. Fibrinogen stimulates macrophage chemokine secretion through toll-like receptor 4. *The Journal of Immunology*, 167(5):2887–2894, 2001.

[218] Eric Brown. *Complement Receptors, Adhesion, and Phagocytosis Molecular Mechanisms of Phagocytosis*. Springer US, 2005.

[219] A. C. Wang and L. Fu. Fibronectin regulates the activation of THP-1 cells by TGF-beta1. *Inflammation Research*, 50(3):142–148, 2001.

[220] D. Morgan, V. V. Cherny, R. Murphy, B. Z. Katz, and T. E. DeCoursey. The pH dependence of NADPH oxidase in human eosinophils. *Journal of Physiology-London*, 569(2):419–431, 2005.

[221] Y. Suzuki and R. I. Lehrer. NAD(P)H oxidase activity in human neutrophils stimulated by phorbol myristate acetate. *The Journal of Clinical Investigation*, 66(6):1409–1418, 1980.

[222] V. K. Salloum, S. Chakraborty, and A. Bidani. Effect of temperature on superoxide production by THP1 monocytes. *Chest*, 128:166S, 2005.

[223] P. Tölgyessy, E. Buchlerova, and J. Brtko. Effect of dissolved oxygen on the inactivation of bacteriophages in water by gamma radiation: important

role of HO_2 radicals. *Journal of Radioanalytical and. Nuclear Chemistry, Letters*, 126(2):139–143, 1988.

[224] DH Park, SK Kim, IH Shin, and YJ Jeong. Electricity production in biofuel cell using modified graphite electrode with Neutral Red. *Biotechnology Letters*, 22(16):1301–1304, 2000.

[225] K Kano and T Ikeda. Fundamentals and practices of mediated bioelectrocatalysis. *Analytical Sciences*, 16(10):1013–1021, 2000.

[226] S. Calabrese Barton, J. Gallaway, and P. Atanassov. Enzymatic Biofuel Cells for Implantable and Microscale Devices. *Chemical Reviews*, 104(10):4867–4886, 2004.

[227] Bruce E. Logan. *Microbial Fuel Cells*. John Wiley & Sons, Inc., New Jersey, 2008.